UNIVERSITY OF CALIFORNIA
RIVERSIDE

Conflict Over Control in the Legume-Rhizobia Symbiosis

A Dissertation submitted in partial satisfaction
of the requirements for the degree of

Doctor of Philosophy

in

Evolution, Ecology, and Organismal Biology

by

Kenjiro Wake Quides

December 2018

Dissertation Committee:
Dr. Joel L. Sachs, Chairperson
Dr. Cheryl Y. Hayashi
Dr. Quinn S. McFrederick

The Dissertation of Kenjiro Wake Quides is approved:

_____

_____

_____

Committee Chairperson

University of California, Riverside

ACKNOWLEDGEMENTS

I am very thankful to have Joel Sachs as my advisor. He provided me with many opportunities to excel as a graduate student and propel my professional development. He created an ideal lab environment for me to grow personally as an eager young adult. I also want to thank other members of the Sachs Lab, past and present, for their lasting friendship and ongoing support. A special thank you to all of the undergraduates I have worked with.

Cheryl Hayashi and Quinn Mcfrederick have been fantastic committee members. I am extremely grateful to have known them throughout my graduate school career. Much of this work could not have been done without many other mentors, collaborators, and providers of biological materials: Jeff Chang, Elizabeth Savory, Alexandra Weisberg, Elizabeth Braker, David Carter, Kurt Anderson, Mike Fugate, Dale Noel, Masayoshi Kawaguchi, Tim Payne, Emma Aronson, and Carolyn Rasmussen.

I also must acknowledge my support network. Carol Findlay has been the best mental trainer I could have asked for, and the EEOB graduate student community has introduced me to amazing people and lifelong friends. Finally, I would not have the persistence to finish my PhD without my family.

Chapter 1 of this dissertation was previously published in PLoS ONE, September 28, 2017.

DEDICATION

I dedicate this to my family, especially my parents, Cathy and Rey Quides. Their ongoing support has encouraged me to view the world through a curious lens.

ABSTRACT OF THE DISSERTATION

Conflict Over Control in the Legume-Rhizobia Symbiosis

by

Kenjiro Wake Quides

Doctor of Philosophy, Graduate Program in Evolution, Ecology, and Organismal Biology
University of California, Riverside, December 2018
Dr. Joel L. Sachs, Chairperson

Microbes can dramatically alter the fitness of host organisms, ranging in effect from mutualistic to antagonistic. Across this spectrum of fitness effects the microbial symbiont is predicted to optimize its own fitness benefits either through positive feedback (i.e., mutualism) or exploitation (i.e., antagonism). The legume-rhizobium symbiosis has emerged as a powerful system to study the control mechanisms of hosts and the corresponding subversion of control by symbionts. Rhizobial bacteria are housed in legume root nodules where they provide the costly services of nitrogen fixation in return for host derived carbon. However, variation in symbiont quality and lifestyle strategies can result in fitness conflict between host and symbiont. I used the symbiosis between *Lotus japonicus* and *Mesorhizobium loti* to investigate host control over symbionts across the mutualism-antagonism spectrum. For chapter 1 I investigated the effects of host control on symbiont fitness when symbionts vary in their fitness effects. I found that the *L. japonicus* host can adaptively alter the fitness of symbionts dependent on symbiotic nitrogen fixation. For chapter 2 I examined how varying host investment into symbiosis

affects the fitness of hosts and symbionts. I found host control was maintained when host investment into symbiosis was altered. However, at high levels of host investment in symbiosis with a high-quality symbiont I uncovered evidence that host fitness is optimized, while symbiont fitness continues to increase. For chapter 3 I tested the effects of host control and varying levels of host investment on the evolution of symbiont services to hosts. After experimentally evolving rhizobial symbionts of mediocre quality in multiple experiments, the phenotypic data was most consistent with a shift towards antagonistic phenotypes. Together, these results highlight the intense conflict over resources that can lead to the destabilization or breakdown of the mutualism between legumes and rhizobia.

TABLE OF CONTENTS

General Introduction……1

Chapter 1: ***Lotus japonicus*** **alters** ***in planta*** **fitness of** ***Mesorhizobium loti*** **dependent on symbiotic nitrogen fixation**……4

Chapter 2: **Over-investment by legumes triggers antagonistic fitness consequences by their symbionts**…….28

Chapter 3: **Exposure to static host genotypes leads to rapid shifts in symbiotic rhizobia phenotypes**…….53

General Conclusions……..93

References……..95

Appendices……...114

LIST OF TABLES

Table 1.1 Host control phenotypes when inoculated with two symbionts……17

Table 2.1 List of functions used for AICc comparisons……41

Table 2.2 Proportional *in planta* fitness of the beneficial symbiont MAFF at 5wpi…….43

Table 3.1 Metadata for symbiont passaging……..65

Table 3.2 Phenotypic comparison of ancestral and final derived symbionts…….81

Table 3.3 Fraction of 20 clonal isolates from final derived population with mutation….86

LIST OF FIGURES

Figure 1.1 Traits of host and symbiont in growth chamber experiment……11

Figure 1.2 Traits of host and symbiont in greenhouse experiment……13

Figure 1.3 Sanctions are triggered continuously with nitrogen fixation……17

Figure 2.1 *L. japonicus* nodulation varied significantly among host genotypes……...42

Figure 2.2 Rhizobia fitness varied significantly among host genotypes……...44

Figure 2.3 Host benefits from nodulation varied significantly among host genotypes….46

Figure 2.4 Host and symbiont fitness functions…….47

Figure 3.1 Symbiont passaging protocol……...68

Figure 3.2 Phenotypic evolution of CE3 symbionts on *har1* hosts……...83

Figure 3.3 Nodule structure of ancestral and derived CE3 infected nodule……..84

Figure 3.4 Number of mutations identified with whole genome resequencing…….86

LIST OF APPENDICES

Appendix 1.1 Summary of data collected during harvests…….see attached

Appendix 1.2 Estimated rhizobial fitness determined by culturing nodules…..see attached

Appendix 2.1 Host and symbiont data collected for the 3.5wpi harvest…….115

Appendix 2.2 Host phenotype data collected at the time of harvest……..see attached

Appendix 2.3 Estimated viable rhizobia per nodule……..see attached

Appendix 2.4 Histology measurements of MAFF infected nodules at 5wpi….see attached

Appendix 2.5 Elemental and isotopic leaf tissue analysis at 5wpi…….see attached

Appendix 2.6 Fitness functions and corresponding AICc values for host shoot mass dependent on number of nodules formed…….117

Appendix 2.7 Fitness functions and corresponding AICc values for estimated rhizobia population size per plant dependent on number of nodules formed……118

Appendix 3.1 Relative read depth of each sample……...119

General Introduction

Mutualistic interactions with microbes can dramatically improve the fitness of eukaryotic hosts. However, these benefits are not guaranteed or fixed and many of these interactions shift in fitness outcome from mutualism to antagonism (Bronstein 1994, 2001; Neuhauser and Fargione 2004; Thompson 1988). Microbes have a profound evolutionary advantage over hosts due to a vastly greater effective population size and rapid reproduction rates. Thus, rapid evolution of mutant microbes that extract more and or give less resources to hosts can rapidly spread through a population (Joel L. Sachs et al. 2004; Foster and Wenseleers 2006). Both plant and animals hosts are predicted to evolve control mechanisms that decrease the fitness advantage gained by such antagonistic symbiont genotypes (Axelrod and Hamilton 1981; Chaparro et al. 2012; Denison 2000; Fine 1975; Haney et al. 2015; Joel L. Sachs et al. 2004). For example, host plants can influence the microbial ecology around their roots (Busby et al. 2017), while the bobtail squid host can alter allele frequencies of their symbionts by creating a harsh *in vivo* environment for non-mutualistic symbionts (McFall-Ngai 2014).

The legume-rhizobia interaction is a powerful model to study microbial symbionts that fall along the mutualism-antagonism spectrum and the corresponding evolutionary dynamics that maintain this symbiosis (Denison 2000; Mus et al. 2016; Joel L. Sachs, Quides, and Wendlandt 2018; J. I. Sprent et al. 1987). Legumes provide photosynthates while rhizobia fix atmospheric nitrogen, and both provide substantial fitness benefits to the other. The interaction begins when host roots release flavonoids into the soil whereby receptive rhizobia release Nod factors that trigger a cascade of transcriptional changes in

host roots (Liu and Murray 2016). Once inside host tissue, the rhizobia colonize individual plant cells (Coba de la Peña et al. 2018). As the intracellular rhizobia begin to proliferate, the host root tissue grows into a novel organ, a nodule, which can house millions of rhizobia that fix atmospheric nitrogen for the host (Quides et al. 2017). As the growth season progresses, nodules gradually senesce and resources are diverted away from nodule maintenance (and corresponding rhizobia fitness) and towards host seed production. Throughout nodule senescence, a subset of rhizobia residing within the nodule are released into the soil where they can infect a future host (Puppo et al. 2004). At each step in this process, hosts have evolved control mechanisms that can limit harmful interactions with rhizobia (Joel L. Sachs, Quides, and Wendlandt 2018). Nonetheless, the host mechanisms that prevent the sweep of antagonistic rhizobial symbionts in a population remain unresolved.

Lotus japonicus is a genomic model for legume research with a diversity of mutants available for both host and symbiont (LegumeBase). By using this host I was able to ask specific questions using near-isogenic hosts and symbionts. Furthermore, there is a large assemblage of established methods to study this interaction (Márquez 2005). In chapter 1, I inoculated *L. japonicus* with three near-isogenic symbionts varying in their capacity to fix nitrogen. I tested the ability of *L. japonicus* to bias *in planta* fitness of symbionts based upon the nitrogen fixed by each strain. The prediction is that hosts should adjust investment in a way that optimizes host fitness. For chapter 2, I used four near-isogenic *L. japonicus* hosts varying in their investment into nodules. I examined variation in the host and symbiont fitness dependent on the degree of host investment into

the symbiotic structures. The prediction is that hosts must balance costs and benefits of any interaction to invest optimally (Joel L. Sachs, Quides, and Wendlandt 2018). For chapter 3, I used *in vitro* evolution to test the capacity of *L. japonicus* to select for beneficial genotypes of rhizobia. Using the *L. japonicus* host I examined the effects of host control mechanisms across the symbiosis spectrum providing insight into the intricate interaction between this eukaryotic host and its microbial symbionts. Additionally, I tested how variation in host control affected a rhizobial symbionts position on the spectrum and I suggest ways that we can adapt these finding to other plant-microbe interactions.

Chapter 1

Lotus japonicus alters *in planta* fitness of *Mesorhizobium loti* dependent on symbiotic nitrogen fixation

Abstract

Rhizobial bacteria are known for their capacity to fix nitrogen for legume hosts. However ineffective rhizobial genotypes exist and can trigger the formation of nodules but fix little if any nitrogen for hosts. Legumes must employ mechanisms to minimize exploitation by the ineffective rhizobial genotypes to limit fitness costs and stabilize the symbiosis. Here we address two key questions about these host mechanisms. What stages of the interaction are controlled by the host, and can hosts detect subtle differences in nitrogen fixation? We provide the first explicit evidence for adaptive host control in the interaction between *Lotus japonicus* and *Mesorhizobium loti*. In both single inoculation and co-inoculation experiments, less effective rhizobial strains exhibited reduced *in planta* fitness relative to the wildtype *M. loti*. We uncovered evidence of host control during nodule formation and during post-infection proliferation of symbionts within nodules. We found a linear relationship between rhizobial fitness and symbiotic effectiveness. Our results suggest that *L. japonicus* can adaptively modulate the fitness of symbionts as a continuous response to symbiotic nitrogen fixation.

Introduction

Rhizobial bacteria instigate the formation of root nodules on legumes where the bacteria fix atmospheric nitrogen for the host, a process that can greatly enhance plant growth and fitness (Sprent et al. 1987). In exchange for fixed nitrogen the plant provides photosynthates that allow rhizobia to proliferate *in planta* and after nodule senescence, replenish the soil (Puppo et al. 2004). However, legumes often encounter ineffective rhizobia that trigger the formation of nodules but fix little if any nitrogen (Bromfield et al. 2010; Burdon et al. 1999; Chen et al. 2002; Collins, Thies, and Abbott 2002; Denton et al. 2000; Ehinger et al. 2014; Fening and Danso 2002; Gaur and Lowther 1980; Gibson et al. 1975; Moawad, Badr El-Din, and Abdel-Aziz 1998; Quigley et al. 1997; Rangin et al. 2008; Sachs et al. 2009; Sachs, Ehinger, and Simms 2010). By not providing fixed nitrogen ineffective rhizobia have the potential to exploit resources from the host without paying the high energetic expense of fixing nitrogen (Porter and Simms 2014; Ratcliff and Denison 2009; Sachs, Ehinger, and Simms 2010; Trainer and Charles 2006; West et al. 2002a). To maximize net fitness benefits of symbiosis, legumes must exhibit 'host control' traits that constrain the effects of ineffective rhizobial genotypes and select against symbiont exploitation (Denison 2000; West et al. 2002a, 2002b).

There are two stages of the interaction where legumes have the potential to bias investment towards beneficial rhizobia and limit physiological inputs into ineffective genotypes. In a 'partner choice' model, legumes could discriminate between different genotypes of rhizobia during the process of nodule organogenesis (Cooper 2007; Sachs et al. 2004; Simms and Taylor 2002). Evidence suggests legumes restrict certain

genotypes of rhizobia at the early stages of nodule development (Djordjevic et al. 1988; Kosch et al. 1994; Lotocka et al. 2000; Martin Parniske et al. 1994; Vasse, Billy, and Truchet 1993) or block nodulation caused by toxin-producing rhizobia (Devine, Kuykendall, and O'Neill 1990; Devine and Kuykendall 1996). However, it is unclear whether nitrogen fixation is expressed early in the process for legumes to discriminate between effective and ineffective genotypes (Amarger 1981a, 1981b; de Boer and Djordjevic 1995; Champion et al. 1992; Hahn and Studer 1986; Kuykendall and Elkan 1976; Ling et al. 2013; Noel, Vandenbosch, and Kulpaca 1986; Westhoek et al. 2017; Yasuda et al. 2016). In a 'sanctions' model, after nodule organogenesis is complete, legumes have the potential to selectively target rhizobia that fail to fix sufficient amounts of nitrogen within the nodule and reduce their fitness relative to beneficial genotypes (Denison 2000; West et al. 2002a, 2002b). Several experiments have demonstrated that nodules with nitrogen-fixing rhizobia grow (and the rhizobia within rapidly proliferate) whereas nodules with ineffective rhizobia tend to stay small (and the rhizobia within have reduced fitness) (Kiers et al. 2003; Oono, Anderson, and Denison 2011; Regus et al. 2014; Sachs et al. 2010; Simms et al. 2006). Some experiments have failed to find evidence for sanctions but this could be a consequence of challenges in controlling for variation in competitive ability and host specificity among rhizobial genotypes (Gubry-Rangin, Garcia, and Bena 2010; Heath and Tiffin 2009; Ling et al. 2013; Marco et al. 2009). Experiments have found evidence for partner choice and/or sanctions in diverse legumes (Amarger 1981a; Champion et al. 1992; Gubry-Rangin, Garcia, and Bena 2010; Heath and Tiffin 2009; Kiers et al. 2003; Kiers, Rousseau, and Denison 2006; Oono,

Anderson, and Denison 2011; Regus et al. 2014, 2015; Sachs et al. 2010; Simms et al. 2006; Singleton and Stockinger 1983; Westhoek et al. 2017). While the molecular dialogue that occurs prior to nodule formation has been well characterized (Cooper 2007; Limpens, van Zeijl, and Geurts 2015), the triggers for sanctions have received little attention (Kiers, Rousseau, and Denison 2006; Regus et al. 2014).

Mesorhizobium loti MAFF303099 (MAFF) fixes nitrogen for the host *Lotus japonicus*, a perennial herbaceous diploid, allowing hosts to grow without any other source of nitrogen (Jiang and Gresshoff 1997). *L. japonicus* forms determinate nodules that lack a continuous meristem. *L. japonicus* nodules have a relatively homogenous population of differentiated intracellular rhizobia (i.e., bacteroids), cease growth after nodule development is complete, and because the bacteroids do not terminally differentiate, allow rhizobia to escape back into the soil during nodule senescence. This is in contrast to other legumes such as *Medicago truncatula* that form indeterminate nodules that grow throughout the functional association, and have a spatial gradation of bacteroids in different developmental stages. The bacteroids of indeterminate nodules tend to terminally differentiate and cannot escape the nodule, but nonetheless a subset of viable rhizobia can be released upon nodule senescence (Crespo-Rivas et al. 2016; Puppo et al. 2004; Oono et al. 2010).

In the *Lotus-Mesorhizobium* symbiosis both symbiotic partners have been developed as models for the molecular and cellular basis of nodulation (Kaneko 2000; Kawaguchi et al. 2002). Mutants of MAFF have been generated by signature-tagged mutagenesis and their insertion sites have been identified (Shimoda et al. 2008). Several

mutants affected in nitrogen fixation have been identified. STM30 has a transposon inserted in mll0343, encoding glutamine synthetase I (strain ID 10T05g06). The mutant is significantly reduced in its ability to fix nitrogen, as measured by acetylene reduction (ca. 45%, Chungopast et al. 2014). Glutamine synthetase (along with glutamine synthase) is responsible for the assimilation of ammonium in legume nodules, which is the main product of nitrogen fixation (Chungopast et al. 2014). The MAFF mutant STM6 has a transposon inserted in mlr5906, which is the nitrogenase gene *nifD* (strain ID 17T02d02). This mutant is incapable of fixing nitrogen (Shimoda et al. 2008). Nitrogenases are a family of metalloenzymes that catalyze the reduction of dinitrogen to ammonia. In MAFF, the majority of the genes necessary for nodulation and nitrogen fixation are clustered in a symbiosis island (Kaneko 2000).

The goals of our experiment were to (i) test whether mildly effective and ineffective mutants of *M. loti* nodulate *L. japonicus* hosts at reduced rates when competing against wildtype MAFF, (ii) examine whether the MAFF mutants are reduced in population sizes within singly infected and co-infected host nodules, and (iii) investigate the triggering of sanctions in response to varying amounts of nitrogen fixation. We inoculated *L. japonicus* hosts with single and mixed inocula of MAFF, STM30, and STM6 in order to estimate symbiotic effectiveness (effects on host growth in the absence of other nitrogen sources), host investment in symbionts (nodule biomass), and symbiont fitness (viable within-nodule population size). Additionally, we tested models of nodulation rates for each strain and host response to rhizobia that differ in symbiotic effectiveness.

Results

Host and symbiont growth in a controlled environment

MAFF, STM30, and STM6 were singly inoculated on *L. japonicus* seedlings growing in sterilized growth pouches filled with N-free Jensen's fertilizer and in an environmentally-controlled setting (Somasegaran and Hoben 1994). Experimental treatments each began with 20 seeds, but after germination the number of surviving plants ranged from 10 to 18 (Appendix 1.1). Plants were harvested from 3 weeks post infection (wpi) to 8wpi. These time points were selected based on data from pilot experiments and visualization of key morphological differences, such as observable differences in nodule size, flowering, and senescence. At the earliest time point, there were no detectable differences in shoot biomass between inoculation treatments (ANOVA, $F_{2,38} = 0.994$, $P = 0.380$; Figure 1.1A). By 5wpi, a significant difference was observed, with MAFF-inoculated plants having significantly greater shoot biomass than hosts inoculated with STM30 or STM6, and this pattern was maintained at 6wpi (5wpi: ANOVA, $F_{2,44} = 19.052$, $P < 0.001$; 6wpi: ANOVA, $F_{2,36} = 11.758$, $P < 0.001$; Figure 1.1A). As the experiment progressed, the differences in shoot biomass of plants inoculated with MAFF and mutants became greater. At 7 and 8wpi MAFF-inoculated plants were significantly larger than hosts inoculated with STM30 which were significantly greater larger than hosts inoculated with STM6 (7wpi: ANOVA, $F_{2,42} = 30.212$, $P < 0.001$; 8wpi: ANOVA, $F_{2,34} = 20.215$, $P < 0.001$; Figure 1.1A).

To quantify fitness effects on the symbiont, we measured characteristics of nodules that reflect host investment into *in planta* rhizobia. We focused on 6 and 8wpi,

time points in which variation in symbiotic benefit was detected and natural senescence of nodules had not occurred. At 6wpi we did not detect differences in average nodule biomass infected with different genotypes (ANOVA, $F_{2,9} = 4.543$, $P = 0.054$; Figure 1.1B), At 8wpi, nodules housing MAFF had a greater average biomass than nodules of STM30 which were larger than STM6 (ANOVA, $F_{2,11} = 17.156$, $P < 0.001$; Figure 1.1B). To examine the possibility that differences in nodule biomass reflected fitness differences of the bacteria, we also dissected and successfully cultured 86 out of 115 nodules to quantify the viable *in planta* rhizobia (Appendix 1.2). MAFF population sizes estimated from cultured nodules at 6 and 8wpi were significantly greater than STM30 and STM6, while no differences were detected between STM30 and STM6 (6wpi: ANOVA, $F_{2,38} = 4.673$, $P < 0.05$; 8wpi: ANOVA, $F_{2,46} = 11.789$, $P < 0.001$; Figure 1.1C). Thus, under controlled conditions, singly inoculated hosts grew smaller with the less effective rhizobia which were simultaneously reciprocated fewer resources than the more effective genotype.

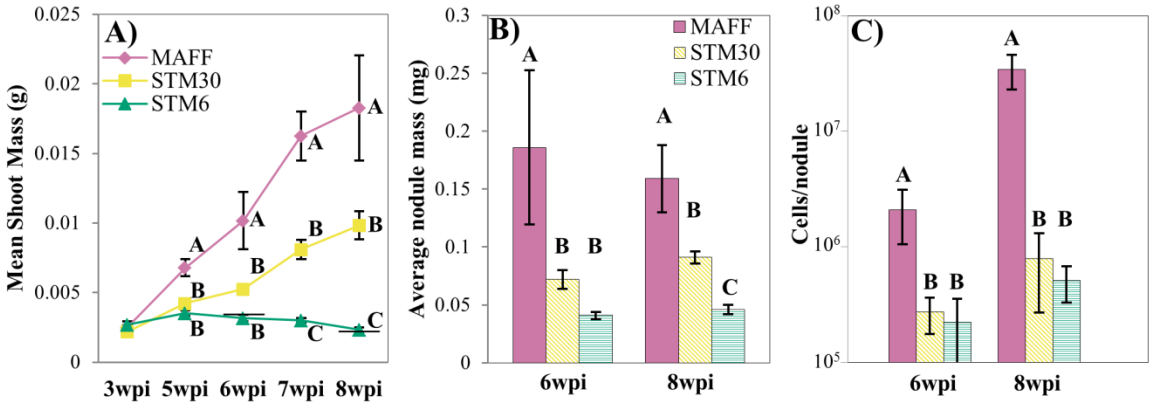

Figure 1.1 Traits of host and symbiont in growth chamber experiment

L. japonicus hosts were inoculated with near-isogenic *M. loti* strains MAFF, STM30, and STM6 and host and symbiont phenotypes were measured at times indicated. **(A)** Symbiont effectiveness was measured as dried shoot biomass. **(B)** Host investment in symbionts was measured as average individual biomass of nodules (dry weight). **(C)** Rhizobial fitness was estimated based on CFUs from serially diluted extracts of crushed nodules. Error bars indicate one standard error from the mean. Horizontal lines **(A)** represent the mean dried shoot biomass for uninoculated controls at 6 (0.003g) and 8wpi (0.002g). Data points demarked with different letters indicate significant differences between strains at a given wpi. (one-way ANOVA, post-hoc Student's t-test, α=0.05).

Host and symbiont growth under ambient conditions

Results were repeatable with plants grown in the less controlled environment of greenhouse. In this experiment plants were harvested only at 4wpi and 7wpi, during which plants were rapidly growing and had not flowered. Only two time points were used because of the greater challenges in greenhouse experiments. At 4 and 7wpi hosts inoculated with MAFF had significantly more shoot biomass than those infected with either STM30 or STM6, and plants inoculated with STM30 had significantly greater shoot biomass than those inoculated with the ineffective strain STM6 (4wpi: ANOVA, $F_{2,35} = 19.334$, $P < 0.001$; 7wpi: ANOVA, $F_{2,35} = 89.744$, $P < 0.001$; Figure 1.2A). We also harvested nodules at these times. Again, consistent with results from growth chamber experiments, nodules infected with MAFF had the greatest average biomass at both 4 and 7wpi, while the average biomass of STM30-infected nodules was significantly greater than those from STM6-infected plants at 7wpi (4wpi: ANOVA, $F_{2,26} = 6.739$, $P < 0.005$; 7wpi: ANOVA, $F_{2,29} = 55.839$, $P < 0.001$; Figure 1.2B). Of the 224 nodules cultured, rhizobia were successfully cultured from 177 nodules (Appendix 1.2). Of the nodules harvested at 4wpi, there were no significant differences in the number of cultured rhizobia (ANOVA, $F_{2,36} = 0.852$, $P = 0.435$; Figure 1.2C). At 7wpi, MAFF population size was significantly greater than that of STM6, but the population size of STM30 was not different relative to the population sizes of either of the other two genotypes (ANOVA, $F_{2,40} = 3.782$, $P < 0.05$; Figure 1.2C).

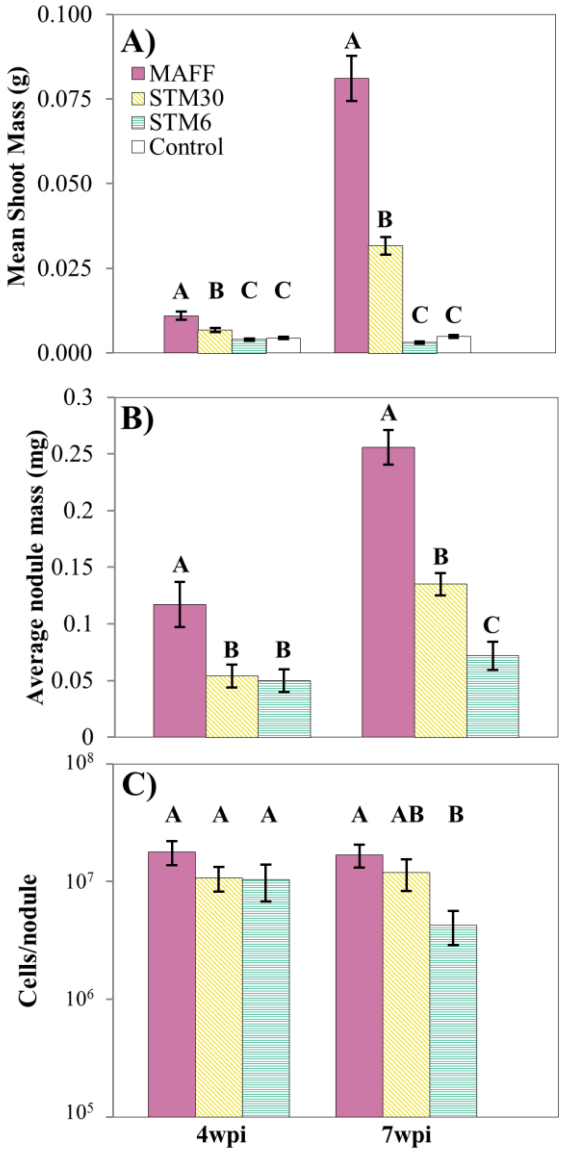

Figure 1.2 Traits of host and symbiont in greenhouse experiment

L. japonicus hosts were grown in sterilized quartzite sand supplemented with N-free Jensen's fertilizer. Hosts were singly inoculated or co-inoculated with the near-isogenic *M. loti* strains MAFF, STM30, and STM6 and mean host and symbiont phenotypes were measured. **(A)** Symbiont effectiveness measured as dried shoot biomass. **(B)** Host investment in symbionts was measured as average individual biomass of nodules (dry weight). **(C)** Rhizobial fitness was estimated based on colony forming units (CFUs) from serially diluted extracts of crushed nodules. Error bars indicate one standard error from the mean. Data points demarked with different letters indicate significant differences between strains at a given wpi (one-way ANOVA, post-hoc Student's t-test, α=0.05).

Testing models of host control over *in planta* rhizobial fitness

First, we tested whether STM30 or STM6 are compromised for fitness by measuring *in vitro* growth rate and nodulation rate, as these factors could affect the outcome of our experiments. We can reject the possibility that STM30 or STM6 were compromised for our tested fitness measures. The mean doubling times ± standard error in minutes for MAFF, STM30 and STM6 were 210 ± 32, 175 ± 28 and 220 ± 25, respectively, and there were no significant differences in growth rate between the three strains (ANOVA; $F_{2,32}$ = 0.6687; P = 0.52). We can also reject the possibility that STM30 or STM6 were compromised for nodulation relative to MAFF nodulation relative to MAFF by comparing early nodulation rates in a single inoculation scenario (4wpi, greenhouse experiment; ANOVA; $F_{2,35}$ = 2.2326; P = 0.1232). We co-inoculated 96 greenhouse-grown plants with MAFF paired with each of the less effective genotypes to test models of partner choice and sanctions. The proportion of nodules with MAFF present and the proportion of MAFF within nodules were quantified. We tested the null model that ratios of recovered rhizobia should approximate the ratios used in the initial inoculations, which assumes that nodulation rates and rates of rhizobial *in planta* growth are equal. Under a partner choice model, plants will form more nodules with symbionts that provide greater benefits (Sachs et al. 2004; Simms and Taylor 2002). Under a sanctions model, there will be greater *in planta* proliferation of the more effective genotype (Denison 2000).

We inoculated plants with a 1:1 and 1:9 (MAFF:STM mutant) ratio of genotypes. A fraction of the mixtures was plated and each genotype was scored based on colony color (the MAFF strain used expressed red fluorescent protein) to retrospectively

determine actual proportions used. The proportion of MAFF in MAFF:STM30 mixtures were close to the expected proportions: 0.517 ± 0.030 for the planned 1:1 ratio inoculum and 0.118 ± 0.001 for the planned 1:9 inoculum. In contrast, the proportion of MAFF for the MAFF:STM6 mixtures were more biased towards the mutant than expected and were 0.289 ± 0.032 for the planned 1:1 inoculum and 0.045 ± 0.005 for the 1:9 inoculum. Thus, for the latter combination, the actual ratios of inoculated genotypes were 3:7 and 1:19.

In all but one comparison, MAFF was present in significantly more nodules than the null expectation (Table 1.1). When MAFF and STM30 were inoculated at equal proportions, MAFF was present in significantly more nodules at 4 and 7wpi (4wpi: two-tailed GoF test, n = 16, $P < 0.05$; 7wpi: two-tailed GoF test, n = 10, $P < 0.01$). The same pattern was observed at 4 and 7wpi when MAFF was co-inoculated at a 3:7 ratio with STM6 (4wpi: two-tailed GoF test, n = 15, $P < 0.01$; 7wpi: two-tailed GoF test, n = 12, $P < 0.01$). Likewise, at both 4 and 7wpi MAFF was present in significantly more nodules than expected when inoculated at a 1:9 ratio with STM30 (4wpi: two-tailed GoF test, n = 11, $P < 0.01$; 7wpi: two-tailed GoF test, n = 9, $P < 0.01$). Additionally, the proportion of nodules with MAFF present was significantly greater than expected at 7wpi (two-tailed GoF test, n =12, $P < 0.05$), but not 4wpi (two-tailed GoF test, n = 12, $P = 1$), when in a mixed inoculum of 1:19 with STM6. These data are inconsistent with predictions of the null model and suggest that even at the earliest stages of infection *L. japonicus* can bias infections rates towards the more beneficial symbiont.

In all but the 1:19 MAFF:STM6 (4wpi) treatment, MAFF achieved a higher *in planta* population size than the paired mutant (Table 1.1). But this pattern was only significant in nodules of plants infected with a 3:7 ratio of MAFF:STM6 at 7wpi (one-sample t-test, $t = 4.444$, $df = 3$, $P < 0.05$). Additionally, at 4wpi in plants inoculated with a 1:19 ratio of MAFF:STM6, MAFF was estimated at significantly lower than expected proportions (one-sample t-test, $t = 499$, $df = 2$, $P < 0.01$). These results are inconsistent with the null model and suggest that the host can efficiently sanction ineffective strains, but the efficacy of sanctions may be lower with mediocre strains or when the beneficial strain is greatly outnumbered.

Models assume that sanctions are either triggered when fixed nitrogen is below a minimal threshold (e.g., sanctioning only of ineffective strains) or are scaled linearly according to the amount of fixed nitrogen (West et al. 2002b). To test these models, we investigated the relationship between symbiotic effectiveness and rhizobial fitness *in planta*. There was a significant correlation between shoot biomass and estimated rhizobial population size, at 6 and 8wpi of plants grown in the growth chamber (6wpi: $R^2 = 0.181$, $F_{1,38} = 8.197$, $P < 0.01$; 8wpi: $R^2 = 0.226$, $F_{1,46} = 13.1525$, $P < 0.01$; Figure 1.3). While a similar pattern was observed for plants grown in the greenhouse, we could not detect a statistically significant correlation (4wpi: $R^2 = 0.087$, $F_{1,37} = 3.4437$, $P = 0.07$; 7wpi: $R^2 = 0.047$, $F_{1,40} = 1.9376$, $P = 0.17$). These results suggest that the host alters *in planta* fitness of symbionts in a continuous fashion dependent on symbiotic effectiveness.

Table 1.1 Host control phenotypes when inoculated with two symbionts

Harvest	Proportion of MAFF[a] when coinoculated with near-isogenic mutants (STM30 or STM6)	Proportion of nodules with MAFF present on co-inoculated hosts (partner choice)[b]	Proportional population size of MAFF in nodules of co-inoculated hosts (sanctions)[c]	Fraction of co-infected nodules[d]
4wpi	0.5 (STM30)	0.813[e]	0.827±0.169	3/16
	0.3 (STM6)	0.867[f]	0.680±0.231	3/15
	0.1 (STM30)	0.455[f]	0.509±0.176	4/11
	0.05 (STM6)	0.083	0.0001±0.0001[f]	1/12
7wpi	0.5 (STM30)	1[f]	0.765±0.214	2/10
	0.3 (STM6)	0.667[f]	0.840±0.121[e]	2/12
	0.1 (STM30)	0.556[f]	0.459±0.154	2/9
	0.05 (STM6)	0.25[e]	0.161±0.093	2/12

[a] Proportion of MAFF in inocula were used as null expectations

[b] Observed proportion of nodules with MAFF present on co-inoculated hosts analyzed with a binomial goodness of fit test

[c] Observed±one standard error from the mean proportion of viable MAFF in nodules of co-inoculated hosts analyzed with a one-sample t-test

[d] Proportion of co-infected nodules pooled by treatment and harvest

P-values are indicated with [e]($P < 0.05$) and [f]($P < 0.01$)

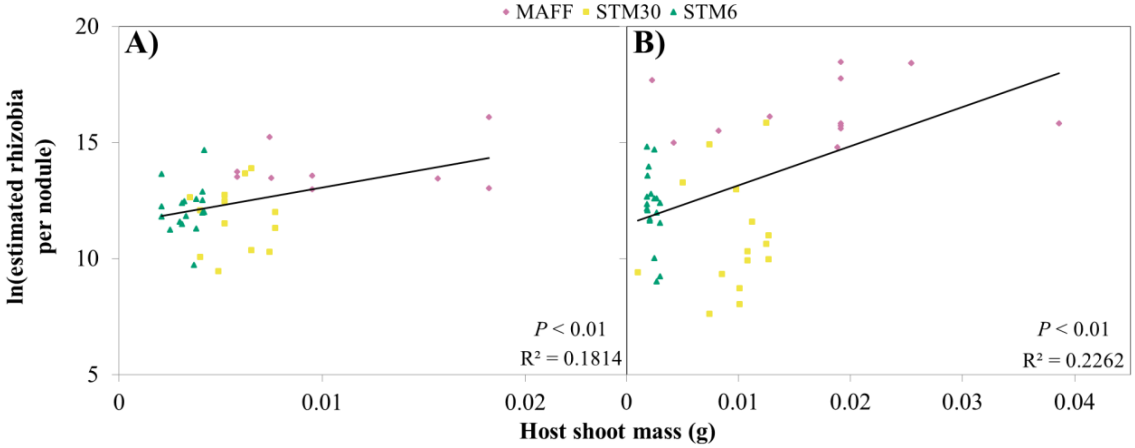

Figure 1.3 Sanctions are triggered continuously with nitrogen fixation

Linear regression of the natural log of estimated rhizobia per nodule (counting CFUs of serially diluted extracts of crushed nodules) against the shoot biomass of the host (dry weight) Hosts were singly inoculated with near-isogenic *M. loti*: MAFF (pink diamond), STM30 (yellow square) and STM6 (green triangle). Each symbol represents one nodule. **(A)** Hosts harvested at 6wpi; $F_{1,38} = 8.197$. **(B)** Hosts harvested at 8wpi; $F_{1,46} = 13.1525$.

Discussion

Using the *L. japonicus-M. loti* symbiosis we found support for three key hypotheses about host control in legumes: (i) host plants bias nodulation rates against less beneficial rhizobia, (ii) hosts bias *in planta* fitness against less beneficial rhizobia when singly infected and co-infected, and (iii) hosts adjust the severity of sanctions based on symbiotic effectiveness.

Consistent with partner choice theory (Simms and Taylor 2002; Simms et al. 2006), MAFF was significantly enriched, relative to the less-effective STM30 or STM6 near-isogenic mutants, in nodules of plants that had received mixed-strain inocula (Table 1.1). Given that near-isogenic pairs of symbionts were tested, we suggest that *L. japonicus* can detect and respond to differences in symbiotic effectiveness during the early stages of nodule formation. These results are similar to those in which mutant strains varying in nitrogen fixation led to biased infection towards the effective strain (Amarger 1981a; Champion et al. 1992). However, four other experiments found, regardless of whether hosts formed determinant or independent nodules, no such evidence (Amarger 1981a; Hahn and Studer 1986; Kuykendall and Elkan 1976; Ling et al. 2013; Westhoek et al. 2017). One possible confounding factor is that the mutations introduced in the strains of previous studies had pleiotropic effects on growth and the ability to compete for nodulation sites. STM30 and STM6 were not compromised in *in vitro* growth nor in their ability to nodulate plants, when clonally infected. Furthermore, the use of a mediocre but a near-isogenic mutant (STM30) allowed us to test sanctions

hypotheses in a scenario that is more similar to nature, while limiting confounding genetic differences among strains.

Our data suggest that *L. japonicus* has a mechanism to detect symbiotic quality before nodule maturation is complete. Histological data of nodule primordia has exhibited phenotypes consistent with a hypersensitive response found in pathogenic infections when symbiont exopolysaccharide genes were mutated (Djordjevic et al. 1988; Kosch et al. 1994; Parniske et al. 1994), symbionts were maladapted for the inoculated host (Ivanova et al. 2015; Noel, Vandenbosch, and Kulpaca 1986; Yasuda et al. 2016), or the host was satiated for nitrogen (Lotocka et al. 2000; Vasse, Billy, and Truchet 1993). Because nitrogen fixation is not expressed at the time of infection, we hypothesize that the hosts are aborting some nodules before we assayed plants. A mechanism of nodule abortion could explain why the less beneficial genotypes were consistently present in fewer nodules than expected when strains differed in their capacity to fix dinitrogen. However more work is needed to understand the capacity for legumes to detect fixed nitrogen provided by their symbionts, to uncover the cellular and molecular mechanisms for this detection, and to understand how these mechanisms have evolved.

Consistent with models of sanctions (Denison 2000; West et al. 2002a, 2002b), *L. japonicus* can alter the *in planta* proliferation of *M. loti* dependent on the symbiotic benefit provided. Given that the host has no method to calibrate the benefit received and no alternative choice for receiving fixed nitrogen, it has been debated whether legumes can impose host control when inoculated with a single genotype of symbiont (Friesen and Heath 2013; Kiers, Ratcliff, and Denison 2013; Regus et al. 2014). Here, evidence of

sanctions was derived from both single inoculation and co-inoculation experiments (Figure 1.2; Table 1.1). Moreover, data suggested that sanctions in *L. japonicus* are triggered in a continuous fashion and are scaled to the nitrogen fixed by each rhizobial genotype. Similar results were obtained from experiments in which *Glycine max* had received variable rhizobial benefit, which was artificially manipulated by adjusting the amounts of dinitrogen available for fixation (Kiers, Rousseau, and Denison 2006), and *Acmispon strigosus* (formerly *L. strigosus*) inoculated with natural strains that varied in nitrogen fixation (Regus et al. 2015).

In both natural and agricultural soils, legumes invariably encounter multiple rhizobial genotypes (Bromfield et al. 2010; Burdon et al. 1999; Chen et al. 2002; Collins, Thies, and Abbott 2002; Denton et al. 2000; Ehinger et al. 2014; Fening and Danso 2002; Gaur and Lowther 1980; Gibson et al. 1975; Moawad, Badr El-Din, and Abdel-Aziz 1998; Quigley et al. 1997; Rangin et al. 2008; Sachs et al. 2009; Sachs, Ehinger, and Simms 2010). Previous models have suggested that legumes impose sanctions at the level of the whole nodule (West et al. 2002a, 2002b), and that this is dependent upon the production of fixed nitrogen regardless of whether it is a clonal or mixed infection. But our data adds to the growing body of literature that suggests hosts can sanction rhizobia at a finer scale within individual nodules. In co-inoculated hosts we consistently found mixed nodules in which MAFF was present at a greater proportion than expected of the null model (Table 1.1) – (15 out of 19 mixed nodules; Appendix 1.2). These data are consistent with other studies that have found sanctions to be effective within determinate nodules of *A. strigosus* (Regus et al. 2014, 2017; Sachs et al. 2010).

Evidence for whole nodule sanctions has been found in single inoculation experiments with *Pisum sativa and M. truncatula* that inhibited nitrogen fixation with the use of argon in place of dinitrogen (Oono, Anderson, and Denison 2011). However, it has recently been suggested that indeterminate nodules of *P. sativa* (Westhoek et al. 2017) and *M. sativa* (Checcucci et al. 2016) can be infected by multiple genotypes and the less effective strains have decreased *in planta* fitness. Unlike determinate nodules studied here, indeterminate nodules grow indefinitely and have a spatial gradation of rhizobia in different developmental stages (Puppo et al. 2004). This mixture of rhizobia at various life stages, including nitrogen fixing bacteroids that are terminally differentiated (in most cases; Singleton and Stockinger 1983), makes a within nodule mechanism of sanctions more difficult to envision. If an indeterminate nodule is infected by a symbiont that can fix nitrogen, it is only the rhizobia that have terminally differentiated that are providing benefit, while the undifferentiated rhizobia are not. Under this scenario if nitrogen fixation is the trigger for sanctions the host would wrongfully target undifferentiated beneficial symbionts, unless the viable bacteria are able to suppress mechanisms of sanctions, which has been suggested to involve functional nitrogenase (Berrabah, Ratet, and Gourion 2015). Furthermore, if a nodule is mixed the host would be unable to distinguish symbiont quality of undifferentiated rhizobia, thus targeting rhizobia based on nitrogen fixation would not effectively decrease the relative fitness of less beneficial strains. More research is needed on sanctions in hosts that form indeterminate nodules to examine whether the mechanisms of sanctions are independent from the patterns we have described for species that form determinate nodules.

Historically, scientists have tried to leverage this symbiosis to improve agronomically important leguminous crops, but native low quality symbionts often outcompete elite rhizobial inocula (Beattie, Clayton, and Handelsman 1989; Moawad, Badr El-Din, and Abdel-Aziz 1998; Parniske et al. 1990). Co-inoculation experiments are important because they model the multistrain competition for infections that occur in nature (Zgadzaj et al. 2016), and also because they can enhance our understanding of the effects of nodule co-infection(Checcucci et al. 2016; Gano-Cohen et al. 2016; Regus et al. 2014; Sachs et al. 2010; Westhoek et al. 2017). Accordingly, researchers that study sanctions should not neglect the role mixed nodules could play in this complex symbiosis and its evolutionary trajectory. Early models of sanctions focused on a whole nodule mechanism, but if sanctions occur at a finer scale many of these models could be adapted to the plant cell level, or smaller (West et al. 2002a, 2002b). This study demonstrates the utility of combining single inoculation and co-inoculation experimental designs for future studies of host control as we continue to unravel this symbiosis and its stabilizing mechanisms.

Methods

Biological Materials

L. japonicus ecotype MG-20 seeds were acquired from LegumeBase (University of Miyazaki, Japan). MG-20 hosts were grown for one generation at the University of California, Riverside (UCR) to generate seeds for this experiment. Seeds were germinated on N-free Jensen's (Somasegaran and Hoben 1994) agar plates (1.5% w/v) prior to planting in one gallon pots filled with a plaster sand and peat moss mixture supplemented with nitrogen, phosphorus, potassium, calcium and trace minerals (UCR soil mix #3). Plants were grown under ambient light from July to October in an insect free greenhouse and watered with a 1:100 dilution of Peters Excel 21-5-20 (Scotts Professional, Marysville, Ohio, USA).

We used a MAFF strain with DsRed integrated into the genome (red fluorescent protein visible under natural light; M. Hayashi, personal communication), andtwo near-isogenic mutants STM30 and STM6, previously generated by signature tagged mutagenesis (Shimoda et al. 2008). We acquired the rhizobial strains from LegumeBase. Bacteria were grown in a liquid medium of Modified Arabinose Gluconate (MAG, 29˚C, 180rpm; Sachs et al. 2009).

In vitro MAFF growth assays

Flasks of MAG were inoculated with MAFF, STM30, or STM6 and grown to log-phase growth. Cell density readings were measured optically on a colorimeter and a subset of readings were confirmed via quantitative plating. Doubling time was calculated by

estimating cell density at sequential time points (Roth 2006) and the three fastest doubling times for each flask were averaged. An average doubling time was calculated for eleven independent flasks of each strain.

Growth Chamber Experiment

MG-20 seeds were sterilized in bleach (5.25% sodium hypochlorite) for five minutes, followed by seven one-minute rinses in sterile ddH_2O. Seeds were nick scarified with a sterile razor blade and immediately placed into sterilized CYG germination pouches (Mega International; Newport, MN, USA) filled with 13ml of sterile N-free Jensen's fertilizer. Bundles of four pouches containing five or ten seeds each were wrapped in aluminum foil and placed in clear plastic boxes (Sterilite 18058606; 13.1"x7.6"x4.5"). The inoculated pouches were maintained in a controlled growth facility (14h:10h day:night cycle; 17-27˚C; relative humidity 31%-65%) and plants were fertilized weekly with 10ml of N-free Jensen's per pouch for the duration of the experiment. When true leaves formed (ca. two weeks) seedlings were inoculated with 50ul of rhizobia, which had been washed, resuspended in 50ul of sterile ddH_2O at a density of 10^9 cells ml^{-1}, and dripped directly on to the roots. Rhizobial treatments included MAFF, STM30, and STM6. A negative control, using 50ul sterile ddH_2O was also included.

Plants were harvested at 3, 5, 6, 7, and 8wpi. Excess fertilizer was removed from pouches and photographs of each plant were taken for reference. Nodules were counted, dissected, and photographed. Shoots, roots, and nodules were separated and dried at 60˚C

≥3 days prior to weighing biomass. At 6 and 8wpi 15-21 nodules from each treatment group were randomly selected for quantitative culturing. Uninoculated controls were also harvested at this time.

Greenhouse Experiment

Seeds were sterilized and nicked as described above and germinated in sterile ddH_2O in the dark at 20˚C for ca. one week. Germinated seedlings were planted in sterilized Conetainers (SC10; Steuwe and Sons, Tangent, OR, USA) filled with autoclaved quartzite sand. The sand is inert and offers negligible nutrients for plant growth (Sachs, Ehinger, and Simms 2010). Seedlings were initially maintained in a controlled growth facility and watered three times a week until true leaves emerged (ca. two weeks). After true leaves formed, seedlings were fertilized weekly with 5ml of N-free Jensen's. One day after the second fertilization seedlings were moved to the greenhouse and arranged by size which was determined based on the number of leaves. After three days of acclimation, groups of eight size-matched plants were randomly assigned to one of the following inoculation treatments: sterile ddH_2O, MAFF, STM30, STM6, MAFF:STM30 (1:1), MAFF:STM6 (3:7), MAFF:STM30 (1:9) and, MAFF:STM6 (1:19). Treatments within a block were randomly assigned to a location in the greenhouse. For each treatment, either 5ml of sterile ddH_2O or 5ml of washed rhizobial cells (10^8 cells ml^{-1}) were inoculated directly into the sand. The realized ratios were empirically measured by serially diluting each inoculum treatment, spread plating (10^{-6} dilution), and CFUs. Plants were harvested at 4wpi and 7wpi. At harvest, shoots, roots, and nodules were dried at

60˚C, ≥3 days prior to weighing biomass. There were 24 blocks in total, 12 for each harvest, with four randomly picked for nodule culturing at each harvest. Four randomly selected plants per treatment per harvest were picked to measure proxies of rhizobial fitness. Four nodules from each selected plant were randomly selected for quantitative culturing.

Nodule Culturing

Nodules were individually surface sterilized in bleach for a minimum of 45 seconds (ca. one minute per mm of nodule diameter), rinsed three times in sterile ddH_20, and crushed with a sterile pestle in sterile ddH_20. The nodule slurry was serially diluted in sterile ddH_2O, spread plated on MAG (10^{-3}, 10^{-5} dilutions; 1.8% agar w/v) and incubated at 29 ˚C for 3 days. Colonies were counted to estimate rhizobial population sizes within a nodule. Nodules from co-inoculated plants were cultured as above and were used to estimate total rhizobial population size within a nodule and the proportion of MAFF by scoring colony color (i.e., red versus white colonies).

Data Analysis

Dry shoot biomass was used as a proxy for symbiotic effectiveness of each rhizobial strain given that the rhizobia provided the sole external source of nitrogen for growing plants in our experiments (Regus et al. 2014, 2015). We used mean individual nodule biomass as a proxy for host investment. Rhizobial population size within a nodule was used as a proxy for rhizobial fitness. Symbiotic effectiveness, host investment in symbionts, symbiont fitness, and number of nodules formed were compared among

treatments using analysis of variance (ANOVA) and post-hoc Student's t-tests (JMP Pro 12.0.1). At 8wpi in the growth chamber experiment two hosts singly inoculated with MAFF were removed from the analysis due to constrained growth within the pouches.

For each mixed strain treatment we quantified the proportion of cultured nodules occupied by MAFF at each harvest and used a binomial goodness of fit test of the realized inocula ratios against the observed proportions of nodules containing MAFF. Estimated fitness of each strain from nodules of mixed strain treatment hosts was measured and proportion of MAFF was calculated per individual host. Hosts from the same treatment were analyzed with a one-sample t-test using realized inocula ratios as the null expected proportions. To test for a correlation between symbiotic effectiveness and symbiont fitness we performed a linear regression (JMP Pro 12.0.1). To normalize estimates of rhizobial population size per nodule the natural log of population size was used.

Chapter 2

Over-investment by legumes triggers antagonistic fitness consequences by their symbionts

Abstract

Microbial mutualists provide substantial benefits to hosts which feeds back to enhance fitness of the associated microbes. But antagonism is predicted to emerge over the magnitude of individual resource expenditures by each species into the mutualism. We investigated the scope of antagonism in the association between *Lotus japonicus* and its root-nodulating symbiont, *Mesorhizobium loti*. We employed experimental inoculations with near isogenic host and symbiont variants and analyzed fitness effects on each partner over a range of host investment into symbiotic root nodules. *M. loti* fitness increased linearly as the host plant formed additional root nodules. Conversely, *L. japonicus* genotypes exhibited a unimodal fitness function for nodulation, revealing host-symbiont antagonism over a broad parameter space of host investment into nodules. Finally, fitness data from mixed-strain coinoculations revealed that host sanctions of non-beneficial *M. loti* genotypes occurs independently of host mechanisms that regulate nodulation.

Introduction

Microbial mutualists can dramatically improve the fitness of plants and animals. Associations with microbes can accelerate host growth (Sprent et al. 1987), enhance immune defense (Gerardo and Parker 2014; Pieterse et al. 2014), increase stress tolerance (Rubin, van Groenigen, and Hungate 2017; Schützendübel and Polle 2002), and improve host interactions with predators, pathogens, and competitors (Friesen et al. 2011). However, the net fitness rewards that define these microbial mutualisms can conceal underlying costs that each partner must pay to partake in specific interactions. For instance, the reduction of atmospheric nitrogen by rhizobial symbionts requires 16 ATP per dinitrogen molecule (Dixon and Kahn 2004), and the synthesis of essential amino acids by insect endosymbionts can cost up to 10 ATP (Douglas 2016). These energetic costs are ultimately subsidized by the hosts (Ankrah, Luan, and Douglas 2017; White et al. 2007), but the exchange of costly services makes each partner vulnerable to being exploited by the other. Microbial partners exhibit a substantial evolutionary advantage over hosts by having greater population sizes and faster reproduction rates. Thus, microbial mutants can rapidly evolve to downregulate or arrest services to hosts while gaining a fitness advantage over beneficial genotypes (Foster and Wenseleers 2006; Sachs et al. 2004). What prevents the invasion of such uncooperative mutants in mutualist populations remains a central question in evolutionary biology.

Two frameworks model the evolutionary maintenance of costly mutualistic traits in microbial populations, here termed the partner fidelity feedback (PFF) and host sanctions (HS) models. PFF predicts that microbial enhancement of host fitness can feed

back to proportionally improve the microbe's fitness, and vice versa (Axelrod and Hamilton 1981; Fine 1975; Sachs et al. 2004). Fitness feedbacks can arise because the partners are engaged in intimate or long term association, if partners exist in highly structured populations, or because partners have evolved mechanisms that automatically facilitate such feedbacks (Foster and Wenseleers 2006). Under PFF, feedbacks occur passively, without the need for partner recognition, and the fitness interests of both partners are correlated insofar as the fitness feedbacks are maintained. Conversely, HS models predict that microbial cooperation is maintained by host mechanisms of selective reward and/or punishment that impose selection against uncooperative partners (Denison 2000; West al. 2002a). Under HS models, the host must detect the level of cooperation from its microbial partner, and actively alter the fitness of the microbe accordingly (Denison 2000; Koch et al. 2014). Unlike PFF, the HS framework predicts that the fitness interests of partners are not correlated (Sachs et al. 2004).

The mutualism between legumes and rhizobia provides a powerful system to study the evolutionary maintenance of costly mutualistic traits and examine fitness interactions among partners (Kiers et al. 2003; Porter and Simms 2014; Sachs et al. 2010; Sachs, Quides, and Wendlandt 2018; Simms et al. 2006). Diverse legumes form symbiotic root nodules in which rhizobia fix nitrogen for the plant host in exchange for photosynthates. The interaction is initiated when the host roots attract rhizobia with flavonoids, followed by rhizobial secretion of Nod factors, that trigger morphological changes in the roots (Liu and Murray 2016). Within root cells, rhizobia are encased in organelle-like structures called symbiosomes where they begin fixing atmospheric

nitrogen. Each partner takes on substantial costs in the interaction that must be reciprocated by the other to generate a net benefit. For legumes, a predominant cost of interacting with rhizobia is attributed to the formation and maintenance of root nodules (Krusell et al. 2002; Nishimura et al. 2002). For rhizobia, a key cost is the fixation of atmospheric nitrogen for the host (White et al. 2007).

Both the PFF and HS models predict that rhizobia gain fitness rewards from hosts dependent on the magnitude of the benefit the rhizobia provides to the host plant. The models differ in whether fitness feedbacks are sufficient to align fitness interests between partners, and thus resolve conflict (Foster and Wenseleers 2006; Sachs et al. 2004). Two data sources can support a model of fitness feedbacks. First, evidence of plant-bacterial cycling of amino acids has been hypothesized to automatically link nitrogen fixation by rhizobia with the supply of resources provided in return by the host (Lodwig et al. 2003). But the molecular details of the coupled exchange of metabolites has been challenged (Prell et al. 2009). Second, a meta-analysis of fitness outcomes from diverse legume and rhizobia genotypes suggests that fitness interests of both partners are widely aligned (Regus et al. 2014). However, this dataset has been questioned due to potential artifacts of primarily analyzing clonal inoculation experiments (Friesen and Heath 2013; Kiers, Ratcliff, and Denison 2013). Contrary to automatic feedbacks, many researchers argue that the population biology of legume-rhizobia interactions is inconsistent with PFF. Multiple genotypes of rhizobia infect individual legume hosts and rhizobia are transmitted horizontally to unrelated hosts, both of which would make feedbacks difficult to maintain (Kiers et al. 2003, 2011; Oono, Anderson, and Denison 2011; Quides et al.

2017; Regus et al. 2014, 2017; Westhoek et al. 2017). Instead, HS by legumes is predicted to be necessary and sufficient to select for cooperation by rhizobia (Denison 2000; Kiers et al. 2003). For instance, by inoculating legumes with multiple rhizobia strains, experimenters have repeatedly demonstrated that nodules infected with non-fixing (or poorly-fixing rhizobia) are smaller and house fewer rhizobia compared to nodules infected with nitrogen fixing rhizobia (Kiers et al. 2003, 2011; Oono, Anderson, and Denison 2011; Quides et al. 2017; Regus et al. 2014, 2017; Simms et al. 2006; Westhoek et al. 2017).

Here, we investigated the scope of antagonism in the association between *Lotus japonicus* and its root-nodulating symbiont, *Mesorhizobium loti*. We used four *L. japonicus* genotypes that vary genetically in their regulation of nodule formation (i.e., investment into rhizobia). *L. japonicus* 'Miyakojima' MG-20 (MG-20) and *L. japonicus* Gifu B-129 (Gifu) are closely related ecotypes with natural variation in the number of nodules they form (Kawaguchi 2000). We also used two nearly-isogenic mutants of MG-20: *plenty*, a mutant with moderate hyper-nodulation (Yoshida, Funayama-Noguchi, and Kawaguchi 2010) and *har1*, which carries a knockout mutation for autoregulation of nodulation (AON) and exhibits extreme hyper-nodulation (Krusell et al. 2002; Nishimura et al. 2002). To examine fitness interactions in clonal host-symbiont associations, we singly inoculated each of the four hosts with the compatible nitrogen fixing strain *M. loti* MAFF303099 (MAFF) or a near isogenic mutant lacking in nitrogen fixation function (STM6; Quides et al. 2017). For host plants we measured fitness effects of nodulation using shoot mass, percent nitrogen content, and stable isotope analysis of nitrogen

fixation ($\delta^{15}N$). For rhizobia, we measured fitness effects of nodulation by estimating *in planta* rhizobial population size (via quantitative culturing) and by examining histological features of *in planta* rhizobia in nodules. In a parallel experiment, we coinoculated each of the host genotypes with equal ratios of MAFF and STM6 to test for interactions between control over number of nodules formed and host sanctions. The goals of our study were to i) investigate variation in host fitness dependent on the magnitude of investment into nodules, ii) quantify *in planta* variation in symbiont fitness dependent on the number of nodules formed, iii) integrate plant and bacterial fitness datasets to resolve whether hosts and symbionts experience antagonism over nodulation

Methods

Biological Materials

L. japonicus ecotypes MG-20 and Gifu seeds were acquired from LegumeBase (University of Miyazaki, Japan). Previous work found that MG-20 forms slightly fewer nodules compared to Gifu (Kawaguchi 2000). Additionally, the nearly isogenic MG-20 mutants, *plenty* and *har1*, were acquired from Masayoshi Kawaguchi (National Institute for Basic Biology, Okazaki, Aichi, Japan). The *plenty* mutant forms approximately twice as many nodules as the wildtype (Yoshida, Funayama-Noguchi, and Kawaguchi 2010) and *har1* forms six times as many nodules as the MG-20 wildtype (Yoshida, Funayama-Noguchi, and Kawaguchi 2010). The *PLENTY* gene is on chromosome 2 and grafting experiments demonstrated that it controls nodulation from root tissue (Yoshida, Funayama-Noguchi, and Kawaguchi 2010). The *HAR1* gene is on chromosome 3 and is

part of the AON pathway, a root-shoot-root positive feedback system that controls nodulation dependent on the plant's nitrate demand (Krusell et al. 2002; Nishimura et al. 2002).

All *L. japonicus* lines were grown to generate seeds at the University of California, Riverside (UCR) following published protocols (Quides et al. 2017). Briefly, seeds were surface sterilized in bleach (5.25% sodium hypochlorite, 5 minutes) and rinsed seven times (one minute each) in sterile reverse osmosis purified water (ROH_2O). Surface-sterilized seeds were then nick scarified with a razor blade and germinated on N-free Jensens plates (1.5% agar w/v; Somasegaran and Hoben 1994). Seedlings were planted in one gallon pots filled with UCR soil mix #3 (plaster sand and peat moss supplemented with nitrogen, phosphorus, potassium, calcium and trace minerals). Plants were maintained in a greenhouse under natural lighting from July to October and watered as needed with a 1:100 dilution of Peters Excel® 21-5-20 (Scotts Professional, Marysville, Ohio, USA). To assure that no cross-pollination occurred, the greenhouse was fumigated weekly with the insecticide Talstar® (7.9% Bifenthrin, FMC Corporation, Philadelphia, Pennsylvania, USA).

We used MAFF303099 (MAFF) expressing DsRed integrated into the genome (a red fluorescent protein visible under natural light; Maekawa et al. 2009), and a near-isogenic non-nitrogen fixing mutant with a transposon inserted in the *NifD* gene, mlr5906 (strain ID 17T02d02; STM6). STM6 is easily distinguished from MAFF on plates by colony color (Quides et al. 2017). Bacteria were grown on a solid medium of Modified Arabinose Gluconate (MAG, 1.8% agar w/v, 29° C; Sachs et al. 2009) and have

previously been shown to have no differences in *in vitro* growth rate on MAG (Quides et al. 2017).

Inoculation experiments

Seeds were germinated in sterile ROH_2O in the dark at 20˚C from 20th March 2017 to 3rd April 2017. Seedlings were planted in sterilized Conetainers (SC10; Steuwe and Sons, Tangent, OR, USA) filled with sterilized, calcined clay that is inert and offers negligible nutrients (Turface® Pro League®, Turface Athletics, Buffalo Grove, Illinois, USA). Seedlings were grown in a controlled growth facility with daily mist-watering until true leaves emerged. After true leaves formed, seedlings were fertilized weekly with 5mL of N-free Jensens for the duration of the experiment. After two weeks in the controlled growth facility, seedlings were transferred to the greenhouse to harden behind 50% shade cloth on 24th April 2017.

In the greenhouse, plants were arranged into size-matched groups of 16 (four per genotype, by leaf count) and were inoculated with one of four treatments: MAFF, STM6, MAFF:STM6 (coinoculated; 1:1 ratio), or sterile ROH_2O (negative control). Shade cloth was removed and inoculation occurred on 27th April 2017. For each treatment, either 5mL of water or 5mL of washed rhizobial cells were drip inoculated directly into the Turface® at a density of 10^8 cells mL^{-1} ($5x10^8$ cells). Inoculum concentrations and ratios were empirically confirmed by serial dilutions, spread plating (10^{-6} dilution), and counting colonies.

Plants were harvested at 3.5 weeks and 5 weeks post inoculation (wpi), time spans when nodule formation is mostly complete, and when plant growth from nitrogen fixation is near optimum, respectively (Quides et al. 2017). At harvest, the shoots and roots were separated and photographed, and nodules were dissected from roots, counted, and photographed. Plant shoots, roots, and nodules were dried separately at 60˚C ≥3 days prior to weighing dry biomass.

The experimental plants were organized into a full factorial randomized block design with a total of 20 replicates for each host by inoculum combination with one replicate per block. There were 20 blocks, 10 for each harvest, with three randomly picked for nodule culturing at each harvest and one picked for light microscopy (at 5wpi). During an early spring heatwave, 10 plants died within a few days after inoculation (28th April 2017 – 4th May 2017; Appendix 2.2).

In vitro estimation of rhizobial fitness

The fitness of rhizobia in nodules was estimated by quantitative culturing. Three nodules from singly inoculated hosts and five nodules from coinoculated hosts were randomly selected from each of three plants for culturing. Nodules were individually surface sterilized in bleach for a minimum of 30 seconds (ca. one minute per mm of nodule diameter), rinsed three times in sterile ROH_20, and macerated to a slurry with a sterile pestle in sterile ROH_20. The nodule slurry was serially diluted in sterile ROH_2O, spread plated on MAG (10^{-3}, 10^{-5} dilutions) and incubated at 29˚C for three days. Colonies were counted to estimate rhizobial population sizes within a nodule. Nodules from

coinoculated plants were cultured as above and were used to estimate total rhizobial population size of both symbionts within a nodule (i.e., MAFF formed red colonies).

Light Microscopy

Nodules were randomly selected for light microscopy from all four host genotypes inoculated with MAFF at 5wpi. Nodules were fixed in 4% v/v paraformaldehyde, 2.5% v/v glutaraldehyde in 50mM phosphate buffer pH 7.2 for 6-10hrs at 20° C, then 4° C for three days, and dehydrated in a graded alcohol series to 100% EtOH at 20° C. The nodules were infiltrated with JB-4 Plus methacrylate (Poly-sciences, Warrington, Pennsylvania, USA) in catalyzed Solution A and 100% EtOH (1:1 ratio) at 20° C for 6hrs followed by a 3:2 ratio at 4° C overnight. Infiltration with 100% catalyzed Solution A was performed at 20° C for 6hrs and refreshed for final infiltration at 4° C overnight. Finally, nodules were embedded in film caps with polymerized JB-4 plus methacrylate and sealed with Parafilm. All steps at 20° C were done with gentle agitation (John U. Regus et al. 2017)

Individual nodules were removed with a coping saw and polymerized with JB-4 plus methacrylate on metal stubs for sectioning. Sections of 2-4µm thickness were prepared parallel to the long axis of the parent root using a glass knife and H/I Bright 5030 Microtome (Hacker Instruments Inc.; Fairfield, New Jersey, USA), mounted on glass slides, and stained with 0.1% w/v aqueous toluidine Blue O to identify plant cells that are infected with rhizobia. Sections were viewed with a Meiji Techo MT4000L Biological Microscope (Meiji Techo CO., LTD.; Miyoshi machi, Iruma-gun, Japan) and

images were acquired with a Nikon D80 DSLR (Nikon Corporations; Minato, Tokyo, Japan) attached to the trinocular tube using Meiji specific adapters and ControlMyNikon tethering software (Tetherscript Technology Corporation; Vancouver, British Colombia, Canada).

An average of 11 sections per nodule were analyzed (range 7-17) from each of 3-4 nodules per host. Mean infected cell size was estimated by measuring the total area of all infected plant cells in a nodule section (via observation of toluidine stained nodule cells) divided by the number of infected cells counted. Mean uninfected cortex cell size was estimate using a subset of cortex cells since it is difficult to preserved the entire cortex (mean = ca. 53; range = 8-110; lack of toluidine staining). The cortex was defined as the plant cells one cell layer away from the central infection region. Vascular bundles were not measured (Regus et al. 2017). For both cell size measures, means were calculated per nodule.

Leaf Tissue Analysis

We compared %N and $\delta^{15}N$ for all host by inoculum treatment combinations at 5wpi. When plants incorporate symbiotic nitrogen fixed by rhizobia, the leaf tissue exhibited $\delta^{15}N$ relative to uninfected plants because of isotopic fractionation by rhizobia (Regus et al. 2014). Dry leaves were removed from stems and powdered using a bead beater for 10 seconds at $4ms^{-1}$ with a 5mm steel bead. Samples were analyzed at UC Santa Cruz Stable Isotope Laboratory. In many cases one plant did not provide enough leaf tissue for

analysis, thus we pooled leaf tissue from up to four plants in a treatment. Due to pooling each treatment has 2-8 replicates.

Data Analysis

To quantify host investment into rhizobia we counted the number of nodules formed, and calculated the ratio of dry nodule biomass to shoot biomass (relative nodule mass). Relative nodule mass minimizes the confounding effects of correlations between total plant biomass and nodule biomass. We tested for main effects (fixed; host genotype, inoculum) and the interaction effect using a Standard Least Squares Fit Model (JMP Pro 13) with block as a random effect. For significant fixed effects in our model we performed a post-hoc LSMeans Tukey HSD test for pairwise comparisons. To investigate host investment into rhizobia at the cellular level, we measured the sizes of infected and uninfected cells within nodules. We compared mean measures of infected cells and uninfected cortex cells using a one-way analysis of variance (ANOVA) with a post-hoc Tukey-HSD test for pairwise comparisons (JMP Pro 13).

We calculated host growth benefits from nodulation as the difference in dry shoot biomass between inoculated hosts and uninoculated controls ($Host^{inoculum}(g) - Host^{control}(g)$), as well as leaf tissue %N content and $\delta^{15}N$. To test for main effects of host genotype and inoculum (fixed effects) and an interaction effect we used a Standard Least Squares Fit Model (JMP Pro 13) with block as a random effect (not applicable for %N or $\delta^{15}N$ due to pooling). We used a post-hoc LSMeans Tukey HSD test for significant fixed effects to look for significant pairwise comparisons (JMP Pro 13).

To quantify rhizobial fitness, we estimated the total population size of rhizobia per plant. We multiplied average rhizobial population per nodule from an individual plant by the number of nodules on that plant. Total rhizobial population per plant was Log_{10} transformed to improve normality and analyzed with a Standard Least Squares Fit Model to test for main effects of host genotype and inoculum (fixed effects) and an interaction effect. Post-hoc comparisons were done with an LSMeans Tukey HSD test for the host (multiple pairwise comparisons) and a Student's t-test for the symbiont (one comparison). To analyze symbiont fitness in coinoculated hosts we used a one-way t-test to compare our mean observed proportion of MAFF (N-fixing genotype) per plant to an expected proportion 0.5 (i.e., inoculated at equal ratios).

We combined analyses of host and symbiont fitness functions to test the alternative hypotheses of fitness alignment versus antagonism over nodulation. We used dry shoot biomass as a proxy of host fitness, rhizobial cells per plant for symbiont fitness (dependent variables), and the number of nodules formed was used as the independent variable (Table 2.1). For each host and symbiont inoculum combination and for each harvest we independently fit each basic fitness function to our measure of host or symbiont fitness using Nonlinear Specialized Modeling (JMP Pro 13). Up to 10^7 iterations were used to converge on parameter values of our functions that best fit our data set. Y-intercepts were set to the mean host or symbiont fitness values of the given uninoculated treatment (i.e., without nodules). Functions that we selected among included a linear function (i.e., assumes a fixed return with no costs), as well as square root, Log_{10}, and negative exponential functions, each of which assumes a fixed cost with diminishing

returns. We assessed goodness of fit by calculating the corrected Akaike information criterion (AICc) for each function of each data set:

$$\text{AICc} = 2k + n * \log_{10}(MSE) + \frac{2k^2+2k}{n-k-1},$$

where *k* is the number of parameters in a given function, n is the number of data points, and MSE is the mean squared error calculated for the best fit function of each data set.

Table 2.1 List of functions used for AICc comparisons.

Function name	Equation
linear	$k1 * x$
square root	$(k1 * \sqrt{x}) - (k2 * x)$
Log_{10}	$k1 * \log_{10}(x + 1) - (k2 * x)$
Negative exponential	$\left(k1 * (1 - e^{-k2*x})\right) - (k3 * x)$

x = number of nodules
ki = parameter

Results

Genotypic variation in nodulation

The *har1* hosts formed the greatest number of nodules per plant, followed by *plenty*, Gifu, and MG-20 at 5wpi (Figure 2.1A). We found a significant effect of host genotype on the number of nodules formed at 5wpi ($F_{3,\ 97.73}$ = 57.683; $P < 0.0001$). While we uncovered a significant effect of inoculum ($F_{2,93.7}$ = 3.4383, P = 0.0362), we were unable to detect any significant pairwise comparisons among symbiont genotypes. We did not find an interaction effects between host and inoculum ($F_{6,93.67}$ = 1.4737, P = 0.1956). The *har1* hosts also formed the greatest relative nodule mass at 5wpi followed by *plenty*, Gifu, and MG-20 (Figure 2.1B). We found a significant effect of host genotype on relative nodule mass at 5wpi ($F_{3,\ 78.82}$ = 32.540; $P < 0.0001$), but we did not find an effect

of inoculum ($F_{2,78.78}$ = 2.0794, P = 0.1318), or an interaction effect between host and inoculum ($F_{6,78.6}$ = 2.0745, P = 0.0656). Nodulation patterns were similar in the 3.5wpi harvest (Appendix 2.1).

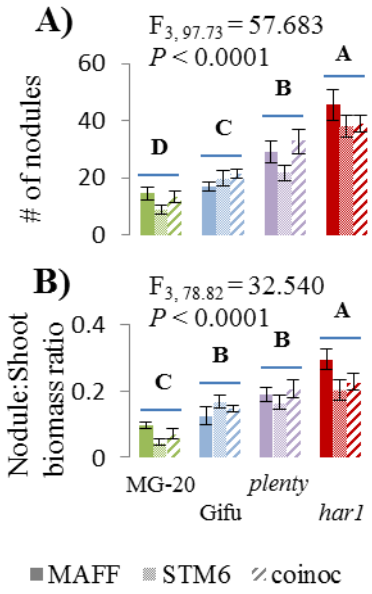

Figure 2.1 *L. japonicus* nodulation varied significantly among host genotypes
Nodulation patterns were assessed at 5wpi for all host and symbiont genotype combinations. The mean number of nodules per plant **(A)**, and the mean nodule to shoot biomass ratio **(B)** varied significantly among host genotypes. Error bars represent one standard error from the mean. F ratios and *P-values* are provided for host comparisons. A connecting letter report indicates significant differences among hosts (Standard Least Squares Fit Model, post-hoc LSMeans Tukey HSD test, α = 0.05). Hosts receiving MAFF, STM6, or a mixed-strain coinoculum are represented by solid bars, dotted bars, or striped bars, respectively. Green bars = MG-20 host, blue = Gifu, purple = *plenty*, and red = *har1*. Pairwise comparisons among symbiont genotypes were not statistically significant.

Genotypic variation in fitness of rhizobia

For rhizobial population size per plant, we found a significant effect of host genotype ($F_{3,16}$ = 6.580, P = 0.0042) and inoculum ($F_{1,16}$ = 9.1970, P = 0.0052; post-hoc Student's t-test, t = 2.11991, df = 1, P = 0.0079), but no interaction effect ($F_{3,16}$ = 1.2241, P = 0.3333). The hosts *har1* and *plenty* housed the greatest rhizobia population size per plant at 5wpi, followed by MG-20 and Gifu (Figure 2.2A). For all host genotypes, the fitness within nodules of coinoculated plants appeared higher for MAFF at 5wpi, but this difference was only significant with *plenty* (Table 2.2). Mean size of infected and uninfected cells in nodules varied significantly among host genotypes (infected: $F_{3,10}$ = 9.562, P = 0.0028; uninfected: $F_{3,10}$ = 7.556, P = 0.0063). MG-20 nodule cells were the largest, followed by Gifu, *plenty*, and *har1* when these hosts were infected with MAFF. This pattern was consistent in both infected cells (Figure 2.2B) and cortex cells (Figure 2.2C).

Table 2.2 Proportional *in planta* fitness of the beneficial symbiont MAFF at 5wpi

Host Genotype	Proportion MAFF	Fraction of coinfected nodules
MG-20	0.736‡	5/13
Gifu	0.594	3/13
plenty	0.689*	3/12
har1	0.895‡	3/14

one-way t-test of the proportion of MAFF compared to the expected proportion of 0.5 based on coinoculation ratio

‡ $P < 0.1$

* $P < 0.05$

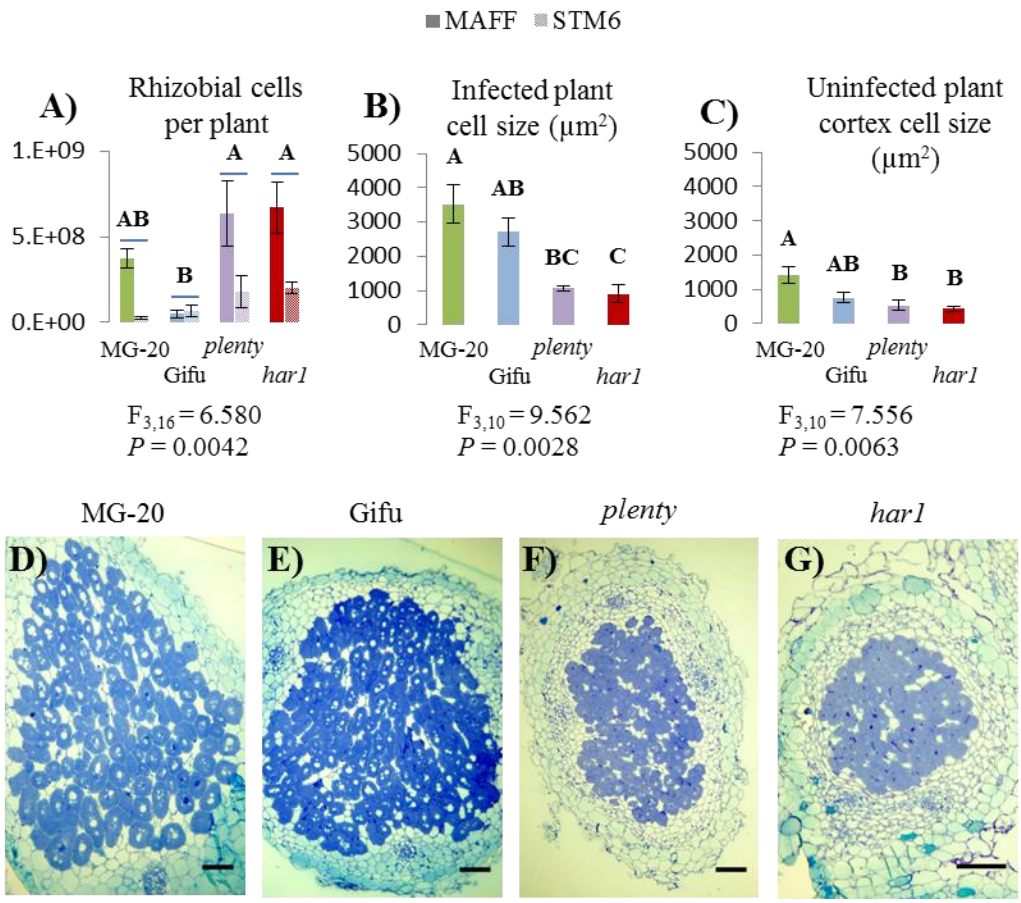

Figure 2.2 Rhizobia fitness varied significantly among host genotypes

Rhizobial fitness was estimated at the plant level and nodule level using culturing data and histology data, respectively. Genotypic variation in *in planta* rhizobial fitness was analyzed using rhizobial population size per plant when MAFF and STM6 symbiont genotypes were singly inoculated **(A)**, and histological features to assess per nodule fitness of MAFF **(B,C)** at 5wpi. Errors bars represent one standard error from the mean **(A-C)**. F ratios and *P-values* are provided for host comparisons. A connecting letter report indicates significant differences among hosts (Standard Least Squares Fit Model, post-hoc LSMeans Tukey HSD Test, A; one-way ANOVA, post-host Tukey HSD test, B-C; $\alpha = 0.05$). Hosts receiving MAFF or STM6 are represented by solid bars or dotted bars, respectively. Green bars = MG-20 host, blue = Gifu, purple = *plenty*, and red = *har1*. Representative light micrographs of nodules formed by each host genotype infected with MAFF are shown (scale bars = 100µm; **D-G**). Infected cells are darkly stained with 0.1% Toluidine Blue O **(B)** whereas uninfected cells remain clear **(C)**. Images **(E-F)** were adjusted to enhance contrast and sharpness for visualization after measurements were taken.

Host benefits from symbiosis

For host growth benefits from nodulation ($Host^{inoculum}(g) - Host^{control}(g)$) we found a significant effect of host genotype ($F_{3,95.12} = 13.566$, $P < 0.0001$; Figure 2.3A), inoculum ($F_{2,95.03} = 35.9451$, $P < 0.0001$), and the interaction effect ($F_{6,94.97} = 2.356$, $P = 0.0364$). The host genotypes that formed more nodules consistently received lower growth benefits from nodulation. For leaf %N, we also found a significant effect of host genotype ($F_{3,49} = 15.006$, $P < 0.0001$), inoculum ($F_{2,49} = 194.955$, $P < 0.0001$), and an interaction effect ($F_{6,49} = 2.733$, $P = 0.0227$). The host with the greatest %N in leaf tissue was *plenty*, followed by Gifu, MG-20, and *har1* (Figure 2.3B). The low shoot growth but high leaf %N for *plenty* hosts suggests that this host line might gain higher gross benefits from nodulation, but that these benefits are outweighed by the large costs to nodule maintenance. For isotopic $\delta^{15}N$ data we also found significant effects for hosts ($F_{3,49} = 24.1427$, $P < 0.0001$), inoculum ($F_{2,49} = 19.6125$, $P < 0.0001$), and the interaction effect ($F_{6,49} = 3.0350$, $P = 0.0133$). $\delta^{15}N$ data indicates that Gifu received the least amount of symbiotic nitrogen with no significant differences for the other three host genotypes (Figure 2.3C). Uninoculated controls were not statistically distinguishable from STM6 and were not included in the %N or $\delta^{15}N$ analyses (for raw data see table S4).

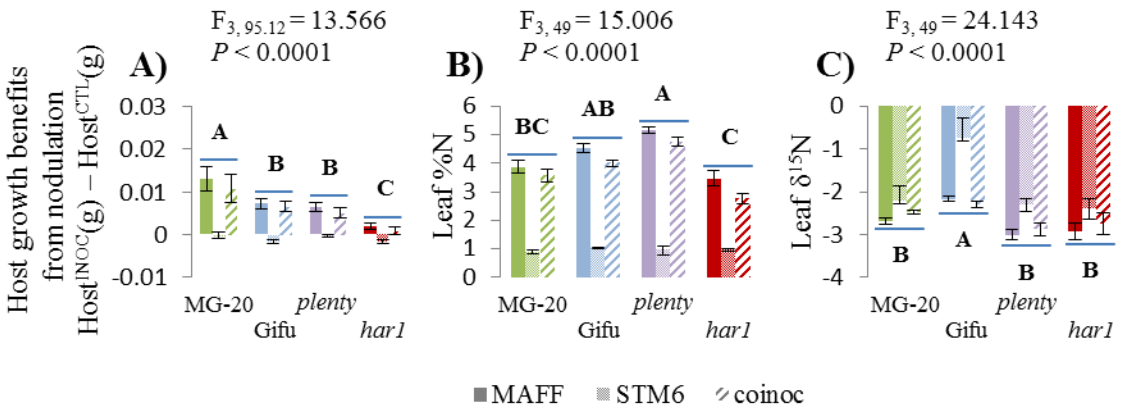

Figure 2.3 Host benefits from nodulation varied significantly among host genotypes
Host growth benefits from nodulation was compared among host genotypes ($Host^{inoculum}(g) - Host^{control}(g)$) **(A)**, as well as leaf %N **(B)** and $\delta^{15}N$ **(C)** for all rhizobial inoculum at 5wpi. Error bars represent one standard error from the mean. F ratios and *P-values* are provided for host comparisons. A connecting letter report indicates significant differences among hosts (Standard Least Squares Fit Model, post-hoc LSMeans Tukey HSD Test, A; $\alpha = 0.05$). Hosts receiving MAFF, STM6, or a mixed-strain coinoculum are represented by solid bars, dotted bars, or striped bars, respectively. Green bars = MG-20 host, blue = Gifu, purple = *plenty*, and red = *har1*.

Host and symbiont fitness functions

AICc values indicated that the Log_{10} and square root unimodal functions for host growth dependent on nodulation were the best fit for the host fitness data set (square root visually depicted; Figure 2.4A,B). For the rhizobial fitness data set AICc values estimated the linear function as the best fit (Figure 2.4A,C). We also calculated AICc values of our four functions for host and symbiont fitness at 3.5wpi for all inocula as well as the remaining two inocula at 5wpi (Appendix 2.6, 2.7).

A)

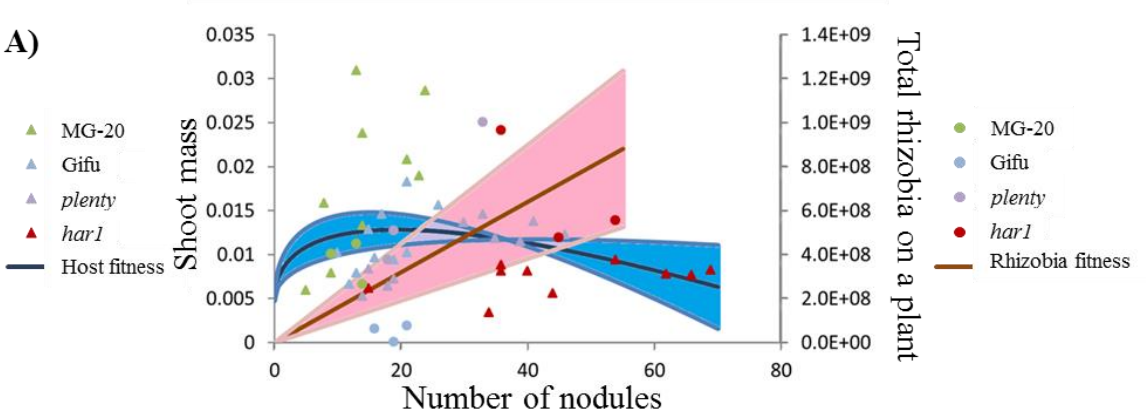

B)

Shoot mass of all four hosts inoculated with the Fix+ symbiont at 5wpi
y-intercept = 0.0047769

Function name	f(x); x = # of nodules	n	MSE	AICc
Linear	0.0001692598 * x	39	5.94E-05	-162.727
Square root	0.0036598490 * $\sqrt{x}$ - 0.0004152124 * x	39	3.65E-05	-168.749
$\log_{10}$	$\log_{10}(x+1)$ * (0.0094199389) - (0.0002207508 * x)	39	3.65E-05	-168.740
Negative exponential	0.0140423277 * (1 - $e^{(-0.0976359555 * x)}$) - (0.0001812257 * x)	39	3.69E-05	-166.237

C)

Total rhizobial cells on a plant for all four hosts inoculated with the Fix+ symbiont at 5wpi
y-intercept = 0.000

Function name	f(x); x = # of nodules	n	MSE	AICc
Linear	16017437.465 * x	12	8.22E+16	205.311
Square root	64367483.650 * $\sqrt{x}$ - (-4972124.511 * x)	12	8.34E+16	208.147
Log_{10}	$\log_{10}(x+1)$ * (159746129.838) - (-8689136.900 * x)	12	8.37E+16	208.166
Negative exponential	153357489.262 * (1 - $e^{(-8620023.755 * x)}$) - (-11230556.298 * x)	12	8.40E+16	211.490

Figure 2.4 Host and symbiont fitness functions

Hosts exhibited a unimodal fitness function for nodulation, while symbionts had a linear fitness function. Best fit functions for host shoot mass **(A)** and symbiont population size on a plant **(B)** are provided with AICc values. Functions with the lowest AICc values are then graphed along with data points used to generate these functions **(C)**. Host shoot mass (g) was used as a proxy for host fitness of the left y-axis (triangle data points) and the best fit function is represented with the blue curve. Estimated rhizobial population size per plant was used to quantify symbiont fitness on the right y-axis (circle data points) and the best fit function is represented by the red line. Green data points = MG-20 host, blue = Gifu, purple = *plenty*, and red = *har1*. Shading around the function lines represent one standard error from the mean for the parameter(s) calculated for each function.

Discussion

The evolutionary stability of microbial mutualisms depends in large part on the magnitude of costs of services exchanged between microbes and hosts (Foster and Wenseleers 2006; Sachs et al. 2004). At the extreme of little or no costs, microbial byproducts can be beneficial to plant or animal growth and/or defense (Sachs, Skophammer, and Regus 2011). When microbial services are byproducts there is little opportunity for fitness conflict to arise between the partners since the microbial services are produced automatically, occur independent of host action, and bear negligible costs to express (Foster and Wenseleers 2006; Sachs et al. 2004). However, many microbial mutualisms involve the exchange of costly services between partners. The existence of costly services can promote fitness conflict as each partner is selected to minimize costs and maximize gains. When costly services are exchanged in a mutualism, partner fidelity feedback (PFF) and/or host sanctions (HS) are needed to constrain conflict. A challenging aspect of PFF is that some degree of fitness feedback is a near universal feature of microbial mutualisms. Microbial colonization can alter a host's fitness in a positive or negative way which creates an opportunity for the fitness effects on the host to feedback on the microbe's fitness. For instance, fitness feedbacks play a critical role in selecting against the most virulent genotypes of pathogens (Bull 1994) just as PFF can favor more cooperative microbial genotypes of mutualists (Kaltenpoth et al. 2014; Mueller 2002; Sachs and Wilcox 2006). While PFF can be difficult to quantify, models predict that the fitness feedbacks between partners must be strong and consistent for PFF alone to stabilize a microbial mutualism, such as when mutualists are vertically

transmitted (Foster and Wenseleers 2006). Our current understanding of the routes of microbial transmission suggests that most microbial mutualisms lack the repeated or long-term interactions required for PFF, suggesting that other stabilizing mechanisms must be in place (Sachs, Skophammer, and Regus 2011).

Host legumes have evolved multiple, independent mechanisms that constrain investment into nodules (Sachs, Quides, and Wendlandt 2018). The initiation of nodule development is a complex, multistep process controlled by dozens of plant genes that minimize non-specific infection (i.e., rhizobia specificity; Liu and Murray 2016). After nodule formation, legumes can drastically reduce investment into nodules that house non-beneficial symbionts and redirect host resources towards beneficial symbionts (i.e., HS; Kiers et al. 2003, 2011; Oono, Anderson, and Denison 2011; Quides et al. 2017; Regus et al. 2014, 2017; Simms et al. 2006; Westhoek et al. 2017). Finally, even when symbionts are both compatible and beneficial, legumes must autoregulate continued nodulation dependent on the plant's nitrogen demand to stop nodulation when the costs outweigh the benefits (i.e., AON; Reid et al. 2011). Host genes related to the AON pathway suggest at least two independent mechanisms by which legumes can regulate nodule number (Yoshida, Funayama-Noguchi, and Kawaguchi 2010).

Conversely, rhizobia have evolved multiple mechanisms to gain access to host root cells (Masson-Boivin and Sachs 2018), in some cases by subverting host control over nodulation. In one extreme example, two genotypes of rhizobia (*Ensifer fredii*: NGR234, USDA257) can produce a cocktail of Nod factors that allow them to nodulate scores of host species while providing negligible benefit to the majority of the infected

hosts (Pueppke and Broughton 1999). Similarly, a genotype of *E. meliloti* bears a plasmid that makes it hypercompetitive for nodulation on some genotypes of *Medicago truncatula*, but provides minimal benefit to the host (Crook et al. 2012). For this strain, the presence of a 'host range' plasmid is key to controlling nodulation; the plasmid encodes a protein that appears to interfere with host-symbiont communication by potentially manipulating type III effector proteins or exopolysaccharides (Crook et al. 2012). Lastly, *Bradyrhizobium elkanii* USDA61 nodulates its soybean host and provides little benefit when it has a defective type III secretion system (T3SS; Yasuda et al. 2016). However if the T3SS is not defective, soybeans with the *Rj4* allele can terminate nodulation by USDA61 (Yasuda et al. 2016). Interestingly, this soybean defense mechanism has been found to be susceptible to seven other USDA61 knockout mutants suggesting the potential for an on-going arms race between partners (Faruque et al. 2015). At a more general level, rapid evolution of symbiosis loci, such as can be observed in the genome of *M. truncatula* (Yoder 2016), is consistent with an ongoing arms-race between this host and its rhizobial symbionts (Yoder and Tiffin 2017).

The various mechanisms that hosts have to restrict nodulation, and the multiple pathways that rhizobia have to subvert host control, suggest that legumes and rhizobia have conflicting selection regimes for the number of nodules formed. Moreover, the results presented here go further by estimating the fitness functions for both legume and rhizobium partners dependent on nodulation. Our results suggest that MAFF experiences directional selection to increase nodule number, but *L. japonicus* experiences stabilizing selection around an optimal number of nodules. The shape of the fitness functions further

suggests that the *Lotus*-MAFF mutualism may be on a knife's edge of stability as optimal host nodulation occurs right on the edge of the zone of conflict (Figure 2.4; Sachs, Quides, and Wendlandt 2018). While wildtype hosts express phenotypes that are near their physiological optimum for net benefits from nodulation, natural selection could favor rhizobia mutants that increase nodulation rates and would push the host over the edge. A unimodal fitness function suggesting mutualistic instability is not limited to host legumes interacting with rhizobia. The host dynamics of this model have been suggested as a general feature of many mutualisms (Bronstein 1998; Fonseca 1993; Holland, DeAngelis, and Bronstein 2002).

A convenient aspect of the legume-rhizobium symbiosis is the joint phenotype of nodule number. Adapting this approach to other symbioses could be a matter of quantifying investment into symbionts while integrating measures of symbiont fitness. For instance, our measure of investment is the generation of new biomass to house rhizobia (nodule formation) which can subsequently be used to compare host and symbiont fitness benefits from host investment. A similar approach could be applied to hosts such as the Bobtail squid, *Euprymna scolopes* (McFall-Ngai 2014) or beewolf wasps (Kaltenpoth et al. 2014) as they both allocate tissue space to symbionts in a measurable way. Alternatively, if metabolic investment (by the host) can be reliably measured, it could be possible to measure 'return on investment' (host metabolite benefits), and 'profitability' (symbiont metabolite benefits) by directly measuring ATP production and consumption (Dixon and Kahn 2004; Douglas 2016) or tracing shared isotopes (Pringle 2016).

We uncovered fitness conflict between legumes and rhizobia over host investment into nodules. But the parameter space over which we found conflict might not commonly persist in nature given the fitness costs to the host. Moreover, our model also suggests that fitness would be aligned when hosts underinvest in symbiosis. The data presented here and the corresponding models highlight the infrequent, and sometimes hidden, conflict in symbioses that are mutualistic. Interactions that are not overwhelmingly antagonistic, or that are only antagonistic in some environments, can make antagonism difficult to detect. But a firm understanding of the transmission mode and phenology of an interaction can lead to novel approaches to study the coevolution of a symbiosis (McFall-Ngai 2014; Mueller 2002; Sachs, Quides, and Wendlandt 2018). Just as host-symbiont antagonism appears to be a largely hidden aspect of interactions between legumes and rhizobia, evidence of fitness conflict between male and female *Drosophila melanogaster* heavily influenced how we now think about coevolution (Rice 1996). In a parallel way, our data highlights the evolution of symbiont traits in legumes and rhizobia and the often overlooked conflict in mutualistic interactions.

Chapter 3

Exposure to static host genotypes leads to rapid shifts in symbiotic rhizobia phenotypes

Abstract

A major question in plant biology and agronomy is to understand the degree to which plants can reshape their microbiome to improve host fitness. Legumes have multiple traits to optimize their interactions with root nodulating rhizobia, but the effects of these traits on rhizobial evolution remain poorly understood. Host legumes can limit infection by rhizobia that provide low levels of benefit, and bias *in planta* fitness if rhizobia provide low levels of benefit. Host legumes also can control the number of nodules they form dependent on nitrogen demand, as forming excessive nodules can have negative fitness consequences for a legume. In this study we mimic agricultural conditions whereby symbionts repeatedly interact with the same plant genotype and evolve while the plant host does not. We experimentally evolved two mediocre rhizobial symbionts through a series of *in vitro*-*in planta* passages on two host genotypes of *Lotus japonicus* that vary in symbiont investment. *Rhizobium etli* CE3 forms nodules on *L. japonicus* that prematurely senesce, and *Ensifer fredii* NGR234 forms nodules that mature slowly. After a series of symbiont passaging, we tested symbiont phenotypes for evidence of enhanced mutualistic, antagonistic, or free-living evolution. Additionally, we resequenced the genomes of the symbionts to link phenotypes to genotypes. We uncovered positive and negative shifts in host and symbiont fitness, but our data suggest this occurred independent of nitrogen fixation. Our most consistent phenotypic data suggest evolution

of antagonism, and the corresponding genomic data suggest communication via polysaccharides might play a role in this phenotypic evolution.

Introduction

Plants interact with diverse soil microbes that can enhance the host plant's health and fitness (Bakker et al. 2012; Busby et al. 2017; Kroll, Agler, and Kemen 2017; Friesen et al. 2011). The benefits provided by a plant's microbiome can include increased growth rate and seed production (Sprent et al. 1987), protection against drought (Rubin, van Groenigen, and Hungate 2017) and other stressors (Schützendübel and Polle 2002), as well as host immune system priming to more efficiently defend against pathogens (Pieterse et al. 2014), but these benefits are not guaranteed or fixed. Fitness outcomes for a plant can range from mutualistic (i.e., net fitness benefits from microbes) to antagonistic (i.e., net fitness cost) depending upon the host and microbe genotypes as well as environmental parameters that influence the interactions (Bronstein 1994, 2001; Neuhauser and Fargione 2004; Thompson 1988). To deal with this variation, plants hosts have also evolved "host control traits" that selectively acquire and provision cooperative microbial genotypes while limiting interactions with harmful strains (Denison 2000; Kiers et al. 2003; Sachs et al. 2010).

An emerging set of methods, described as microbiome engineering seek to leverage host control by plants to artificially select for soil microbial communities that promote desirable effects on hosts (Bakker et al. 2012; Busby et al. 2017; Foo et al. 2017; U.G. Mueller and Sachs 2015). In a typical protocol axenic plants are exposed to diverse microbial soil communities which are then artificially selected on the basis of desired plant traits, such as rapid growth, early flowering, drought tolerance, or disease resistance (Swenson, Wilson, and Elias 2000; Mendes et al. 2011; Lau and Lennon 2011, 2012;

Panke-Buisse et al. 2015). The soil that yields plants with desired traits is passaged onto a new generation of axenic plants, thus imposing a degree of artificial selection on the soil microbial community based on the effect it has on the plant hosts. Other sources of variance can be limited through the use of clonal or inbred plants as well as controlled environmental conditions (U.G. Mueller and Sachs 2015; Swenson, Wilson, and Elias 2000; Williams and Lenton 2007). Microbiome engineering is hypothesized to alter soil microbial communities via ecological processes and evolutionary processes (U.G. Mueller and Sachs 2015). Plants release metabolites that attract beneficial microbes (Chaparro et al. 2012), or that inhibit antagonistic ones (Haney et al. 2015), which can alter the relative abundance of different microbial taxa in bulk soil, the rhizosphere, and the root endosphere (Miranda-Sánchez, Rivera, and Vinuesa 2016; Zgadzaj et al. 2016). Host traits also have the capacity to alter allele frequencies within a species directly affecting their evolution (U.G. Mueller and Sachs 2015). An important aspect of this approach is that it allows for change in the microbial community without the opportunity for plants to coevolve.

Microbiome engineering has received increased attention in recent years, but key assumptions of its predictive models remain untested (Busby et al. 2017; Foo et al. 2017; U.G. Mueller and Sachs 2015; Pineda, Kaplan, and Bezemer 2017; Rillig, Tsang, and Roy 2016; Trivedi et al. 2017). One tacit assumption is that the host is the dominant driver of ecological and evolutionary shifts in microbial function. However, most plant-associated microbes also experience a free-living phase in the soil wherein the microbes can experience a different set of selection pressures (Busby et al. 2017; Mapelli et al.

2018; Sachs, Russell, and Hollowell 2011; Sachs, Skophammer, and Regus 2011; Tkacz et al. 2015). Second is the assumption that plant traits invariably impose strong selection for microbes that increase symbiotic benefit towards the host (Bakker et al. 2014; Burghardt et al. 2018; Panke-Buisse et al. 2015; Sachs, Russell, and Hollowell 2011; Tkacz et al. 2015). This might be unlikely though as microbes have a massive evolutionary advantage over their plant hosts in terms of generation time and population size leaving the host vulnerable to microbes that evolve exploitative phenotypes (Heath 2010; Porter and Simms 2014; Sachs, Ehinger, and Simms 2010). Based on these assumptions, we predict three broad evolutionary outcomes for microbiome engineering. Microbes could evolve enhanced benefit provided to the host, phenotypes that exploit the host, and traits that improve life in the soil. To test these predictions, an experimental system needs to simulate the biphasic life cycle of many plant microbial symbionts, and there must be robust fitness phenotypes for host and symbiont to investigate the relative importance of host control traits, symbiont traits that exploit the host, and traits independent of symbiosis.

The symbiosis between legumes and root nodulating rhizobia is one of the best-studied models of a beneficial plant-microbe interaction (Sprent, Ardley, and James 2017). The interaction is initiated when host roots release flavonoids into the soil and rhizobia respond with the release of Nod factors which induce transcriptional and morphological changes in host roots (Liu and Murray 2016). Upon infection, rhizobia colonize intracellularly wherein they fix atmospheric nitrogen for the host (Coba de la Peña et al. 2018), and ongoing communication limits persistence in host tissue by non-

beneficial rhizobia (Acosta-Jurado et al. 2016; Kawaharada et al. 2017). When the interaction between plant and bacteria is cooperative, both partners gain substantial fitness benefits from this exchange (Denison 2000; Mus et al. 2016; Sachs, Quides, and Wendlandt 2018). The whole nodule eventually senesces as host resources are redirected to seed production and a subset of rhizobia are released back into the soil (Puppo et al. 2004).

The fixation of atmospheric nitrogen by rhizobial symbionts has historically been a dominant source of biologically available nitrogen, but industrialization has made nitrogen more readily available in many terrestrial ecosystems (Cleveland et al. 1999). In agriculture, increased use of nitrogen fertilizer has often led to rapid and devastating changes to ecosystems. Even in legume fields, which represent 25% of global crop production, chemical fertilizers are used heavily (Ferguson et al. 2010). For decades there has been an attempt to inoculate rhizobia on legume crops to reduce or replace the use of expensive and polluting nitrogen fertilizer (Ferguson et al. 2010; Tilman et al. 2002), but it has been difficult to create rhizobial inoculum that provide high levels of benefit under field conditions. Although, the genetic basis for rhizobial success on field crops in unknown, the outcome is clear, non-beneficial rhizobial symbionts tend to dominate in agricultural soil and in nodules (Yates et al. 2011). Thus, in many agricultural fields the benefit provided by rhizobia is largely mediocre leaving room for selection of mutualistic traits.

Here, we used an experimental evolution system inspired by microbiome engineering techniques to test the capacity of host plants to impose selection on simple

microbial populations. By initiating our experiments with clonal populations of rhizobia we focus on the microevolutionary processes of microbiome engineering, as opposed to ecological shifts in the soil microbial communities. The design simulates agricultural conditions where microbes repeatedly interact with consistent plant genotypes with which they share little or no evolutionary history of interaction (Busby et al. 2017). We used a replicated factorial design in which two genotypes of *Lotus japonicus* were each independently paired with rhizobial populations initiated with one of two ancestral clones (four independent experiments, each replicated). Hosts included the *L. japonicus* ecotype MG-20 (Kawaguchi 2000) and a near isogenic mutant with a hypernodulating phenotype (*har1*; produces 6x nodules; Yoshida, Funayama-Noguchi, and Kawaguchi 2010). Rhizobial populations were initiated with either *Rhizobium etli* CE3 or *Ensifer fredii* NGR234, both of which provide low levels of benefit to *L. japonicus*. *Rhizobium etli* CE3 forms nodules on *L. japonicus* that exhibit poor nitrogen fixation and premature senescence (Banba et al. 2001). *Ensifer fredii* NGR234, on the other hand, exhibits poor nitrogen fixation early in the interaction because of delayed nodule development (Schumpp et al. 2009). Each experiment involved an alternating series of *in planta* and *in vitro* passages that simulate the natural cycle of host infection and free-living phases of life that most plant associated symbionts experience (Sachs, Skophammer, and Regus 2011). At the end of the experiment we compared ancestral clones with the derived populations, using inoculation and *in* vitro experiments, nodule histology analysis, and whole genome resequencing. Our design differs in three key ways from previous experimental evolution of rhizobia. First, we initiated the evolution with two nodule

forming, marginally beneficial symbionts allowing ample opportunity for positive selection to improve nitrogen fixation (Guan et al. 2013; Marchetti et al. 2010, 2014). Second, we used host genotypes that vary their input into nodulation, thus we varied the structure and proportion of the rhizobial population that is affected by host selection (Marchetti et al. 2017). Finally, although we included an *ex planta* growth phase which allowed for rhizobia to evolved under free-living conditions (Sachs, Russell, and Hollowell 2011), we alternated free-living phases with symbiosis with legumes. The goals of our experiment were i) to investigate what subset of microbial phenotypes would be selected for during our experimental evolution (i.e., enhancement of mutualism, antagonism, or free-living traits) ii) to identify genes or genomic regions under selection during interactions with the host and in the environment, and iii) to link phenotype to genotype.

Methods

Biological materials

L. japonicus MG-20 seeds were acquired from LegumeBase (University of Miyazaki, Japan). MG-20 is an early flowering ecotype that is amenable to growth under artificial light (Kawaguchi 2000). The near-isogenic MG-20 mutant, *har1* (Yoshida, Funayama-Noguchi, and Kawaguchi 2010) was received from Masayoshi Kawaguchi. The gene *HAR1* is on chromosome 3 and mutations to this gene result in a shoot-derived hypernodulator (Krusell et al. 2002; Nishimura et al. 2002) that forms approximately six times as many nodules as MG-20 under tested conditions (Yoshida, Funayama-Noguchi,

and Kawaguchi 2010). MG-20 and *har1* hosts were grown to generate seeds at the University of California, Riverside (UCR) following published protocols (Quides et al. 2017). Briefly, seeds were surface sterilized in bleach (5.25% sodium hypochlorite, 5 minutes) and rinsed seven times (one minute each) in sterile reverse osmosis purified water (ROH_2O). Surface-sterilized seeds were nick scarified and germinated on agar plates with micronutrients (1.5% agar w/v, nitrogen-free Jensens solution; Somasegaran and Hoben 1994). Seedlings were planted in one gallon pots filled with UCR soil mix #3 (plaster sand and peat moss supplemented with nitrogen, phosphorus, potassium, calcium and trace minerals). Plants were maintained in a greenhouse under natural lighting from July to October and watered as needed with a 1:100 dilution of Peters Excel® 21-5-20 (Scotts Professional, Marysville, Ohio, USA). Greenhouses were fumigated weekly with the insecticide Talstar® (7.9% Bifenthrin, FMC Corporation, Philadelphia, Pennsylvania, USA) to assure no cross-pollination occurred.

Rhizobium etli strain CE3 (hereafter CE3) is a beneficial symbiont of *Phaseolus vulgaris* (Gonzalez et al. 2006; Noel et al. 1984). When CE3 infects *L. japonicus* the nodules prematurely senesce starting as early as 3 weeks post inoculation (wpi; Banba et al. 2001). The genome of CE3 includes a 4.38Mb chromosome and six plasmids ranging from 194kb to 643kb (total is 6.53Mb; Gonzalez et al. 2006). CE3 was provided by Dale Noel (Marquette University, Milwaukee, WI, USA).

Ensifer fredii strain NGR234 (hereafter NGR) can nodulate a large diversity of legumes (Pueppke and Broughton 1999) including *L. japonicus*. When NGR infects *L. japonicus* MG-20 the nodules can take up to 20 weeks to fix nitrogen and produce

leghemoglobin, an oxygen carrier vital to nitrogen fixation (Schumpp et al. 2009). The genome of NGR included a 3.926Mb chromosome and two plasmids that are 2.43Mb and 536kb (Schmeisser et al. 2009). NGR was provided by Jeff Chang (Oregon State University, Corvallis, OR, USA).

Experimental Evolution protocol

Plant preparation and inoculation: Seeds were surface sterilized, nick scarified, and immediately placed into sterilized CYG germination pouches (Mega International; Newport, Minnesota, USA) filled with 20mL of sterile nitrogen-free Jensens fertilizer. Bundles of four pouches containing five seeds each were wrapped in aluminum foil and placed in clear plastic boxes with holes for ventilation. Plants were grown for ~2.5 weeks prior to inoculation. Plants were maintained in a growth chamber with a light dark cycle of 14:10 hours at ~600 Lux, 18-27.5˚C, and relative humidity of 40-65% for the duration of the experiment (Conviron® A1000 with a CMP6010 control system; Winnipeg, Manitoba, Canada).

When seedlings had at least two true leaves they were inoculated following published protocol (Quides et al. 2017). Briefly, liquid cultures of rhizobia were grown to log-phase, cells were separated from spent media and resuspended in sterile ROH_2O at a density of 10^9 cells mL^{-1}. A volume of 50µL (5×10^7cells) was dripped directly on host roots. For the initial round of host infection (passage 0) we infected hosts with clonal liquid cultures of CE3 or NGR (ancestors). Subsequent rounds of inoculation were initiated from rhizobia extracted from the nodules of the previous passage (descendant

passages). Plants were fertilized weekly with 10mL of nitrogen-free Jensens per pouch. Each of the four host and symbiont combinations were passaged in two replicated lineages for a total of eight independent experiments (Table 1).

Plants were harvested for passaging of symbionts at 4wpi (Figure 1). In experiments with CE3 we predict 4wpi will select for symbionts that do not initiate premature senescence at 3wpi (Banba et al. 2001). For NGR experiments, we predict that 4wpi will select for symbionts that fix nitrogen given that leghemoglobin is already present in nodules (Schumpp et al. 2009). Excess fertilizer was removed from pouches and photographs of each plant were taken for reference. Nodules were counted, dissected, and photographed. Shoots were dried at 60˚C for three days prior to weighing dry biomass. All nodules from a host and symbiont replicate passage were pooled and surface sterilized (bleach; three min.), rinsed in sterile ROH_2O (7 times, 1 min. each), crushed with a sterile glass rod, and resuspended in 5mL of liquid MAG. From the 5mL of nodule extract, 200µL was mixed with 200µL of MAG:glycerol (1:1) to archive viable cells, 100µL was serially diluted and spread plated (10^6) to quantify rhizobia population size within nodules, and 3.2mL was used to inoculate a flask of MAG to grow cells for the next passage. This phase of *in vitro* growth simulates the free-living state rhizobia experience between host infections and allowed us to inoculate the next round of hosts with a consistent number of cells every passage. All nodules were surface sterilized within 24 hours of harvesting and crushed within 24 hours of sterilization. Each experiment was named after the symbiont (CE3 or NGR), host (MG-20 or *har1*), and replicate (‘a’ or ‘b’; Table 1).

The CE3 strain was evolved for a total of 15 passages on each host (Table 1). The NGR passage lines became contaminated at passage 3 (*har1* hosts) and passage 13 (MG-20 hosts), and a new round of passaging was initiated from archived stocks pre-contamination. As a result of contamination, NGR was only passaged for ten cycles on *har1*. There were a total of ~490 and ~380 estimated generations symbionts passaged 15 times and 10 times, respectively (~3x as many generations *in planta* compared to *in vitro*, Table 1). To try to make up for this reduction, both replicates of the NGR:*har1* combination were exposed to ~450 plants compared to ~260 in the other passage lines (~70% more plants in total) and formed >50% more total nodules than the other *har1* experiments resulting in about twice as many within nodule generations (Table 1).

We estimated rhizobial generations *in planta* and *in vitro* to gather information about the fitness of our symbionts throughout experimental evolution. The data used to generate fitness information was also used to identify the severity of the bottleneck effect in our protocol; only a very small proportion of the rhizobia inocula get inside a nodule and have the chance to be passaged. The number of *in planta* generations for rhizobia was estimated using the number of nodules to infer initial population size and estimated rhizobial population size as the final population size. More than one rhizobia can initiate one nodule, but it is unclear how common this is. One study has estimated that with our inoculation density of 5×10^7cells we should expect 6% of nodules to be dually infected (Gage 2002), therefore we estimate a range of 1-2 rhizobia initiate one nodule. At a 6% coinfection rate all coinfected nodules would have to have ~16 independent rhizobia initiate one nodules to reach an average of two rhizobia starting a nodule.

100µL of nodule extract (see above) was used to estimate the entire population size of rhizobia after the *in planta* growth portion of a passage cycle for a given experiment. The entire population size was divided by the number of nodules formed during this passage to estimate the mean nodule population size. The mean nodule population size was used as a final population size to calculate the number of *in planta* generations using either one or two as the initial population size. The number of generations within nodules was calculated as the product of *in planta* generations and the number of nodules formed during that passage. We also used the entire population size to estimate the starting population size when calculating number of *in vitro* generations using the final estimated cell density within the flask at inoculation as the final population size.

Table 3.1 Metadata for symbiont passaging

Symbiont:Host _replicate	Number of passages	Total number of plants exposed to rhizobia	Total number of nodules formed by rhizobia	Estimated total # of rhizobia cells extracted from nodules	Estimated number of *in planta* generations	Estimated number of generations within nodules	Estimated number of *in vitro* generations
CE3:MG-20_a	15	253	559	2.69E+09	326-341	13,979-14,503	128
CE3:MG-20_b	15	245	660	2.41E+09	355-370	17,432-18,074	137
CE3:*har1*_a	15	255	1895	4.47E+09	368-382	51,041-52,861	121
CE3:*har1*_b	15	260	2258	3.72E+09	359-374	60,666-62,882	130
NGR:MG-20_a	15	278	1208	5.99E+09	341-356	30,792-31,862	109
NGR:MG-20_b	15	289	1464	3.36E+09	353-368	34,840-36,085	126
NGR:*har1*_a	10	448	4381	1.92E+09	268-278	120,057-124,438	95
NGR:*har1*_b	10	454	3622	2.89E+09	283-293	111,354-114,976	94

Plants were harvested for passaging of symbionts at 4wpi (Figure 3.1). Excess fertilizer was removed from pouches and photographs of each plant were taken for reference. Nodules were counted, dissected, and photographed. Shoots were dried at 60˚C for three days prior to weighing dry biomass. All nodules from a host and symbiont replicate passage were pooled and surface sterilized (bleach; three min.), rinsed in sterile ROH_2O (7 times, 1 min. each), crushed with a sterile glass rod, and resuspended in 5mL of liquid MAG. From the 5mL of nodule extract, 200µL was mixed with 200µL of MAG:glycerol (1:1) to archive viable cells, 100µL was serially diluted and spread plated (10^6) to quantify rhizobia population size within nodules, and 3.2mL was used to inoculate a flask of MAG to grow cells for the next passage. The number of *in planta* generations for rhizobia was estimated using the number of nodules to infer initial population size and estimated rhizobial population size as the final population size. We assume an average of 1-2 rhizobia initiate one nodule (estimated to be 1.06; Gage 2002). We also calculated the number generations within a nodule calculated as the product of *in planta* generations and number of nodules formed during that passage. The final population size was then scaled to estimate the starting population size for *in vitro* growth. The number of *in vitro* generation times was then calculated using the final estimated cell density within the flask at inoculation. This phase of *in vitro* growth simulates the free-living state rhizobia experience between host infections and allowed us to inoculate the next round of hosts with a consistent number of cells every passage. All nodules were surface sterilized within 24 hours of harvesting and crushed within 24 hours of sterilization.

The CE3 strain was evolved for a total of 15 passages on each host (Table 3.1). The NGR passage lines became contaminated at passage 3 (*har1* hosts) and passage 13 (MG-20 hosts), and a new round of passaging was initiated from archived stocks pre-contamination. As a result of contamination, NGR was only passaged for ten cycles on *har1*. There were ~490 and ~380 estimated generations for symbionts passaged 15 times and 10 times, respectively. To try to make up for this reduction, both replicates of the NGR:*har1* combination were exposed to ~450 plants compared to ~260 in the other passage lines (~70% more plants in total) and formed >50% more nodules than the other *har1* experiments resulting in about twice as many within nodule generations. It is important to note that our design is not a coevolution experiment which is consistent with microbiome engineering and many agricultural practices.

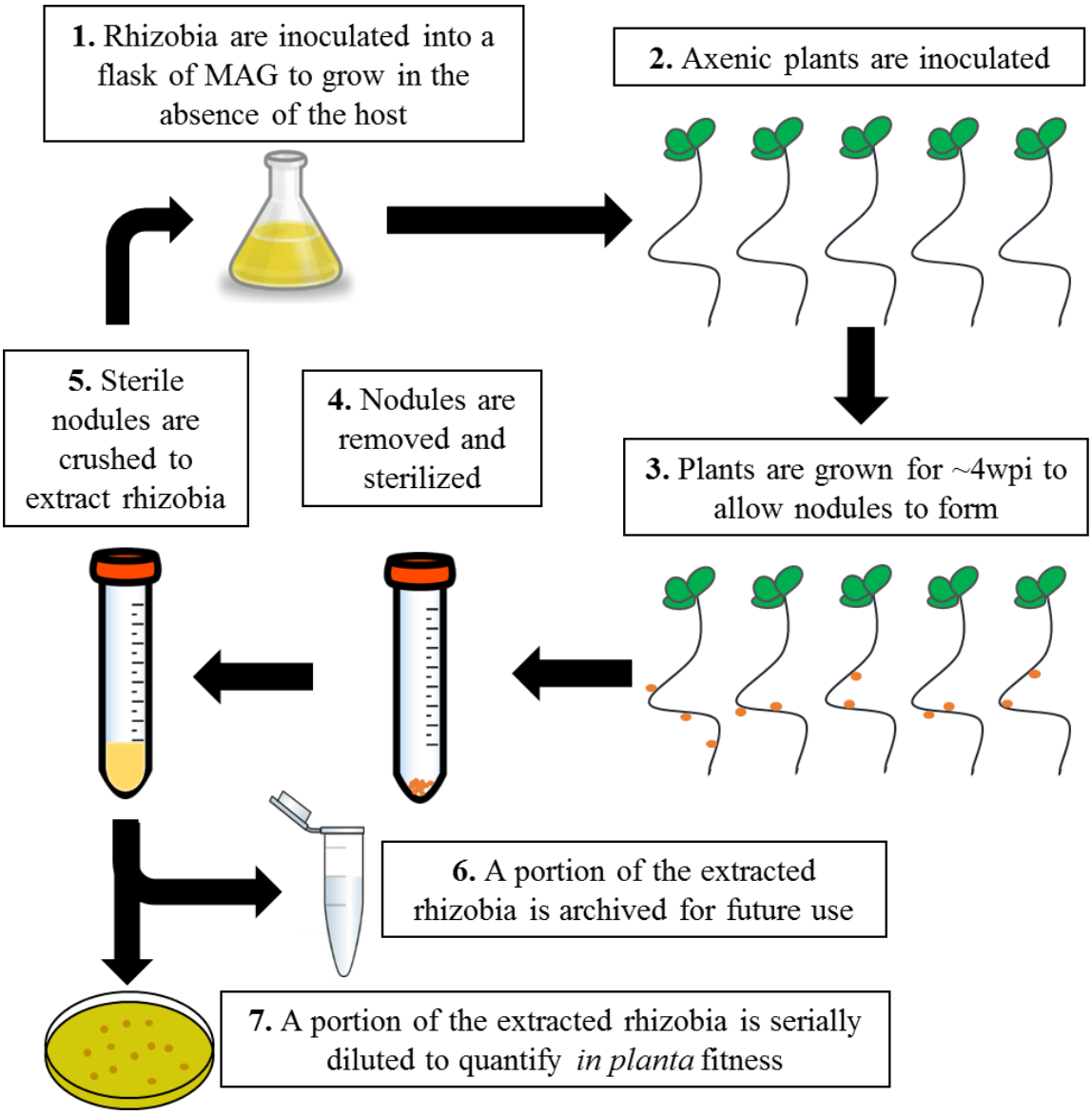

Figure 3.1 Symbiont passaging protocol

It is important to note that our design is not a coevolution experiment which is consistent with microbiome engineering and many agricultural practices. Rhizobia are grown *in vitro* in the absence of host (Step 1). A known density of rhizobia is inoculated on axenic plants and rhizobia begin to experience selection in the presence of the host (Step 2). Plants are grown for ~4wpi. Nodules form and rhizobia continue to experience selection in the presence of the host (Step 3). Nodules are removed (Step 4) so that rhizobia can be extracted (Step 5) to start a new round of *in vitro* growth (Step 1). A portion of the extracted rhizobia were archived in a 1:1 solution of MAG:glycerol for future experiments (Step 6). Another portion of the extracted rhizobia were serially diluted to quantify *in planta* population sizes to estimate growth rate *in planta* and *in vitro*.

Phenotypic Analysis

***In vitro* growth rate and estimating cell density:** Ancestral and derived clones were inoculated from individual colonies into flasks of liquid MAG and grown to log-phase (12-36 hours, 29˚C, 180rpm). Optical density (OD) was measured multiple times over the course of one day. At each OD measurement cell density was estimated by diluting the cultures, spread plating, and counting colony forming units. Growth rate (doubling time) was estimated between sequential time points which were treated as one data point. Differences in growth rate for individual derived symbionts were compared to ancestral symbionts with Welch's two sample t-test for unequal variance. Cell density was plotted against OD to create a cell density linear regression used to quickly estimate cell density from OD. A total of 12-28 independent flasks were inoculated for each strain to compare *in vitro* growth rate and correlate OD to cell density.

Greenhouse experiment to measure symbiont fitness and fitness effects: Seeds of each host type were sterilized and scarified as above and germinated at 20˚C in sterile ROH_2O in the dark for at least two weeks (25^{th} September 2017 – 13^{th} October 2017). Germinated seedlings were planted in sterilized Conetainers (SC10; Steuwe and Sons, Tangent, OR, USA) filled with autoclaved inert calcined clay that offers negligible nutrients (Turface® Pro League®, Turface Athletics, Buffalo Grove, Illinois, USA). Seedlings were grown in a controlled facility with daily mist-watering until true leaves emerged and thereafter were fertilized weekly with 5mL of N-free Jensens solution.

Seedlings were transferred to the greenhouse and were hardened behind 50% shade cloth for four days.

After hardening, seedlings of each host genotype were arranged into size matched groups using leaf counts, and were randomly assigned to inoculation treatments. MG-20 hosts received the following inoculum: sterile ROH_2O (negative control), NGR, NGR:MG-20_a, NGR:MG-20_b, CE3, CE3:MG-20_a, CE3:MG-20_b and *har1* hosts received sterile ROH_2O, NGR, NGR:*har1*_a, NGR:*har1*_b, CE3, CE3:*har1*_a, CE3:*har1*_b. Inoculation occurred on 30th October 2017. For each treatment, either 5mL of water or 5mL of washed rhizobial cells were drip inoculated directly into the sterile clay soil at a density of 10^8 cells mL^{-1} ($5x10^8$ cells). Inoculum concentrations were estimated to be ~10^8 cells mL^{-1} via optical density as above and confirmed by counting colony forming units. The 14 host and inoculum treatment combinations were randomly distributed in the greenhouse with one treatment combination replicate in one of 20 blocks (280 plants total). 10 blocks were removed from the greenhouse for each harvest.

We performed two harvests. The 'early-development harvest' occurred at 4wpi. This is the same timing as passaging and thus matched the time point that was under selection. At 4wpi in pouches (growth during passaging) it can be difficult to detect phenotypic differences even when comparing hosts inoculated with a nitrogen fixing symbiont or a non-fixing symbiont, but by 6wpi there are stark differences as hosts prepare to flower (Quides et al. 2017). We therefore harvested the other half of the plants at 6wpi ('maturity harvest') before hosts would begin to flower and nodules naturally senesce (Puppo et al. 2004). If there was selection for enhanced mutualism we would

expect to see phenotypic evidence of this by 6wpi. Alternatively, if symbionts evolved to become more antagonistic we would not expect our plants to survive much longer than 6wpi (especially CE3, premature senescence phenotype).

Upon harvest, shoots, roots and nodules were separated, photographed, and dried at 60˚C for 3 days prior to weighing dry biomass. True leaves and nodules were counted. We measured shoot biomass, shoot biomass per true leaf, change in true leaves, number of nodules formed, total nodule biomass, and mean nodule biomass. Shoot biomass per true leaf was calculated as the shoot biomass divided by the number of true leaves at harvest to assess leaf size. Change in true leaves was calculated as the difference between the number of true leaves at inoculation and harvest as an indicator of growth potential. Mean nodule biomass was calculated as the total biomass of all nodules on a plant divided by the number of nodules formed on that plant which was used as a proxy for rhizobial fitness. These measures were compared between plants inoculated with derived symbionts versus those inoculated with ancestral symbiont using a Welch's two sample t-test.

Nodule Culturing: *In planta* fitness of rhizobia was quantified by culturing nodules at both harvests. Three blocks of plants were randomly selected to culture nodules from all treatments. From each of the three treatment replicates, four randomly picked nodules per plant were cultured (144 total nodules per harvest). Nodules were individually surface sterilized in bleach for a minimum of 30 seconds (ca. one minute per mm of nodule diameter), rinsed three times in sterile ROH_20, and crushed with a sterile pestle in sterile

ROH_20. The nodule slurry was serially diluted in sterile ROH_2O, spread plated on MAG (10^{-3}, 10^{-5} dilutions) and incubated at 29˚C. For CE3, cultures were incubated overnight, and for NGR, cultures were incubated for three days. Colonies were counted to estimate rhizobial population sizes per nodule. Estimated nodule population size per nodule was log-transformed to improve normality and analyzed with Welch's two sample t-test for unequal variance to compare individual derived symbionts to ancestral symbionts.

Light Microscopy: At each harvest we randomly designated one block of plants to be used for light microscopy. At the early-development harvest we had an insufficient number of nodules formed by MG-20 hosts in our designated block. To ensure an adequate number of nodules for these treatments we also set aside all the nodules from one nodule culturing block that were not randomly picked for culturing. By the second harvest the number of nodules produced by MG-20 hosts was sufficient to collect microscopy data, thus we only had to use the nodules from the one block originally selected for light microscopy.

Nodules were fixed in 4% v/v paraformaldehyde, 2.5% v/v glutaraldehyde in 50mM phosphate buffer pH 7.2 for 6-10 hours at 20° C, then 4° C for three days, and dehydrated in a graded alcohol series to 100% EtOH at 20° C. The nodules were infiltrated with JB-4 Plus methacrylate (Poly-sciences, Warrington, Pennsylvania, USA) in catalyzed Solution A and 100% EtOH (1:1 ratio) at 20° C for 6 hours followed by a 3:2 ratio at 4° C overnight. Infiltration with 100% catalyzed Solution A was performed at 20° C for 6 hours and refreshed for final infiltration at 4° C overnight. Finally, nodules

were embedded in film caps with polymerized JB-4 plus methacrylate and sealed with Parafilm. All steps at 20° C were done with gentle agitation (Regus et al. 2017).

Individual nodules were removed from film caps with a coping saw and polymerized with JB-4 Plus methacrylate on metal stubs for sectioning. Sections of 4µm thickness were prepared parallel to the long axis of the parent root using a glass knife and an H/I Bright 5030 Microtome (Hacker Instruments Inc.; Fairfield, New Jersey, USA). Sections were mounted on glass slides, and stained with 0.1% w/v aqueous toluidine Blue O to identify infected plant cells (dark blue stain). Sections were viewed with a Meiji Techo MT4000L Biological Microscope (Meiji Techo CO., LTD.; Miyoshi machi, Iruma-gun, Japan) and images were acquired with a Nikon D80 DSLR (Nikon Corporations; Minato, Tokyo, Japan) attached to the trinocular tube using Meiji specific adapters and 'ControlMyNikon' tethering software (Tetherscript Technology Corporation; Vancouver, British Colombia, Canada).

An average of 16 sections per nodule were analyzed (range 4-30) from each of 3-4 nodules per host. We calculated the percentage of infected plant cells showing signs of senescence for each section (ruptured or compromised cell wall, blotchy appearance, low density of rhizobia; Regus et al. 2017). To control for variation in cell structure throughout the nodule (Puppo et al. 2004), the mean percentage of senescent plant cells in a section was calculated for all sections from one nodule. The mean percentage of nodule cells infected with the derived symbiont showing signs of senescence was compared to nodules infected with the derived symbiont using Welch's two sample t-test for unequal variance with mean values for each nodule as a data point.

Isotopic Analysis: We quantified %N and $\delta^{15}N$ from dried leaf samples for all host and treatment combinations at both harvests. Dry leaves were removed from stems and powdered using a bead beater for 10 seconds at $4ms^{-1}$ with a 5mm steel bead. When plants incorporate symbiotically fixed nitrogen, the leaf tissue exhibit reduced $\delta^{15}N$ relative to uninfected plants because of isotopic fractionation (Regus et al. 2014). Samples were analyzed at UC Santa Cruz Stable Isotope Laboratory. In many cases one plant did not provide sufficient leaf tissue for analysis, thus we pooled leaf tissue from up to four plants in a treatment. Due to pooling each treatment has a range of 2-5 replicates. Mean %N and $\delta^{15}N$ was compared between hosts inoculated with one of the derived symbionts and corresponding ancestral symbiont using Welch's two sample t-test for unequal variance.

Genome Analysis

Isolation and extraction: CE3 ancestral clones and archived nodule slurries from the CE3 experiments were plated on 25ug/mL cyclohexamide MAG to prevent fungal growth and limit the extraction of plant DNA. We sampled 20 individual colonies from the passage 15 populations of CE3:*har1*_a and CE3:*har1*_b and one CE3 colony. Individual colonies were picked and washed in 500uL of sterile ROH_2O via vortexing and centrifugation (14,000g, 3min). From passages 5 and 10 we sampled CE3:*har1*_a and CE3:*har1*_b. From passage 15 we sampled CE3:*har1*_a, CE3:*har1*_b, CE3:MG-20_a, and CE3:MG-20_b. Plates from these eight populations were scraped and washed in

10mL of sterile ROH_2O. 25uL of washed population cell culture was used for DNA extraction. Genomic DNA was extracted using a Qiagen DNeasy blood & tissue kit.

Genome re-sequencing and mutation identification: Genomic DNA (from clonal isolates) or metagenomics DNA (from derived population samples) were processed as Nextera XT libraries and sequenced (2x 150 bp) on one lane of an Illumina HiSeq 3000 at the Center for Genome Research and Biocomputing (CGRB), Oregon State University. Sequencing reads were checked for quality and/or contamination using FastQC (Andrews 2014). Sequencing adapters and poor-quality reads were trimmed using BBduk v. 35.82 with the options "ktrim = r k = 23 mink = 9 hdist = 1 minlength = 100 tpe tbo" (Bushnell 2014). The CE3 genome was *de novo* assembled using SPAdes v. 3.1.1 with the options "--careful -k 21,33,55,77,99"; and the assembled contigs were aligned to the *R. etli* CFN 42 reference genome (NCBI: GCF_000092045.1) using progressiveMauve with the default options (Bankevich et al. 2012; Darling, Mau, and Perna 2010).

Single nucleotide polymorphisms (SNPs) and indels were called for all samples together as follows. Reads were mapped to the *R. etli* CFN 42 reference genome using bowtie2 v. 2.2.3 with the option "--local" (Langmead et al. 2009). Alignments were converted to bam format using Samtools v. 0.1.18, and sample read groups were added to alignments using Picard tools v. 2.0.1 (Li et al. 2009; Picard Tools, 20015). Mapped read coverage for each sample was calculated using bedtools v2.25.0 "genomecov", and regions with no coverage were identified as putative deletions in each sample (Quinlan and Hall 2010). Per-sample read depth was plotted using the R package Sushi (Phanstiel

et al. 2014). Read depth was normalized to the chromosome mean read depth for each sample. GATK v. 3.7 HaplotypeCaller and the options '-ERC GVCF -ploidy 1' were used to call variants for each sample, and the data were then combined using GenotypeGVCFs (McKenna et al. 2010). Variants were annotated for predicted functional effect using snpEff v. 4.3t and the CFN 42 reference genome annotation (Cingolani et al. 2012). One sequenced isolate (CE3:*har1*_b_20) is predicted to have lost the p42f plasmid due to lack of read coverage on this replicon. Predicted variants resulting from reads that misaligned to this replicon were removed for this sample. Variants were converted into a fasta alignment using bcftools v. 1.3–14-ge0890a1 vcf-to-tab and the perl script vcftab-to-fasta (Li et al. 2009; J. Chen 2012).

Results

Symbiotic effectiveness

CE3:*har1*: We uncovered conflicting data among the harvests for these experiments. At the early-development harvest we detected evolution of enhanced effectiveness (increased shoot biomass; CE3:*har1*_a: t = 3.15, df = 14.1, P = 0.007; CE3:*har1*_b: t = 2.81, df = 11.5, P = 0.016; Figure 2A). By the maturity harvest this pattern was not maintained and we found that hosts inoculated with the derived symbionts had less shoot biomass, on average, than the hosts inoculated with the ancestral symbiont (Figure 2B). For shoot biomass per true leaf, a measure of leaf size, we also found evidence of enhanced benefit at the early-development harvest (Figure 2C) and reduced benefit by the maturity harvest (Figure 2D). Hosts receiving the derived CE3:*har1*_b symbiont formed

significantly heavier leaves than the ancestral CE3 (t = 3.08, df = 15, P = 0.008; Figure 2B), and a similar trend was observed for CE3:*har1*_a. We found no difference in percent nitrogen in leaf tissue or isotopic signature of nitrogen fixation ($\delta^{15}N$). At the early-development harvest we found a trend of decreased percent nitrogen, but a trend of increased nitrogen fixation for both replicates compared to the ancestral CE3. At the maturity harvest we detected a negative trend for CE3:*har1*_a for percent nitrogen, but a positive trend for CE3:*har1*_b. For $\delta^{15}N$ there was a positive trend for CE3:*har1*_a, but a negative trend for CE3:*har1*_b.

CE3:MG-20: For both replicates we found almost no evidence of phenotypic evolution. We found evidence for increased shoot biomass with CE3:MG-20_a at the maturity harvest (t = 2.33, df = 17.4, P = 0.0319), but only a positive trend for CE3:MG-20_b. For both shoot biomass measures at the early-development harvest the trends were positive for both replicates, or there was no difference in the mean value (CE3:MG-20_b: t = 0). For this harvest there was a negative trend for CE3:MG-20_a for both measures of nitrogen, and positive trends with CE3:MG-20_b for both. At the maturity harvest shoot biomass per true leaf, percent nitrogen, and $\delta^{15}N$ increased for CE3:MG-20_a. For replicate 'b' percent nitrogen displayed a positive increase, while shoot biomass per true leaf and $\delta^{15}N$ had negative trends.

NGR:*har1*: In these experiments we found scant evidence for a phenotypic shifts in symbiotic effectiveness at the early-development harvest, and no evidence at the maturity

harvest. For both replicates percent nitrogen in leaf tissue increased, but it was only significant for NGR:*har1*_a (t = 4.58, df = 2.88; *P* = 0.0213). Nitrogen fixation, however, was diminished for both replicates, and shoot biomass measures exhibited decreases or nearly identical means compared to the ancestral NGR on *har1* (NGR:*har1*_a shoot biomass: t = 0; shoot biomass per true leaf: t = 0.003). At the maturity harvest none of the trends were consistent for enhanced or reduced symbiotic effectiveness. Shoot biomass and percent nitrogen in leaf tissue increased for both replicates, while shoot biomass per true leaf and $\delta^{15}N$ decreased for both replicates.

NGR:MG-20: Similar to the other NGR experiment, we only found evidence of increased symbiotic effectiveness at the early-development harvest. Both replicates fixed more nitrogen than their ancestor, but this was only significant for NGR:MG-20_a (t = 3.55, df = 3.44, *P* = 0.0305). While this resulted in a minor increase in percent nitrogen in leaf tissue, it slightly decreased both shoot biomass traits. For NGR_MG-20_b, all three measures were reduced compared to the ancestor. Data collected during the maturity harvest displayed consistent trends for each replicate. NGR:MG-20_a had subtle increases in all four symbiotic effectiveness measures, while NGR:MG-20_b had small decreases.

For all experiments we found no evidence for a change in the number of true leaves developed between inoculation and harvests

Symbiont fitness

CE3:*har1*: In these experiments we found some evidence for the evolution of increased symbiont fitness. In all cases the derived symbionts attained a greater mean population size within nodules (Figure 2E,F), but this was only significant for CE3:*har1*_a at the maturity harvest (t = 3.02, df = 16, *P* = 0.008). Mean total nodule mass, a proxy for rhizobia fitness, was increased at the early-development harvest, but decreased at the maturity harvest for both replicates.

CE3:MG-20: We found no evidence of symbiont fitness evolution in these experiments. At the early-development harvest CE3:MG-20_a had an increased nodule population size, while replicate 'b' a decreasing trend for nodule population size, and both had decreased total nodule mass. By the maturity harvest both were trending towards increased population sizes and total nodule mass.

NGR:*har1*: Evidence for evolution of symbiont fitness was limited, but consistent among replicates. At the early-development harvest both replicates had increased nodule population sizes, but decreased total nodule mass and for NGR:*har1*_a this was significantly reduced (t = -2.36, df = 15.4, *P* = 0.0318). For the maturity harvest both population sizes were decreased compared to the ancestral NGR, but the mean total nodule masses were increased, and significantly so for NGR:*har1*_b (t = 2.5, df = 15.1, *P* = 0.0242)

NGR:MG-20: The derived strains from these experiments provided some evidence of evolved symbiont fitness, but it was not enhanced. At the early-development harvest both derived replicates had significantly decreased mean population sizes within nodules (NGR:MG-20_a: t = -2.59, df = 13.2, *P* = 0.0222; NGR:MG-20_b: t = -2.53, df = 10.9, *P* = 0.028). However this pattern changed for NGR:MG-20_a at the maturity harvest, and nodule population size was trending higher. NGR:MG-20_b continued to have a decreased nodule population size, but the trend was no long significant. For both replicates at the early-development harvest there was a trend of decreased total nodule mass, but at the maturity harvest the trend switched to increasing.

For all experiments we found no significant differences in the number of nodules formed, mean nodule mass, or *in vitro* growth rate.

Table 3.2 Phenotypic comparison of ancestral and final derived symbionts

Phenotype Early-development Harvest	**a_*har1*:CE3**	**b_*har1*:CE3**	**a_MG-20:CE3**	**b_MG-20:CE3**	**a_*har1*:NGR**	**b_*har1*:NGR**	**a_MG-20:NGR**	**b_MG-20:NGR**
Shoot biomass	t = 3.15 ǂ df = 14.1	t = 2.81 ǂ df = 11.5	t = 0.429 df = 16	t = 0 df = 14.3	t = 0 df = 16.7	t = -1 df = 17.5	t = -1.32 df = 16.6	t = -0.845 df = 16.7
Shoot biomass per true leaf	t = 1.6 df = 17.3	t = 3.08 ǂ df = 15	t = 0.092 df = 18	t = 0.497 df = 18	t = 0.003 df = 17.7	t = -0.73 df = 16.2	t = -1.92 df = 13.6	t = -1.58 df = 17.8
Change in true leaf count	t = 0.447 df = 16.6	t = -0.896 df= 12.3	t = -0.249 df = 13.2	t = -0.973 df = 14.1	t = 0.976 df = 13	t = 0.802 df = 15.2	t = 0.305 df = 17.6	t = 1.26 df = 17.9
Percent nitrogen in leaf tissue	t = -0.277 df = 1.9	t = -3 df = 1	t = -0.632 df = 2.44	t = 0.655 df = 3.92	t = 4.58 ǂ df = 2.88	t = 2.4 df = 1.17	t = 1 df = 2	t = -1 df = 2
$\delta^{15}N$	t = 0.975 df = 1.31	t = 1.45 df = 3	t = -0.204 df = 3.87	t = 0.35 df = 3.4	t = -0.16 df = 2.91	t = -4.11 df = 2.07	t = 3.55 ǂ df = 3.44	t = 3.07 df = 2.56
Number of nodules formed	t = 0.476 df = 18	t = 0.56 df = 17.8	t = -0.988 df = 16.9	t = -0.676 df = 14.4	t = -1.83 df = 17.4	t = -0.457 df = 17.3	t = -0.549 df = 16	t = 1.99 df = 14.7
Total nodule mass	t = 0.67 df = 13.2	t = 0.114 df = 13.9	t = -0.679 df = 7.2	t = -0.216 df = 11.1	t = -2.36 ǂ df = 15.4	t = -0.946 df = 13.8	t = -0.362 df = 13.6	t = -0.405 df = 12.9
Average nodule mass	t = 0.515 df = 13.3	t = -1.81 df = 14.7	t = 1.16 df = 9.85	t = 1.45 df = 7.62	t = 0.006 df = 13.2	t = -0.169 df = 15.2	t = 0.614 df = 12.6	t = -2.12 df = 11.6
Log(estimated nodule population size)	t = 0.163 df = 16.7	t = 0.481 df = 16.6	t = 0.226 df = 20	t = -0.382 df = 17.9	t = 0.797 df = 17.2	t = 0.639 df = 14.1	t = -2.59 ǂ df = 13.2	t = -2.53 ǂ df = 10.9
Percent of nodule cells undergoing senescence	NA	NA	NA	NA	NA	NA	NA	NA
in vitro growth rate (doubling time)	t = -0.984 df = 65.2	t = -1.07 df = 59.2	t = -1.19 df = 60.7	t = -0.046 df = 75.4	t = 0.305 df = 177	t = 0.176 df = 174	t = 0.099 df = 146	t = 0.539 df = 128

Table 3.2 Phenotypic comparison of ancestral and final derived symbionts cont.

Phenotype Maturity Harvest	**a_*har1*:CE3**	**b_*har1*:CE3**	**a_MG-20:CE3**	**b_MG-20:CE3**	**a_*har1*:NGR**	**b_*har1*:NGR**	**a_MG-20:NGR**	**b_MG-20:NGR**
Shoot biomass	t = -1.77 df 13.4	t = -1.03 df = 12.3	t = 2.33 ǂ df = 17.4	t = 0.384 df = 18	t = 0.177 df = 17.2	t = 0.186 df = 17.9	t = 0.12 df = 14	t = -0.538 df = 17.3
Shoot biomass per true leaf	t = -2.45 ǂ df = 16	t = -1.03 df = 13	t = 1.16df = 15.1	t = -0.301 df = 14	t = -0.314 df = 17.4	t = -0.26 df = 17.9	t = 1.37 df = 11.3	t = -0.060 df = 15.4
Change in true leaf count	t = 0.246 df = 17.6	t = -0.497 df = 17.5	t = 0.606 df = 18	t = 1.56 df = 17.9	t = 1.28 df = 17.8	t = 1.28 df = 17.8	t = -1.57 df = 17.6	t = 0 df = 13.8
Percent nitrogen in leaf tissue	t = -0.2 df = 1	t = 1 df = 2	t = 1.1 df = 4.41	t = 1.42 df = 4.54	t = 0.459 df = 3.74	t = 0.894 df = 3.67	t = 0.454 df = 2.68	t = -1.26 df = 5.6
$\delta^{15}N$	t = 0.439 df - 1.25	t = -0.222 df = 2.79	t = 0.492 df = 4.03	t = -0.191 df = 5.68	t = -0.792 df = 2.84	t = -2.56 df = 3.57	t = 1.86 df = 3.56	t = -0.257 df = 4.72
Number of nodules formed	t = -0.715 df = 13.9	t = -0.187 df = 16.5	t = 0.741 df = 17.2	t = 0 df = 18	t = 1.24 df = 17.8	t = 1.64 df = 17.3	t = 0.253 df = 16.5	t = 0.219 df = 18
Total nodule mass	t = -1.24 df = 10.9	t = -0.448 df = 16	t = 0.669 df = 16	t = 0.574 df = 15.8	t = 2.13 df = 14.1	t = 2.5 ǂ df = 15.1	t = 0.594 df = 15.5	t = 0.208 df = 16
Average nodule mass	t = -0.366 df = 15.9	t = -0.575 df = 16	t = -0.641 df = 12.2	t = -0.174 df = 15.6	t = 0.055 df = 12.2	t = -0.327 df = 15.4	t = 0.779 df = 14.1	t = 0.196 df = 13.7
Log(estimated nodule population size)	t = 3.02 ǂ df = 16	t = 1.48 df = 21	t = 0.238 df = 18.9	t = 0.161 df = 21.6	t = -0.207 df = 18	t = -1.83 df = 18.2	t = 0.734 df = 21	t = -0.453 df = 20.9
Percent of nodule cells undergoing senescence	t = 4.23 ǂ df = 5.57	t = 1.44 df = 2.99	t = 0.128 df = 5.71	t = 0.804 df = 4.06	NA	NA	NA	NA
in vitro growth rate (doubling time)	see above	see above	see above	see above	see above	see above	see above	see above

Ancestral and derived phenotypes compared with Welch's two sample t-test

t-value compares derived relative to ancestral (ex., t < 1 indicates derived < ancestral)

ǂ indicates $P < 0.05$

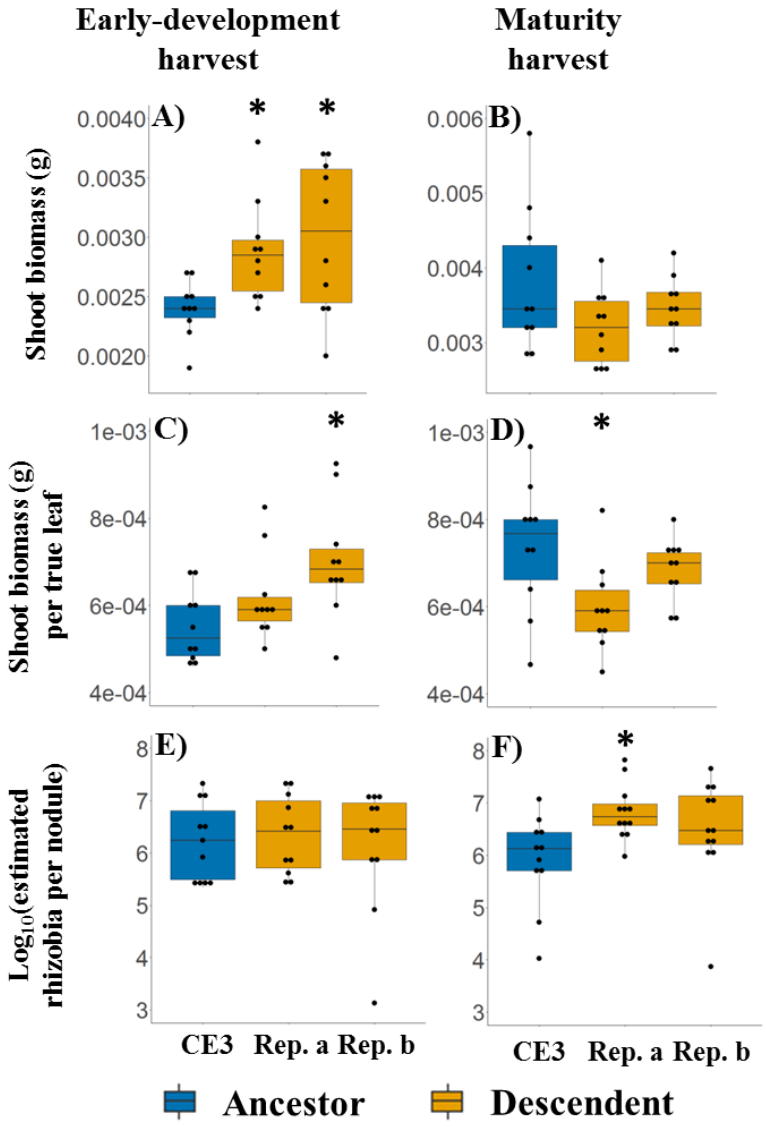

Figure 3.2 Phenotypic evolution of CE3 symbionts on *har1* hosts

We compared ancestral and derived CE3 symbionts on *har1* hosts for measures of symbiotic effectiveness and symbiont fitness at the early-development harvest (A, C, E) and the maturity harvest (B, D, F). Symbiotic effectiveness was measured as shoot biomass (A, B) and shoot biomass per true leaf (C, D). Symbiont fitness was estimated using the mean population size of rhizobia within a nodule (E, F). Blue boxplots represent data of the ancestral symbiont, and orange boxplots correspond to derived symbionts. The following abbreviations are used CE3 = ancestral CE3, Rep. a = CE3:*har1*_a, and Rep. b = CE3:*har1*_b. Asterisks indicate significant differences between the denoted derived symbiont and the ancestral symbiont determined using Welch's two sample t-test.

Nodule Histology

Out of all eight experiments, the data for CE3:*har1*_a at the maturity harvest was most suggestive of phenotypic evolution (Figure2B, D, F). Because of this we chose to focus our light microscopy efforts on the CE3 experiments at the maturity harvest using CE3:MG-20 experiments as a control for passaged symbionts showing limited phenotypic evolution. In both CE3:*har1* experiments we found an increase the percent of cells showing signs of senescence (Figure 3). Strain CE3:*har1*_a exhibited a significantly greater percentage of cells undergoing senescence compared to the ancestral CE3 ($t = 4.228$, $df = 5.567$; $P = 0.007$), while the pattern was similar for CE3:*har1*_b, it was not significant. In both CE3:MG-20 experiments there were an increased number of nodule cells showing signs of senescence, but the differences were not significant (Table 2).

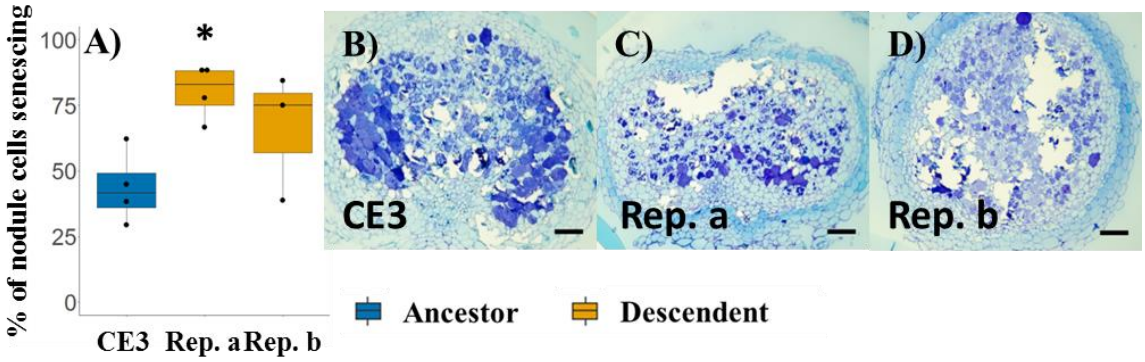

Figure 3.3 Nodule structure of ancestral and derived CE3 infected nodules
The mean number of nodule cells showing signs of senescence (A) was determined using visual appearance of Toluidine Blue O staining for the ancestral CE3 symbiont (B) and derived CE3:*har1*_a (C) and CE3:*har1*_b (D) symbionts. Scale bars are 100µm (E-G). The asterisk indicates a significant difference between the denoted derived symbiont and the ancestral symbiont determined using Welch's two sample t-test.

Mutations in derived CE3 symbionts

As above, we chose to focus our genomic analyses on the CE3:*har1* experiments because we uncovered complimentary evidence of phenotypic evolution. Because we sampled three time points for CE3:*har1*_a and CE3:*har1*_b we were also able to identify the number of mutations that persisted for at least five passages. Across our three time points the total number of mutations were 34 for CE3:*har1*_a and 38 for CE3:*har1*_b with a per time point mean of ~11 and ~13 mutations, respectively (Figure 4). We did not identify any non-synonymous mutations with a known gene product that fixed in either population

We detected six mutations from our 40 clonal isolates (20 from each population) that persisted at low frequency and were thus difficult to detect when re-sequencing the populatin (Table 4). For CE3:*har1*_a we found eight out of the 20 isolates had a SNP in a gene coding for sorbosone dehydrogenase and three out of 20 in a region coding for alpha-L-fucosidase. We also identified deletions in *nifD* and a polymerase, in four and seven out of 20 isolates, respectively. Of the 20 CE3:*har1*_b isolates we found three with a SNP in an aldo/keto reductase gene, 7 with a deletion in *nifD*, 11 with a deletion in a polymerase, and one that lost the entire p42f plasmid. We investigated the loss of plasmid p42f and found this genotype to be at low frequency at passage 5, high frequency at passage 10, and back to low frequency at passage 15 (Figure S1). We did not include mutations that were detected in one out of 20 isolates (5%), with the exception of the loss of plasmid p42f, as these could have been a result of sequencing error.

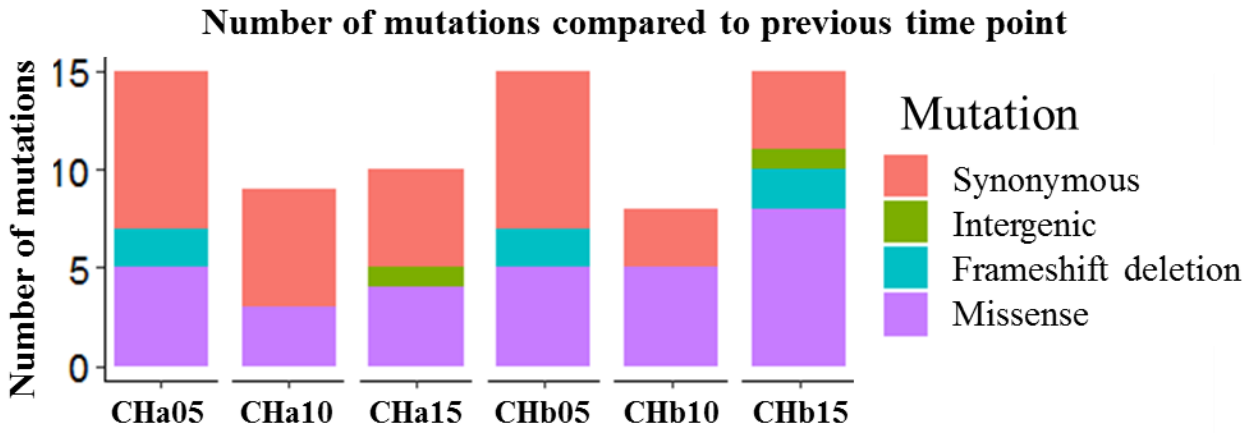

Figure 3.4 Number of mutations identified with whole genome resequencing
Stacked bar graphs indicate the number of mutations detected for our symbiont populations at various passaging time points when compared to the corresponding previous time point. There were a maximum of 15 mutations when comparing a given population to a population five passages earlier. Purple segments of the bar represent missense mutations, blue are frameshift deletions, green are intergenic, and red are synonymous. The following abbreviations are used CHa = CE3:*har1*_a and CHb = CE3:*har1*_b; numbers represent the passage DNA was sampled from.

Table 3.3 Fraction of 20 clonal isolates from final derived population with mutation

Gene or Genome region (mutation)	Replicon	CE3:*har1*_a	CE3:*har1*_b
Sorbosone dehydrogenase (SNP) RHE_CH02735 (T > C; 2848592)	Chromosome	8/20	0/20
Alpha-L-fucosidase (SNP) RHE_PF00304 (C > G; 343028)	p42f	3/20	0/20
aldo/keto reductase (SNP) RHE_PE00404 (G > A; 447009)	p42e	0/20	3/20
nitrogenase molybdenum-iron protein alpha chain (deletion) RHE_RS30400 (218784 -218792)	p42d	4/20	7/20
Polymerase (deletion) RHE_RS22005 (36509-36510)	p42b	7/20	11/20
p42f (loss of plasmid)	p42f	0/20	1/20

Discussion

Using experimental evolution we simulated a natural life cycle for plant associated microbes. We exposed rhizobial symbionts to selection pressures in both the presence and absence of their host through a series of *in planta* and *in vitro* growth cycles. While there are many outcomes that we could have observed, we predicted the evolved symbionts would fall into one of three categories, each based on the efficiency of selection at different stages of the rhizobia life cycle. One possibility is the evolution of improved symbiotic effectiveness driven by the host's capacity to impose strong selection on *in planta* rhizobia (Kiers et al. 2003; Quides et al. 2017; Regus et al. 2017; Sachs et al. 2010). A second outcome would be decreased symbiotic effectiveness driven by selection for rhizobia that exploit their host (Porter and Simms 2014). Lastly, rhizobia could have evolved increased fitness during the free-living phase which would likely favor tradeoff with symbiosis-related traits (Gano-Cohen et al. 2016; Hollowell et al. 2015, 2016). We found some evidence for the evolution of symbiosis related traits, but the observed endpoints of our experimental evolution were more complex than the three outcomes we predicted.

Of our four host-symbiont combinations, CE3 passaged on *har1* had the most evidence to support one of our three predictions. While we found some evidence for increased benefit provided by the derived CE3 strains on *har1* at the early-development harvest, the data were more consistent with antagonism at the maturity harvest. If enhanced symbiotic effectiveness had evolved, we would also expect to see a reciprocated increase in symbiont fitness (Denison 2000; West, Kiers, Pen, et al. 2002;

West, Kiers, Simms, et al. 2002). *L. japonicus* nodules formed by the ancestral CE3 have been observed to prematurely senesce as early as 3wpi (Banba et al. 2001) so another possibility is that our symbionts evolved to delay this premature senescence. It has previously been reported that nodules can prematurely senesce when insufficient amounts of fixed nitrogen are provided (Regus et al. 2017), but this mechanisms is not supported by our data as we did not find any changes in nitrogen fixation at either harvest. Alternatively, miscommunication between host and symbiont could lead to fewer resources being allocated to symbionts, and more towards shoot growth early in development, with the trade-off for the symbiont being increased persistence and scavenging of resources in intercellular space before release into the soil (Timmers et al. 2000). Moreover, derived CE3 symbionts may be attaining higher density within a nodule such that the within nodule population size is greater than their ancestor's after nodules have senesced (strain 2; Sachs et al. 2010). In our other three host-symbiont combinations we found little support for any of our three predictions. CE3:MG-20_a, NGR:*har1*_a, and NGR:MG-20_a had some indication of increased symbiotic effectiveness based on aboveground data, but we found no support for this being translated into increased symbiont fitness. In fact, we found evidence for decreased symbiont fitness for the two derived NGR symbionts. This might be a sign of evolved vulnerability by the symbiont, but it would require additional research to determine what host-symbiont mechanisms are involved, and what trade-offs might exist for the symbionts to evolve decreased *in planta* fitness. In addition to the aforementioned CE3:*har1* experiment, NGR:*har1*_b was the only other experiment that hinted at the potential evolution of antagonism (increased total

nodule mass). Lastly, we found no evidence of a change in *in vitro* (free-living) growth rate in any of our experiments.

We were unable to directly test different effects of host and symbiont genotype on the evolutionary trajectory of the symbionts, but our phenotypic data provides us with some preliminary data for future experiments. We observed more phenotypic shifts in *har1* hosts, but most of these occurred in the CE3:*har1* experiments. One explanation is that *har1* hosts formed 3-4x more nodules, thus exposing a greater proportion of the symbiont population to host selection, resulting increased symbiotic effectiveness, or granting a greater proportion direct access to host resources potentially increasing selection pressure for antagonistic traits. We also found slightly more evidence of a phenotypic shift in the CE3 experiments compared to NGR, but again this was primarily due to the CE3:*har1* experiments. It is possible that the length of the *in planta* passaging (nodule development and nitrogen fixation delayed up to 8wpi, Schumpp et al. 2009) was not sufficient for subtle changes in nitrogen fixation to be selected for by the host. Alternatively, the host may have been able to detect subtle changes in nitrogen fixation, but our greenhouse experiment was not long enough to observe any corresponding phenotypic changes in the derived NGR symbionts.

Focusing on the CE3 symbionts passaged on *har1* we attempted to link phenotype to genotype with genome. The mutations we identified might have a role in communication with the host. Three mutations in the CE3:*har1*_a line represent possible candidates to explore further. Alpha-L-fucosidase is associated with nod factor production by rhizobia (Ihara et al. 2013), so it might also be associated with

communication at other points during the interaction. For instance, signal exchange with polysaccharides has previously been demonstrated to halt the interaction between host and symbiont, butsubsequent mutations by rhizobia have also allowed increased persistence in intercellular space (Acosta-Jurado et al. 2016; Kawaharada et al. 2017). Sorbosone dehydrogenase might also play a similar role in communication between legumes and rhizobia by altering polysaccharides, but this enzyme has not been investigated for a specific function in the symbiosis. A similar evolution experiment also uncovered mutations in genes related to communication with their legume host (Guan et al. 2013; Marchetti et al. 2010, 2014). In these studies a chimeric pathogen carrying a rhizobial symbiotic plasmid had mutations to the virulence regulator *hrpG* and a type three secretion system which allowed for nodulation and persistence within the nodule, but no nitrogen fixation. Resequencing of our samples also identified some isolates with deletions in the one of the core nitrogen fixation genes, *nifD*, but there was no evidence to suggest this had a phenotypic effect on nitrogen fixation. One drastic change that we observed in the CE3:*har1*_b line is the loss of plasmid p42f from some isolates in this population. Population analysis suggests there could be frequency dependent selection based on the alternating proportion of p42f detected at our three sampled time points, but this requires a more robust investigation. It has previously been reported that the loss of p42f reduces nodulation competitiveness, but it is unclear if the loss of this plasmid results in decreased nitrogen fixation (Brom et al. 1992). This could represent a trade-off where the reduced ability to nodulate would decrease the chance of a major fitness boost from nodulation, but if this genotype does nodulate it could experience a superior growth

rate advantage due to the loss of a ~650kb plasmid (~10% of the genome; González et al. 2006). Future experiments could examine population dynamics of the Δp42f genotype across all time points to more accurately assess any selection mechanisms associated with this plasmid.

Our CE3:*har1* experiments are consistent with the broad predictions of virulence theory under horizontal transmission of microbes (Bull 1994). The varying selection pressures experienced by horizontally transmitted microbes are predicted to favor antagonistic evolution in the absence of strong host control due to the large population size and rapid generation time relative to hosts provides rhizobia with an evolutionary advantage (Denison 2000; West, Kiers, Pen, et al. 2002; West, Kiers, Simms, et al. 2002). Maintenance of nodules is also a large energetic cost a host must pay to receive the benefits of nitrogen fixation which can leave the host susceptible to the evolution of symbionts that use more resources than what they provide back to the host (Sachs, Quides, and Wendlandt 2018). For example, rhizobial genotypes have been identified in natural populations that increase their own fitness at the expense of the host fitness (Porter and Simms 2014). The issue of horizontally transmitted rhizobia has been an ongoing struggle in agriculture as non-beneficial rhizobia are often found in high proportions in agricultural soil and in the nodules of leguminous crops (Yates et al. 2011). Our experimental designed attempted to replicate agricultural conditions whereby a constant host genotype was used which only allowed rhizobial symbionts to evolve while hosts were unable to coevolve traits that may aid in enhanced symbiont effectiveness or prevent antagonistic evolution (Sachs, Quides, and Wendlandt 2018).

The evidence most consistent with a shift towards antagonism occurred in our hypernodulating *har1* host (with the CE3 symbiont). Although this host is not an agricultural crop, it does simulate the greater number of nodules formed by some cultivated soybean genotypes compared to wild genotypes (Muñoz et al. 2016). Thus, our results serve as a caution to agronomic approaches where the same host genotypes are replanted in soils for multiple years. New genomic technologies and resources make it increasingly more feasible to dissect microbial communities and determine the drivers of microbial symbiont evolution. As microbiome engineering begins to take hold as a supplement to artificial selection of crops, we have the potential to mitigate the antagonistic evolution of microbes through stringent artificial selection on host plants, and further our understanding of the evolutionary dynamics of microbial symbioses.

General Conclusions

While studies of mutualism tend to focus on the exchange of beneficial resources, it is imperative to understand the energetic cost to produce these resources, and the source of this energy, to accurately predict how interactions may shift along the symbiosis spectrum in our constantly changing world. Legumes acquire their rhizobial symbionts via the soil, as opposed to direct transfer from parent to offspring (Denison 2000). In the soil there is a large diversity of rhizobia that range from beneficial to harmful, but many legumes have evolved host control mechanisms that limit the spread of harmful rhizobial genotypes (Sachs, Quides, and Wendlandt 2018). I found support for host control in *Lotus japonicus* with evidence for biased *in planta* fitness dependent on nitrogen fixation by rhizobial symbionts. Symbionts that fixed more nitrogen received greater fitness benefits from their legume host, and this was maintained even when host investment in symbiosis varied. Despite efficient mechanisms to bias rhizobial fitness at various levels of host investment, the data presented here suggest hosts experience strong balancing selection on host investment into symbiosis, while symbionts experience positive directional selection. This difference in fitness interests between host and symbiont was further addressed using experimental evolution which suggested selection may favor antagonistic symbiont phenotypes in the absence of host coevolution.

The results I have uncovered throughout my dissertation highlight the complex nature of microbial symbioses. While I used the elegant legume-rhizobium system to study intimate plant-microbe interactions, many of these conclusions can be adapted to other microbial symbioses (Sachs, Quides, and Wendlandt 2018). Microbial mutualisms

are largely beneficial, but the exchange of costly fitness benefits can leave the host susceptible to their microbial symbionts. Natural selection on symbionts can vary greatly in the presence and absence of their host which can lead to opposing selection dynamics. Furthermore, the evolutionary advantage that microbes have over their eukaryotic hosts can further intensify these conflicting selection regimes. As microbial symbioses continue to garner increased attention and microbiome engineering begins to establish itself as a new wave of artificial selection, it will be of great interest to further dissect the mechanisms that maintain microbial mutualisms. Microbial symbioses represent an exciting new frontier of research with a wealth of possibilities, but we must continue research with a thorough and biologically realistic pursuit of knowledge.

References

Acosta-Jurado, Sebastián, Dulce-Nombre Rodríguez-Navarro, Yasuyuki Kawaharada, Juan Fernández Perea, Antonio Gil-Serrano, Haojie Jin, Qi An, et al. 2016. "Sinorhizobium Fredii HH103 Invades Lotus Burttii by Crack Entry in a Nod Factor–and Surface Polysaccharide–Dependent Manner." *Molecular Plant-Microbe Interactions* 29 (12): 925–37. https://doi.org/10.1094/MPMI-09-16-0195-R.

Amarger, N. 1981a. "Competition for Nodule Formation between Effective and Ineffective Strains of Rhizobium Meliloti." *Soil Biology and Biochemistry* 13 (6): 475–80. https://doi.org/10.1016/0038-0717(81)90037-7.

———. 1981b. "Selection of Rhizobium Strains on Their Competitive Ability for Nodulation." *Soil Biology and Biochemistry* 13 (6): 481–86. https://doi.org/10.1016/0038-0717(81)90038-9.

Andrews, Simon. 2014. "FastQC: A Quality Control Tool for High Throughput Sequence Data." 2014. http://www.bioinformatics.babraham.ac.uk/projects/fastqc.

Ankrah, Nana Y. D., Junbo Luan, and Angela E. Douglas. 2017. "Cooperative Metabolism in a Three-Partner Insect-Bacterial Symbiosis Revealed by Metabolic Modeling." Edited by George O'Toole. *Journal of Bacteriology* 199 (15): 1–15. https://doi.org/10.1128/JB.00872-16.

Axelrod, R., and W. Hamilton. 1981. "The Evolution of Cooperation." *Science* 211 (4489): 1390–96. https://doi.org/10.1126/science.7466396.

Bakker, Matthew G., Daniel K. Manter, Amy M. Sheflin, Tiffany L. Weir, and Jorge M. Vivanco. 2012. "Harnessing the Rhizosphere Microbiome through Plant Breeding and Agricultural Management." *Plant and Soil* 360 (1–2): 1–13. https://doi.org/10.1007/s11104-012-1361-x.

Bakker, Matthew G., Daniel C. Schlatter, Lindsey Otto-Hanson, and Linda L. Kinkel. 2014. "Diffuse Symbioses: Roles of Plant-Plant, Plant-Microbe and Microbe-Microbe Interactions in Structuring the Soil Microbiome." *Molecular Ecology* 23 (6): 1571–83. https://doi.org/10.1111/mec.12571.

Banba, Mari, Abu-Baker M. Siddique, Hiroshi Kouchi, Katsura Izui, and Shingo Hata. 2001. "Lotus Japonicus Forms Early Senescent Root Nodules with Rhizobium Etli." *Molecular Plant-Microbe Interactions* 14 (2): 173–80. https://doi.org/10.1094/MPMI.2001.14.2.173.

Bankevich, Anton, Sergey Nurk, Dmitry Antipov, Alexey A. Gurevich, Mikhail Dvorkin, Alexander S. Kulikov, Valery M. Lesin, et al. 2012. "SPAdes: A New Genome Assembly Algorithm and Its Applications to Single-Cell Sequencing." *Journal of Computational Biology* 19 (5): 455–77. https://doi.org/10.1089/cmb.2012.0021.

Beattie, G A, M K Clayton, and J. Handelsman. 1989. “Quantitative Comparison of the Laboratory and Field Competitiveness of Rhizobium Leguminosarum Biovar Phaseoli.” *Applied and Environmental Microbiology* 55 (11): 2755–61. http://aem.asm.org/content/55/11/2755.short.

Berrabah, F., P. Ratet, and B. Gourion. 2015. “Multiple Steps Control Immunity during the Intracellular Accommodation of Rhizobia.” *Journal of Experimental Botany* 66 (7): 1977–85. https://doi.org/10.1093/jxb/eru545.

Boer, Margreet H. de, and M. A. Djordjevic. 1995. “The Inhibition of Infection Thread Development in the Cultivar-Specific Interaction OfRhizobium and Subterranean Clover Is Not Caused by a Hypersensitive Response.” *Protoplasma* 185 (1–2): 58–71. https://doi.org/10.1007/BF01272754.

Brom, S, A García de los Santos, T Stepkowsky, M Flores, G Dávila, D Romero, and R Palacios. 1992. “Different Plasmids of Rhizobium Leguminosarum Bv. Phaseoli Are Required for Optimal Symbiotic Performance.” *Journal of Bacteriology* 174 (16): 5183–89. http://www.ncbi.nlm.nih.gov/pubmed/1644746.

Bromfield, E. S. P., J. T. Tambong, S. Cloutier, D. Prevost, G. Laguerre, P. van Berkum, T. V. T. Thi, R. Assabgui, and L. R. Barran. 2010. “Ensifer, Phyllobacterium and Rhizobium Species Occupy Nodules of Medicago Sativa (Alfalfa) and Melilotus Alba (Sweet Clover) Grown at a Canadian Site without a History of Cultivation.” *Microbiology* 156 (2): 505–20. https://doi.org/10.1099/mic.0.034058-0.

Bronstein, Judith L. 1998. “The Contribution of Ant-Plant Protection Studies to Our Understanding of Mutualism1.” *Biotropica* 30 (2): 150–61. https://doi.org/10.1111/j.1744-7429.1998.tb00050.x.

Bronstein, Judith L. 1994. “Conditional Outcomes in Mutualistic Interactions.” *Trends in Ecology & Evolution* 9 (6): 214–17. https://doi.org/10.1016/0169-5347(94)90246-1.

———. 2001. “The Costs of Mutualism.” *American Zoologist* 41 (4): 825–39. https://doi.org/10.1093/icb/41.4.825.

Bull, J. J. 1994. “VIRULENCE.” *Evolution* 48 (5): 1423–37. https://doi.org/10.1111/j.1558-5646.1994.tb02185.x.

Burdon, J. J., A. H. Gibson, Suzette D. Searle, M. J. Woods, and J. Brockwell. 1999. “Variation in the Effectiveness of Symbiotic Associations between Native Rhizobia and Temperate Australian Acacia: Within-Species Interactions.” *Journal of Applied Ecology* 36 (3): 398–408. https://doi.org/10.1046/j.1365-2664.1999.00409.x.

Burghardt, Liana T., Brendan Epstein, Joseph Guhlin, Matt S. Nelson, Margaret R. Taylor, Nevin D. Young, Michael J. Sadowsky, and Peter Tiffin. 2018. "Select and Resequence Reveals Relative Fitness of Bacteria in Symbiotic and Free-Living Environments." *Proceedings of the National Academy of Sciences* 115 (10): 2425–30. https://doi.org/10.1073/pnas.1714246115.

Busby, Posy E., Chinmay Soman, Maggie R. Wagner, Maren L. Friesen, James Kremer, Alison Bennett, Mustafa Morsy, Jonathan A. Eisen, Jan E. Leach, and Jeffery L. Dangl. 2017. "Research Priorities for Harnessing Plant Microbiomes in Sustainable Agriculture." *PLOS Biology* 15 (3): e2001793. https://doi.org/10.1371/journal.pbio.2001793.

Bushnell, Brian. 2014. "BBMap Short Read Aligner, and Other Bioinformatic Tools." 2014. http://sourceforge.net/projects/bbmap/.

Champion, Rebecca A., James N. Mathis, Daniel W. Israel, and Patrick G. Hunt. 1992. "Response of Soybean to Inoculation with Efficient and Inefficient Bradyrhizobium Japonicum Variants." *Crop Science* 32 (2): 457. https://doi.org/10.2135/cropsci1992.0011183X003200020034x.

Chaparro, Jacqueline M., Amy M. Sheflin, Daniel K. Manter, and Jorge M. Vivanco. 2012. "Manipulating the Soil Microbiome to Increase Soil Health and Plant Fertility." *Biology and Fertility of Soils* 48 (5): 489–99. https://doi.org/10.1007/s00374-012-0691-4.

Checcucci, Alice, Elisa Azzarello, Marco Bazzicalupo, Marco Galardini, Alessandra Lagomarsino, Stefano Mancuso, Lucia Marti, et al. 2016. "Mixed Nodule Infection in Sinorhizobium Meliloti–Medicago Sativa Symbiosis Suggest the Presence of Cheating Behavior." *Frontiers in Plant Science* 7 (June): 1–11. https://doi.org/10.3389/fpls.2016.00835.

Chen, Jifeng. 2012. "Vcf_tab_to_fasta_alignment.Pl."

Chen, Lu, Antonio Figueredo, Hugo Villani, Javier Michajluk, and Mariangela Hungria. 2002. "Diversity and Symbiotic Effectiveness of Rhizobia Isolated from Field-Grown Soybean Nodules in Paraguay." *Biology and Fertility of Soils* 35 (6): 448–57. https://doi.org/10.1007/s00374-002-0493-1.

Chungopast, Sirinapa, Pilunthana Thapanapongworakul, Hiroyuki Matsuura, Tan Van Dao, Toshimasa Asahi, Kuninao Tada, Shigeyuki Tajima, and Mika Nomura. 2014. "Glutamine Synthetase I-Deficiency in Mesorhizobium Loti Differentially Affects Nodule Development and Activity in Lotus Japonicus." *Journal of Plant Physiology* 171 (5): 104–8. https://doi.org/10.1016/j.jplph.2013.10.015.

Cingolani, Pablo, Adrian Platts, Le Lily Wang, Melissa Coon, Tung Nguyen, Luan Wang, Susan J. Land, Xiangyi Lu, and Douglas M. Ruden. 2012. "A Program for Annotating and Predicting the Effects of Single Nucleotide Polymorphisms, SnpEff." *Fly* 6 (2): 80–92. https://doi.org/10.4161/fly.19695.

Cleveland, Cory C., Alan R. Townsend, David S. Schimel, Hank Fisher, Robert W. Howarth, Lars O. Hedin, Steven S. Perakis, et al. 1999. "Global Patterns of Terrestrial Biological Nitrogen (N2) Fixation in Natural Ecosystems." *Global Biogeochemical Cycles* 13 (2): 623–45. https://doi.org/10.1029/1999GB900014.

Coba de la Peña, Teodoro, Elena Fedorova, José J. Pueyo, and M. Mercedes Lucas. 2018. "The Symbiosome: Legume and Rhizobia Co-Evolution toward a Nitrogen-Fixing Organelle?" *Frontiers in Plant Science* 8 (January): 1–26. https://doi.org/10.3389/fpls.2017.02229.

Collins, M. T., J. E. Thies, and L. K. Abbott. 2002. "Diversity and Symbiotic Effectiveness of Rhizobium Leguminosarum Bv. Trifolii Isolates from Pasture Soils in South-Western Australia." *Australian Journal of Soil Research* 40 (8): 1319. https://doi.org/10.1071/SR01052.

Cooper, J.E. 2007. "Early Interactions between Legumes and Rhizobia: Disclosing Complexity in a Molecular Dialogue." *Journal of Applied Microbiology* 103 (5): 1355–65. https://doi.org/10.1111/j.1365-2672.2007.03366.x.

Crespo-Rivas, Juan C., Ibtissem Guefrachi, Kenny C. Mok, José A. Villaécija-Aguilar, Sebastián Acosta-Jurado, Olivier Pierre, José E. Ruiz-Sainz, Michiko E. Taga, Peter Mergaert, and José M. Vinardell. 2016. "S Inorhizobium Fredii HH103 Bacteroids Are Not Terminally Differentiated and Show Altered O-Antigen in Nodules of the Inverted Repeat-Lacking Clade Legume G Lycyrrhiza Uralensis." *Environmental Microbiology* 18 (8): 2392–2404. https://doi.org/10.1111/1462-2920.13101.

Crook, Matthew B., Daniel P. Lindsay, Matthew B. Biggs, Joshua S. Bentley, Jared C. Price, Spencer C. Clement, Mark J. Clement, Sharon R. Long, and Joel S. Griffitts. 2012. "Rhizobial Plasmids That Cause Impaired Symbiotic Nitrogen Fixation and Enhanced Host Invasion." *Molecular Plant-Microbe Interactions* 25 (8): 1026–33. https://doi.org/10.1094/MPMI-02-12-0052-R.

Darling, Aaron E., Bob Mau, and Nicole T. Perna. 2010. "ProgressiveMauve: Multiple Genome Alignment with Gene Gain, Loss and Rearrangement." Edited by Jason E. Stajich. *PLoS ONE* 5 (6): e11147. https://doi.org/10.1371/journal.pone.0011147.

Denison, R. Ford. 2000. "Legume Sanctions and the Evolution of Symbiotic Cooperation by Rhizobia." *The American Naturalist* 156 (6): 567–76. https://doi.org/10.1086/316994.

Denton, M.D., D.R. Coventry, W.D. Bellotti, and J.G. Howieson. 2000. "Distribution, Abundance and Symbiotic Effectiveness of Rhizobium Leguminosarum Bv. Trifolii from Alkaline Pasture Soils in South Australia." *Australian Journal of Experimental Agriculture* 40 (1): 25–35. https://doi.org/10.1071/EA99035.

Devine, T. E., and L. D. Kuykendall. 1996. "Host Genetic Control of Symbiosis in Soybean (Glycine Max L.)." *Plant and Soil* 186 (1): 173–87. https://doi.org/10.1007/BF00035072.

Devine, T E, L D Kuykendall, and J J O'Neill. 1990. "The Rj4 Allele in Soybean Represses Nodulation by Chlorosis-Inducing Bradyrhizobia Classified as DNA Homology Group II by Antibiotic Resistance Profiles." *TAG. Theoretical and Applied Genetics. Theoretische Und Angewandte Genetik* 80 (1): 33–37. https://doi.org/10.1007/BF00224012.

Dixon, Ray, and Daniel Kahn. 2004. "Genetic Regulation of Biological Nitrogen Fixation." *Nature Reviews Microbiology* 2 (8): 621–31. https://doi.org/10.1038/nrmicro954.

Djordjevic, S P, R W Ridge, H C Chen, J W Redmond, M. Batley, and B G Rolfe. 1988. "Induction of Pathogenic-like Responses in the Legume Macroptilium Atropurpureum by a Transposon-Induced Mutant of the Fast-Growing, Broad-Host-Range Rhizobium Strain NGR234." *Journal of Bacteriology* 170 (4): 1848–57. http://www.ncbi.nlm.nih.gov/pubmed/2832384.

Douglas, Angela E. 2016. "How Multi-Partner Endosymbioses Function." *Nature Reviews Microbiology* 14 (12): 731–43. https://doi.org/10.1038/nrmicro.2016.151.

Ehinger, Martine, Toni J Mohr, Juliana B Starcevich, Joel L Sachs, Stephanie S Porter, and Ellen L Simms. 2014. "Specialization-Generalization Trade-off in a Bradyrhizobium Symbiosis with Wild Legume Hosts." *BMC Ecology* 14 (1): 8. https://doi.org/10.1186/1472-6785-14-8.

Faruque, Omar M., Hiroki Miwa, Michiko Yasuda, Yoshiharu Fujii, Takakazu Kaneko, Shusei Sato, and Shin Okazaki. 2015. "Identification of Bradyrhizobium Elkanii Genes Involved in Incompatibility with Soybean Plants Carrying the Rj4 Allele." Edited by C. R. Lovell. *Applied and Environmental Microbiology* 81 (19): 6710–17. https://doi.org/10.1128/AEM.01942-15.

Fening, J.O., and S.K.A. Danso. 2002. "Variation in Symbiotic Effectiveness of Cowpea Bradyrhizobia Indigenous to Ghanaian Soils." *Applied Soil Ecology* 21 (1): 23–29. https://doi.org/10.1016/S0929-1393(02)00042-2.

Ferguson, Brett J., Arief Indrasumunar, Satomi Hayashi, Meng-Han Lin, Yu-Hsiang Lin, Dugald E. Reid, and Peter M. Gresshoff. 2010. "Molecular Analysis of Legume Nodule Development and Autoregulation." *Journal of Integrative Plant Biology* 52 (1): 61–76. https://doi.org/10.1111/j.1744-7909.2010.00899.x.

Fine, P E. 1975. "Vectors and Vertical Transmission: An Epidemiologic Perspective." *Annals of the New York Academy of Sciences* 266 (1 Pathobiology): 173–94. https://doi.org/10.1111/j.1749-6632.1975.tb35099.x.

Fonseca, Carlos Roberto. 1993. "Nesting Space Limits Colony Size of the Plant-Ant Pseudomyrmex Concolor." *Oikos* 67 (3): 473. https://doi.org/10.2307/3545359.

Foo, Jee Loon, Hua Ling, Yung Seng Lee, and Matthew Wook Chang. 2017. "Microbiome Engineering: Current Applications and Its Future." *Biotechnology Journal* 12 (3): 1–11. https://doi.org/10.1002/biot.201600099.

Foster, K R, and T Wenseleers. 2006. "A General Model for the Evolution of Mutualisms." *Journal of Evolutionary Biology* 19 (4): 1283–93. https://doi.org/10.1111/j.1420-9101.2005.01073.x.

Friesen, Maren L., and Katy D. Heath. 2013. "One Hundred Years of Solitude: Integrating Single-Strain Inoculations with Community Perspectives in the Legume-Rhizobium Symbiosis." *New Phytologist* 198 (1): 7–9. https://doi.org/10.1111/nph.12173.

Friesen, Maren L., Stephanie S. Porter, Scott C. Stark, Eric J. von Wettberg, Joel L. Sachs, and Esperanza Martinez-Romero. 2011. "Microbially Mediated Plant Functional Traits." *Annual Review of Ecology, Evolution, and Systematics* 42 (1): 23–46. https://doi.org/10.1146/annurev-ecolsys-102710-145039.

Gage, Daniel J. 2002. "Analysis of Infection Thread Development Using Gfp- and DsRed-Expressing Sinorhizobium Meliloti." *Journal of Bacteriology* 184 (24): 7042–46. https://doi.org/10.1128/JB.184.24.7042-7046.2002.

Gano-Cohen, Kelsey A., Peter J. Stokes, Mia A. Blanton, Camille E. Wendlandt, Amanda C. Hollowell, John U. Regus, Deborah Kim, Seema Patel, Victor J. Pahua, and Joel L. Sachs. 2016. "Nonnodulating Bradyrhizobium Spp. Modulate the Benefits of Legume-Rhizobium Mutualism." Edited by C. Vieille. *Applied and Environmental Microbiology* 82 (17): 5259–68. https://doi.org/10.1128/AEM.01116-16.

Gaur, Y. D., and W. L. Lowther. 1980. "Distribution, Symbiotic Effectiveness, and Fluorescent Antibody Reaction of Naturalised Populations of Rhizobium Trifolii in Otago Soils." *New Zealand Journal of Agricultural Research* 23 (4): 529–32. https://doi.org/10.1080/00288233.1980.10417878.

Gerardo, Nicole M, and Benjamin J Parker. 2014. “Mechanisms of Symbiont-Conferred Protection against Natural Enemies: An Ecological and Evolutionary Framework.” *Current Opinion in Insect Science* 4 (October): 8–14. https://doi.org/10.1016/j.cois.2014.08.002.

Gibson, A.H., B.C. Curnow, F.J. Bergersen, J. Brockwell, and A.C. Rominson. 1975. “Studies of Field Populations of Rhizobium: Effectiveness of Strains of Rhizobium Trifolii Associated with Trifolium Subterraneum L. Pastures in South-Eastern Australia.” *Soil Biology and Biochemistry* 7 (2): 95–102. https://doi.org/10.1016/0038-0717(75)90005-X.

Gonzalez, V., R. I. Santamaria, Patricia Bustos, I. Hernandez-Gonzalez, Arturo Medrano-Soto, Gabriel Moreno-Hagelsieb, Sarath Chandra Janga, et al. 2006. “The Partitioned Rhizobium Etli Genome: Genetic and Metabolic Redundancy in Seven Interacting Replicons.” *Proceedings of the National Academy of Sciences* 103 (10): 3834–39. https://doi.org/10.1073/pnas.0508502103.

Guan, Su Hua, Carine Gris, Stéphane Cruveiller, Cécile Pouzet, Lena Tasse, Aurélie Leru, Aline Maillard, et al. 2013. “Experimental Evolution of Nodule Intracellular Infection in Legume Symbionts.” *The ISME Journal* 7 (7): 1367–77. https://doi.org/10.1038/ismej.2013.24.

Gubry-Rangin, C., M. Garcia, and G. Bena. 2010. “Partner Choice in Medicago Truncatula-Sinorhizobium Symbiosis.” *Proceedings of the Royal Society B: Biological Sciences* 277 (1690): 1947–51. https://doi.org/10.1098/rspb.2009.2072.

Hahn, Matthias, and Daniel Studer. 1986. “Competitiveness of a Nif- Bradyrhizobium Japonicum Mutant against the Wild-Type Strain.” *FEMS Microbiology Letters* 33 (1): 143–48. https://doi.org/10.1111/j.1574-6968.1986.tb01228.x.

Haney, Cara H., Buck S. Samuel, Jenifer Bush, and Frederick M. Ausubel. 2015. “Associations with Rhizosphere Bacteria Can Confer an Adaptive Advantage to Plants.” *Nature Plants* 1 (6): 15051. https://doi.org/10.1038/nplants.2015.51.

Heath, Katy D., and Peter Tiffin. 2009. “Stabilizing Mechanisms in a Legume-Rhizobium Mutualism.” *Evolution* 63 (3): 652–62. https://doi.org/10.1111/j.1558-5646.2008.00582.x.

Heath, KD. 2010. “Intergenomic Epistasis and Coevolutionary Constraint in Plants and Rhizobia.” *Evolution* 64 (5): 1446–58. http://onlinelibrary.wiley.com/doi/10.1111/j.1558-5646.2009.00913.x/full.

Holland, J. Nathaniel, Donald L. DeAngelis, and Judith L. Bronstein. 2002. “Population Dynamics and Mutualism: Functional Responses of Benefits and Costs.” *The American Naturalist* 159 (3): 231–44. https://doi.org/10.1086/338510.

Hollowell, Amanda C., Kelsey A. Gano, Gabriel Lopez, Kareem Shahin, John U. Regus, Nathaniel Gleason, Stefanie Graeter, Victor Pahua, and Joel L. Sachs. 2015. "Native California Soils Are Selective Reservoirs for Multidrug-Resistant Bacteria." *Environmental Microbiology Reports* 7 (3): 442–49. https://doi.org/10.1111/1758-2229.12269.

Hollowell, Amanda C., John U. Regus, David Turissini, Kelsey A. Gano-Cohen, Roxanne Bantay, Andrew Bernardo, Devora Moore, Jonathan Pham, and Joel L. Sachs. 2016. "Metapopulation Dominance and Genomic-Island Acquisition of Bradyrhizobium with Superior Catabolic Capabilities." *Proceedings of the Royal Society B: Biological Sciences* 283 (1829): 20160496. https://doi.org/10.1098/rspb.2016.0496.

Ihara, Hideyuki, Shinya Hanashima, Hiroki Tsukamoto, Yoshiki Yamaguchi, Naoyuki Taniguchi, and Yoshitaka Ikeda. 2013. "Difucosylation of Chitooligosaccharides by Eukaryote and Prokaryote A1,6-Fucosyltransferases." *Biochimica et Biophysica Acta (BBA) - General Subjects* 1830 (10): 4482–90. https://doi.org/10.1016/j.bbagen.2013.05.013.

Ivanova, Kira A., Anna V. Tsyganova, Nicholas J. Brewin, Igor A. Tikhonovich, and Viktor E. Tsyganov. 2015. "Induction of Host Defences by Rhizobium during Ineffective Nodulation of Pea (Pisum Sativum L.) Carrying Symbiotically Defective Mutations Sym40 (PsEFD), Sym33 (PsIPD3/PsCYCLOPS) and Sym42." *Protoplasma* 252 (6): 1505–17. https://doi.org/10.1007/s00709-015-0780-y.

Jiang, Qunyi, and Peter M. Gresshoff. 1997. "Classical and Molecular Genetics of the Model Legume Lotus Japonicus." *Molecular Plant-Microbe Interactions* 10 (1): 59–68. https://doi.org/10.1094/MPMI.1997.10.1.59.

Kaltenpoth, M., K. Roeser-Mueller, S. Koehler, A. Peterson, T. Y. Nechitaylo, J. W. Stubblefield, G. Herzner, J. Seger, and E. Strohm. 2014. "Partner Choice and Fidelity Stabilize Coevolution in a Cretaceous-Age Defensive Symbiosis." *Proceedings of the National Academy of Sciences* 111 (17): 6359–64. https://doi.org/10.1073/pnas.1400457111.

Kaneko, T. 2000. "Complete Genome Structure of the Nitrogen-Fixing Symbiotic Bacterium Mesorhizobium Loti." *DNA Research* 7 (6): 331–38. https://doi.org/10.1093/dnares/7.6.331.

Kawaguchi, Masayoshi. 2000. "Lotus Japonicus `Miyakojima' MG-20: An Early-Flowering Accession Suitable for Indoor Handling." *Journal of Plant Research* 113 (4): 507–9. https://doi.org/10.1007/PL00013961.

Kawaguchi, Masayoshi, Haruko Imaizumi-Anraku, Hiroyuki Koiwa, Sinobu Niwa, Akira Ikuta, Kunihiko Syono, and Shoichiro Akao. 2002. "Root, Root Hair, and Symbiotic Mutants of the Model Legume Lotus Japonicus." *Molecular Plant-Microbe Interactions* 15 (1): 17–26. https://doi.org/10.1094/MPMI.2002.15.1.17.

Kawaharada, Yasuyuki, Mette W Nielsen, Simon Kelly, Euan K James, Kasper R Andersen, Sheena R Rasmussen, Winnie Füchtbauer, et al. 2017. "Differential Regulation of the Epr3 Receptor Coordinates Membrane-Restricted Rhizobial Colonization of Root Nodule Primordia." *Nature Communications* 8 (February): 14534. https://doi.org/10.1038/ncomms14534.

Kiers, E. T., R. F. Denison, A. Kawakita, and E. A. Herre. 2011. "The Biological Reality of Host Sanctions and Partner Fidelity." *Proceedings of the National Academy of Sciences* 108 (3): E7–E7. https://doi.org/10.1073/pnas.1014546108.

Kiers, E. Toby, William C. Ratcliff, and R. Ford Denison. 2013. "Single-Strain Inoculation May Create Spurious Correlations between Legume Fitness and Rhizobial Fitness." *New Phytologist* 198 (1): 4–6. https://doi.org/10.1111/nph.12015.

Kiers, E. Toby, Rousseau, and R. Ford Denison. 2006. "Measured Sanctions: Legume Hosts Detect Quantitative Variation in Rhizobium Cooperation and Punish Accordingly." *Evolution Ecology Research* 8 (6): 1077–86.

Kiers, E. Toby, Robert A. Rousseau, Stuart A. West, and R. Ford Denison. 2003. "Host Sanctions and the Legume–rhizobium Mutualism." *Nature* 425 (6953): 78–81. https://doi.org/10.1038/nature01931.

Koch, Eric J., Tim Miyashiro, Margaret J. McFall-Ngai, and Edward G. Ruby. 2014. "Features Governing Symbiont Persistence in the Squid-Vibrio Association." *Molecular Ecology* 23 (6): 1624–34. https://doi.org/10.1111/mec.12474.

Kosch, Kerstin, Andreas Jacobi, Martin Parniske, Dietrich Werner, and Peter Müller. 1994. "The Impairment of the Nodulation Process, Induced by a Bradyrhizobium Japonicum Exopolysaccharide Mutant Is Determined by the Genotype of the Host Plant." *Zeitschrift Für Naturforschung C* 49 (11–12): 727–36. https://doi.org/10.1515/znc-1994-11-1206.

Kroll, Samuel, Matthew T. Agler, and Eric Kemen. 2017. "Genomic Dissection of Host–microbe and Microbe–microbe Interactions for Advanced Plant Breeding." *Current Opinion in Plant Biology* 36 (April): 71–78. https://doi.org/10.1016/j.pbi.2017.01.004.

Krusell, Lene, Lene H. Madsen, Shusei Sato, Grégoire Aubert, Aratz Genua, Krzysztof Szczyglowski, Gérard Duc, et al. 2002. "Shoot Control of Root Development and Nodulation Is Mediated by a Receptor-like Kinase." *Nature* 420 (6914): 422–26. https://doi.org/10.1038/nature01207.

Kuykendall, L D, and G H Elkan. 1976. "Rhizobium Japonicum Derivatives Differing in Nitrogen-Fixing Efficiency and Carbohydrate Utilization." *Applied and Environmental Microbiology* 32 (4): 511–19. http://www.ncbi.nlm.nih.gov/pubmed/988784.

Langmead, Ben, Cole Trapnell, Mihai Pop, and Steven L. Salzberg. 2009. "Ultrafast and Memory-Efficient Alignment of Short DNA Sequences to the Human Genome." *Genome Biology* 10 (3): R25. https://doi.org/10.1186/gb-2009-10-3-r25.

Lau, Jennifer A., and Jay T. Lennon. 2011. "Evolutionary Ecology of Plant-Microbe Interactions: Soil Microbial Structure Alters Selection on Plant Traits." *New Phytologist* 192 (1): 215–24. https://doi.org/10.1111/j.1469-8137.2011.03790.x.

———. 2012. "Rapid Responses of Soil Microorganisms Improve Plant Fitness in Novel Environments." *Proceedings of the National Academy of Sciences of the United States of America* 109 (35): 14058–62. https://doi.org/10.1073/pnas.1202319109.

"LegumeBase." n.d. Japan. https://www.legumebase.brc.miyazaki-u.ac.jp/.

Li, Heng, Bob Handsaker, Alec Wysoker, Tim Fennell, Jue Ruan, Nils Homer, Gabor Marth, Goncalo Abecasis, and Richard Durbin. 2009. "The Sequence Alignment/Map Format and SAMtools." *Bioinformatics* 25 (16): 2078–79. https://doi.org/10.1093/bioinformatics/btp352.

Limpens, Erik, Arjan van Zeijl, and Rene Geurts. 2015. "Lipochitooligosaccharides Modulate Plant Host Immunity to Enable Endosymbioses." *Annual Review of Phytopathology* 53 (1): 311–34. https://doi.org/10.1146/annurev-phyto-080614-120149.

Ling, Jun, Huiming Zheng, David S. Katzianer, Hui Wang, Zengtao Zhong, and Jun Zhu. 2013. "Applying Reversible Mutations of Nodulation and Nitrogen-Fixation Genes to Study Social Cheating in Rhizobium Etli-Legume Interaction." Edited by Daniel Ballhorn. *PLoS ONE* 8 (7): e70138. https://doi.org/10.1371/journal.pone.0070138.

Liu, Cheng-Wu, and Jeremy Murray. 2016. "The Role of Flavonoids in Nodulation Host-Range Specificity: An Update." *Plants* 5 (3): 33. https://doi.org/10.3390/plants5030033.

Lodwig, E. M., A. H. F. Hosie, A. Bourdès, K. Findlay, D. Allaway, R. Karunakaran, J. A. Downie, and P. S. Poole. 2003. "Amino-Acid Cycling Drives Nitrogen Fixation in the Legume–Rhizobium Symbiosis." *Nature* 422 (6933): 722–26. https://doi.org/10.1038/nature01527.

Lotocka, B., J. Kopcinska, M. Gorecka, and W. Golinowski. 2000. "Formation and Abortion of Root Nodule Primordia in Lupinus Luteus L." *Acta Biologica Cracoviensia Botanica* 42 (1): 87–102.

Maekawa, Takaki, Makoto Maekawa-Yoshikawa, Naoya Takeda, Haruko Imaizumi-Anraku, Yoshikatsu Murooka, and Makoto Hayashi. 2009. "Gibberellin Controls the Nodulation Signaling Pathway in Lotus Japonicus." *The Plant Journal* 58 (2): 183–94. https://doi.org/10.1111/j.1365-313X.2008.03774.x.

Mapelli, Francesca, Ramona Marasco, Marco Fusi, Barbara Scaglia, George Tsiamis, Eleonora Rolli, Stilianos Fodelianakis, et al. 2018. "The Stage of Soil Development Modulates Rhizosphere Effect along a High Arctic Desert Chronosequence." *The ISME Journal* 12 (5): 1188–98. https://doi.org/10.1038/s41396-017-0026-4.

Marchetti, Marta, Delphine Capela, Michelle Glew, Stéphane Cruveiller, Béatrice Chane-Woon-Ming, Carine Gris, Ton Timmers, et al. 2010. "Experimental Evolution of a Plant Pathogen into a Legume Symbiont." Edited by Graham C. Walker. *PLoS Biology* 8 (1): e1000280. https://doi.org/10.1371/journal.pbio.1000280.

Marchetti, Marta, Camille Clerissi, Yasmine Yousfi, Carine Gris, Olivier Bouchez, Eduardo Rocha, Stéphane Cruveiller, Alain Jauneau, Delphine Capela, and Catherine Masson-Boivin. 2017. "Experimental Evolution of Rhizobia May Lead to Either Extra- or Intracellular Symbiotic Adaptation Depending on the Selection Regime." *Molecular Ecology* 26 (7): 1818–31. https://doi.org/10.1111/mec.13895.

Marchetti, Marta, Alain Jauneau, Delphine Capela, Philippe Remigi, Carine Gris, Jacques Batut, and Catherine Masson-Boivin. 2014. "Shaping Bacterial Symbiosis With Legumes by Experimental Evolution." *Molecular Plant-Microbe Interactions* 27 (9): 956–64. https://doi.org/10.1094/MPMI-03-14-0083-R.

Marco, Diana E., Juan P. Carbajal, Sergio Cannas, Rebeca Pérez-Arnedo, Ángeles Hidalgo-Perea, José Olivares, José E. Ruiz-Sainz, and Juan Sanjuán. 2009. "An Experimental and Modelling Exploration of the Host-Sanction Hypothesis in Legume–rhizobia Mutualism." *Journal of Theoretical Biology* 259 (3): 423–33. https://doi.org/10.1016/j.jtbi.2009.03.033.

Márquez, A. J. 2005. *Lotus Japonicus Handbook*. *Lotus Japonicus Handbook*. Springer Netherlands.

Masson-Boivin, Catherine, and Joel L Sachs. 2018. “Symbiotic Nitrogen Fixation by Rhizobia — the Roots of a Success Story.” *Current Opinion in Plant Biology* 44 (August): 7–15. https://doi.org/10.1016/j.pbi.2017.12.001.

McFall-Ngai, Margaret J. 2014. “The Importance of Microbes in Animal Development: Lessons from the Squid-Vibrio Symbiosis.” *Annual Review of Microbiology* 68 (1): 177–94. https://doi.org/10.1146/annurev-micro-091313-103654.

McKenna, Aaron, Matthew Hanna, Eric Banks, Andrey Sivachenko, Kristian Cibulskis, Andrew Kernytsky, Kiran Garimella, et al. 2010. “The Genome Analysis Toolkit: A MapReduce Framework for Analyzing next-Generation DNA Sequencing Data.” *Genome Research* 20 (9): 1297–1303. https://doi.org/10.1101/gr.107524.110.

Mendes, Rodrigo, Marco Kruijt, Irene de Bruijn, Ester Dekkers, Menno van der Voort, Johannes H M Schneider, Yvette M Piceno, et al. 2011. “Deciphering the Rhizosphere Microbiome for Disease-Suppressive Bacteria.” *Science* 332 (6033): 1097–1100. https://doi.org/10.1126/science.1203980.

Miranda-Sánchez, Fabiola, Javier Rivera, and Pablo Vinuesa. 2016. “Diversity Patterns of R Hizobiaceae Communities Inhabiting Soils, Root Surfaces and Nodules Reveal a Strong Selection of Rhizobial Partners by Legumes.” *Environmental Microbiology* 18 (8): 2375–91. https://doi.org/10.1111/1462-2920.13061.

Moawad, H., S.M.S. Badr El-Din, and R.A. Abdel-Aziz. 1998. “Improvement of Biological Nitrogen Fixation in Egyptian Winter Legumes through Better Management of Rhizobium.” *Plant and Soil* 204 (1): 95–106. https://doi.org/10.1023/A:1004335112402.

Mueller, U.G., and J.L. Sachs. 2015. “Engineering Microbiomes to Improve Plant and Animal Health.” *Trends in Microbiology* 23 (10): 606–17. https://doi.org/10.1016/j.tim.2015.07.009.

Mueller, Ulrich G. 2002. “Ant versus Fungus versus Mutualism: Ant- Cultivar Conflict and the Deconstruction of the Attine Ant- Fungus Symbiosis.” *The American Naturalist* 160 (S4): S67–98. https://doi.org/10.1086/342084.

Muñoz, N, X Qi, M-W Li, M Xie, Y Gao, M-Y Cheung, F-L Wong, and H-M Lam. 2016. “Improvement in Nitrogen Fixation Capacity Could Be Part of the Domestication Process in Soybean.” *Heredity* 117 (2): 84–93. https://doi.org/10.1038/hdy.2016.27.

Mus, Florence, Matthew B. Crook, Kevin Garcia, Amaya Garcia Costas, Barney A. Geddes, Evangelia D. Kouri, Ponraj Paramasivan, et al. 2016. “Symbiotic Nitrogen Fixation and the Challenges to Its Extension to Nonlegumes.” Edited by R. M. Kelly. *Applied and Environmental Microbiology* 82 (13): 3698–3710. https://doi.org/10.1128/AEM.01055-16.

Neuhauser, Claudia, and Joseph E. Fargione. 2004. “A Mutualism–parasitism Continuum Model and Its Application to Plant–mycorrhizae Interactions.” *Ecological Modelling* 177 (3–4): 337–52. https://doi.org/10.1016/j.ecolmodel.2004.02.010.

Nishimura, Rieko, Masaki Hayashi, Guo-Jiang Wu, Hiroshi Kouchi, Haruko Imaizumi-Anraku, Yasuhiro Murakami, Shinji Kawasaki, et al. 2002. “HAR1 Mediates Systemic Regulation of Symbiotic Organ Development.” *Nature* 420 (6914): 426–29. https://doi.org/10.1038/nature01231.

Noel, K D, A Sanchez, L Fernandez, J Leemans, and M a Cevallos. 1984. “Rhizobium Phaseoli Symbiotic Mutants with Transposon Tn5 Insertions.” *Journal of Bacteriology* 158 (1): 148–55. http://www.pubmedcentral.nih.gov/articlerender.fcgi?artid=215392&tool=pmcentrez&rendertype=abstract.

Noel, K D, K A Vandenbosch, and B. Kulpaca. 1986. “Mutations in Rhizobium Phaseoli That Lead to Arrested Development of Infection Threads.” *Journal of Bacteriology* 168 (3): 1392–1401. http://www.ncbi.nlm.nih.gov/pubmed/3782040.

Oono, Ryoko, Carolyn G. Anderson, and R. Ford Denison. 2011. “Failure to Fix Nitrogen by Non-Reproductive Symbiotic Rhizobia Triggers Host Sanctions That Reduce Fitness of Their Reproductive Clonemates.” *Proceedings of the Royal Society B: Biological Sciences* 278 (1718): 2698–2703. https://doi.org/10.1098/rspb.2010.2193.

Oono, Ryoko, Imke Schmitt, Janet I Sprent, and R Ford Denison. 2010. “Multiple Evolutionary Origins of Legume Traits Leading to Extreme Rhizobial Differentiation.” *New Phytologist* 187 (2): 508–20. https://doi.org/10.1111/j.1469-8137.2010.03261.x.

Panke-Buisse, Kevin, Angela C. Poole, Julia K. Goodrich, Ruth E. Ley, and Jenny Kao-Kniffin. 2015. “Selection on Soil Microbiomes Reveals Reproducible Impacts on Plant Function.” *The ISME Journal* 9 (4): 980–89. https://doi.org/10.1038/ismej.2014.196.

Parniske, M., Christa Zimmermann, P. B. Cregan, and D. Werner. 1990. “Hypersensitive Reaction of Nodule Cells in the Glycine Sp./ Bradyrhizobium Japonicum - Symbiosis Occurs at the Genotype-Specific Level*.” *Botanica Acta* 103 (2): 143–48. https://doi.org/10.1111/j.1438-8677.1990.tb00140.x.

Parniske, Martin, Petra E. Schmidt, Kerstin Kosch, and Muller Peter. 1994. “Plant Defense Responses of Host Plants with Determinate Nodules Induced by EPS-Defective ExoB Mutants of Bradyrhizobium Japonicum.” *Molecular Plant-Microbe Interactions* 7 (5): 631. https://doi.org/10.1094/MPMI-7-0631.

Phanstiel, Douglas H., Alan P. Boyle, Carlos L. Araya, and Michael P. Snyder. 2014. “Sushi.R: Flexible, Quantitative and Integrative Genomic Visualizations for Publication-Quality Multi-Panel Figures.” *Bioinformatics* 30 (19): 2808–10. https://doi.org/10.1093/bioinformatics/btu379.

Pieterse, Corné M.J., Christos Zamioudis, Roeland L. Berendsen, David M. Weller, Saskia C.M. Van Wees, and Peter A.H.M. Bakker. 2014. “Induced Systemic Resistance by Beneficial Microbes.” *Annual Review of Phytopathology* 52 (1): 347–75. https://doi.org/10.1146/annurev-phyto-082712-102340.

Pineda, Ana, Ian Kaplan, and T. Martijn Bezemer. 2017. “Steering Soil Microbiomes to Suppress Aboveground Insect Pests.” *Trends in Plant Science* 22 (9): 770–78. https://doi.org/10.1016/j.tplants.2017.07.002.

Porter, Stephanie S., and Ellen L. Simms. 2014. “Selection for Cheating across Disparate Environments in the Legume-Rhizobium Mutualism.” Edited by Richard Bardgett. *Ecology Letters* 17 (9): 1121–29. https://doi.org/10.1111/ele.12318.

Prell, J., J. P. White, A. Bourdes, S. Bunnewell, R. J. Bongaerts, and P. S. Poole. 2009. “Legumes Regulate Rhizobium Bacteroid Development and Persistence by the Supply of Branched-Chain Amino Acids.” *Proceedings of the National Academy of Sciences* 106 (30): 12477–82. https://doi.org/10.1073/pnas.0903653106.

Pringle, Elizabeth G. 2016. “Integrating Plant Carbon Dynamics with Mutualism Ecology.” *New Phytologist* 210 (1): 71–75. https://doi.org/10.1111/nph.13679.

Pueppke, Steven G., and William J. Broughton. 1999. “Rhizobium Sp. Strain NGR234 and R. Fredii USDA257 Share Exceptionally Broad, Nested Host Ranges.” *Molecular Plant-Microbe Interactions* 12 (4): 293–318. https://doi.org/10.1094/MPMI.1999.12.4.293.

Puppo, Alain, Karin Groten, Fabiola Bastian, Raffaella Carzaniga, Mariam Soussi, M. Mercedes Lucas, Maria Rosario De Felipe, Judith Harrison, Hélène Vanacker, and Christine H. Foyer. 2004. “Legume Nodule Senescence: Roles for Redox and Hormone Signalling in the Orchestration of the Natural Aging Process.” *New Phytologist* 165 (3): 683–701. https://doi.org/10.1111/j.1469-8137.2004.01285.x.

Quides, Kenjiro W., Glenna M. Stomackin, Hsu-Han Lee, Jeff H. Chang, and Joel L. Sachs. 2017. "Lotus Japonicus Alters in Planta Fitness of Mesorhizobium Loti Dependent on Symbiotic Nitrogen Fixation." Edited by Ulrich Melcher. *PLOS ONE* 12 (9): e0185568. https://doi.org/10.1371/journal.pone.0185568.

Quigley, P. E., P. J. Cunningham, M. Hannah, G. N. Ward, and T. Morgan. 1997. "Symbiotic Effectiveness of Rhizobium Leguminosarum Bv. Trifolii Collected from Pastures in South-Western Victoria." *Australian Journal of Experimental Agriculture* 37 (6): 623. https://doi.org/10.1071/EA96089.

Quinlan, Aaron R., and Ira M. Hall. 2010. "BEDTools: A Flexible Suite of Utilities for Comparing Genomic Features." *Bioinformatics* 26 (6): 841–42. https://doi.org/10.1093/bioinformatics/btq033.

Rangin, C., B. Brunel, J.C. Cleyet-Marel, M.M. Perrineau, and G. Bena. 2008. "Effects of Medicago Truncatula Genetic Diversity, Rhizobial Competition, and Strain Effectiveness on the Diversity of a Natural Sinorhizobium Species Community." *Applied and Environmental Microbiology* 74 (18): 5653–61. https://doi.org/10.1128/AEM.01107-08.

Ratcliff, William C, and R Ford Denison. 2009. "Rhizobitoxine Producers Gain More Poly-3-Hydroxybutyrate in Symbiosis than Do Competing Rhizobia, but Reduce Plant Growth." *The ISME Journal* 3 (7): 870–72. https://doi.org/10.1038/ismej.2009.38.

Regus, J. U., K. A. Gano, A. C. Hollowell, and J. L. Sachs. 2014. "Efficiency of Partner Choice and Sanctions in Lotus Is Not Altered by Nitrogen Fertilization." *Proceedings of the Royal Society B: Biological Sciences* 281 (1781): 20132587–20132587. https://doi.org/10.1098/rspb.2013.2587.

Regus, J. U., K. A. Gano, A. C. Hollowell, V. Sofish, and J. L. Sachs. 2015. "Lotus Hosts Delimit the Mutualism-Parasitism Continuum of Bradyrhizobium." *Journal of Evolutionary Biology* 28 (2): 447–56. https://doi.org/10.1111/jeb.12579.

Regus, John U., Kenjiro W. Quides, Matthew R. O'Neill, Rina Suzuki, Elizabeth A. Savory, Jeff H. Chang, and Joel L. Sachs. 2017. "Cell Autonomous Sanctions in Legumes Target Ineffective Rhizobia in Nodules with Mixed Infections." *American Journal of Botany* 104 (9): 1299–1312. https://doi.org/10.3732/ajb.1700165.

Reid, Dugald E., Brett J. Ferguson, Satomi Hayashi, Yu-Hsiang Lin, and Peter M. Gresshoff. 2011. "Molecular Mechanisms Controlling Legume Autoregulation of Nodulation." *Annals of Botany* 108 (5): 789–95. https://doi.org/10.1093/aob/mcr205.

Rice, William R. 1996. “Sexually Antagonistic Male Adaptation Triggered by Experimental Arrest of Female Evolution.” *Nature* 381 (6579): 232–34. https://doi.org/10.1038/381232a0.

Rillig, Matthias C., Alia Tsang, and Julien Roy. 2016. “Microbial Community Coalescence for Microbiome Engineering.” *Frontiers in Microbiology* 7 (DEC): 6–8. https://doi.org/10.3389/fmicb.2016.01967.

Roth, V. 2006. “Doubling Time Computing.” 2006. http://www.doubling-time.com/compute.php.

Rubin, Rachel L., Kees Jan van Groenigen, and Bruce A. Hungate. 2017. “Plant Growth Promoting Rhizobacteria Are More Effective under Drought: A Meta-Analysis.” *Plant and Soil* 416 (1–2): 309–23. https://doi.org/10.1007/s11104-017-3199-8.

Sachs, J. L., S. W. Kembel, A. H. Lau, and E. L. Simms. 2009. “In Situ Phylogenetic Structure and Diversity of Wild Bradyrhizobium Communities.” *Applied and Environmental Microbiology* 75 (14): 4727–35. https://doi.org/10.1128/AEM.00667-09.

Sachs, J. L, and T. P Wilcox. 2006. “A Shift to Parasitism in the Jellyfish Symbiont Symbiodinium Microadriaticum.” *Proceedings of the Royal Society B: Biological Sciences* 273 (1585): 425–29. https://doi.org/10.1098/rspb.2005.3346.

Sachs, J L, M O Ehinger, and E L Simms. 2010. “Origins of Cheating and Loss of Symbiosis in Wild Bradyrhizobium.” *Journal of Evolutionary Biology* 23 (5): 1075–89. https://doi.org/10.1111/j.1420-9101.2010.01980.x.

Sachs, J L, J E Russell, Y E Lii, K C Black, G Lopez, and A S Patil. 2010. “Host Control over Infection and Proliferation of a Cheater Symbiont.” *Journal of Evolutionary Biology* 23 (9): 1919–27. https://doi.org/10.1111/j.1420-9101.2010.02056.x.

Sachs, Joel L., Ulrich G. Mueller, Thomas P. Wilcox, and James J. Bull. 2004. “The Evolution of Cooperation.” *The Quarterly Review of Biology* 79 (2): 135–60. http://www.jstor.org/stable/10.1086/383541.

Sachs, Joel L., Kenjiro W. Quides, and Camille E. Wendlandt. 2018. “Legumes versus Rhizobia: A Model for Ongoing Conflict in Symbiosis.” *New Phytologist* 219 (4): 1199–1206. https://doi.org/10.1111/nph.15222.

Sachs, Joel L., James E. Russell, and Amanda C. Hollowell. 2011. “Evolutionary Instability of Symbiotic Function in Bradyrhizobium Japonicum.” Edited by Bas E. Dutilh. *PLoS ONE* 6 (11): e26370. https://doi.org/10.1371/journal.pone.0026370.

Sachs, Joel L., Ryan G. Skophammer, and John U. Regus. 2011. "Evolutionary Transitions in Bacterial Symbiosis." *Proceedings of the National Academy of Sciences* 108 (Supplement_2): 10800–807. https://doi.org/10.1073/pnas.1100304108.

Schmeisser, Christel, Heiko Liesegang, Dagmar Krysciak, Nadia Bakkou, A. Le Quere, Antje Wollherr, Isabelle Heinemeyer, et al. 2009. "Rhizobium Sp. Strain NGR234 Possesses a Remarkable Number of Secretion Systems." *Applied and Environmental Microbiology* 75 (12): 4035–45. https://doi.org/10.1128/AEM.00515-09.

Schumpp, Olivier, Michèle Crèvecoeur, William J Broughton, and William J Deakin. 2009. "Delayed Maturation of Nodules Reduces Symbiotic Effectiveness of the Lotus Japonicus–Rhizobium Sp. NGR234 Interaction." *Journal of Experimental Botany* 60 (2): 581–90. https://doi.org/10.1093/jxb/ern302.

Schützendübel, Andres, and Andrea Polle. 2002. "Plant Responses to Abiotic Stresses: Heavy Metal- induced Oxidative Stress and Protection by Mycorrhization." *Journal of Experimental Botany* 53 (372): 1351–65. https://doi.org/10.1093/jxb/53.372.1351.

Shimoda, Y., H. Mitsui, H. Kamimatsuse, K. Minamisawa, E. Nishiyama, Y. Ohtsubo, Y. Nagata, et al. 2008. "Construction of Signature-Tagged Mutant Library in Mesorhizobium Loti as a Powerful Tool for Functional Genomics." *DNA Research* 15 (5): 297–308. https://doi.org/10.1093/dnares/dsn017.

Simms, E. L, D. L. Taylor, J. Povich, R. P Shefferson, J.L. Sachs, M. Urbina, and Y. Tausczik. 2006. "An Empirical Test of Partner Choice Mechanisms in a Wild Legume-Rhizobium Interaction." *Proceedings of the Royal Society B: Biological Sciences* 273 (1582): 77–81. https://doi.org/10.1098/rspb.2005.3292.

Simms, Ellen L., and D Lee Taylor. 2002. "Partner Choice in Nitrogen-Fixation Mutualisms of Legumes and Rhizobia." *Integrative and Comparative Biology* 42 (2): 369–80. https://doi.org/10.1093/icb/42.2.369.

Singleton, P. W., and K. R. Stockinger. 1983. "Compensation against Ineffective Nodulation in Soybean1." *Crop Science* 23 (1): 69. https://doi.org/10.2135/cropsci1983.0011183X002300010019x.

Somasegaran, P., and H.J. Hoben. 1994. *Handbook for Rhizobia*. New York: Springer-Verlag.

Sprent, J. I., J. M. Sutherland, S. M. de Faria, M. J. Dilworth, H. D. L. Corby, J. H. Becking, L. A. Materon, and J. W. Drozd. 1987. "Some Aspects of the Biology of Nitrogen-Fixing Organisms [and Discussion]." *Philosophical Transactions of the Royal Society B: Biological Sciences* 317 (1184): 111–29. https://doi.org/10.1098/rstb.1987.0051.

Sprent, Janet I., Julie Ardley, and Euan K. James. 2017. “Biogeography of Nodulated Legumes and Their Nitrogen-Fixing Symbionts.” *New Phytologist* 215 (1): 40–56. https://doi.org/10.1111/nph.14474.

Swenson, W., D. S. Wilson, and R. Elias. 2000. “Artificial Ecosystem Selection.” *Proceedings of the National Academy of Sciences* 97 (16): 9110–14. https://doi.org/10.1073/pnas.150237597.

Thompson, John N. 1988. “Variation in Interspecific Interactions.” *Annual Review of Ecology and Systematics* 19 (1): 65–87. https://doi.org/10.1146/annurev.es.19.110188.000433.

Tilman, David, Kenneth G. Cassman, Pamela A. Matson, Rosamond Naylor, and Stephen Polasky. 2002. “Agricultural Sustainability and Intensive Production Practices.” *Nature* 418 (6898): 671–77. https://doi.org/10.1038/nature01014.

Timmers, Antonius C J, Eric Soupène, Marie-Christine Auriac, Françoise de Billy, Jacques Vasse, Pierre Boistard, and Georges Truchet. 2000. “Saprophytic Intracellular Rhizobia in Alfalfa Nodules.” *Molecular Plant-Microbe Interactions* 13 (11): 1204–13. https://doi.org/10.1094/MPMI.2000.13.11.1204.

Tkacz, Andrzej, Jitender Cheema, Govind Chandra, Alastair Grant, and Philip S. Poole. 2015. “Stability and Succession of the Rhizosphere Microbiota Depends upon Plant Type and Soil Composition.” *The ISME Journal* 9 (11): 2349–59. https://doi.org/10.1038/ismej.2015.41.

Trainer, Maria A., and Trevor C. Charles. 2006. “The Role of PHB Metabolism in the Symbiosis of Rhizobia with Legumes.” *Applied Microbiology and Biotechnology* 71 (4): 377–86. https://doi.org/10.1007/s00253-006-0354-1.

Trivedi, Pankaj, Peer M. Schenk, Matthew D. Wallenstein, and Brajesh K. Singh. 2017. “Tiny Microbes, Big Yields: Enhancing Food Crop Production with Biological Solutions.” *Microbial Biotechnology* 10 (5): 999–1003. https://doi.org/10.1111/1751-7915.12804.

Vasse, Jacques, Francoise Billy, and Georges Truchet. 1993. “Abortion of Infection during the Rhizobium Meliloti-Alfalfa Symbiotic Interaction Is Accompanied by a Hypersensitive Reaction.” *The Plant Journal* 4 (3): 555–66. https://doi.org/10.1046/j.1365-313X.1993.04030555.x.

West, S. A., E. T. Kiers, E. L. Simms, and R. F. Denison. 2002. “Sanctions and Mutualism Stability: Why Do Rhizobia Fix Nitrogen?” *Proceedings of the Royal Society B: Biological Sciences* 269 (1492): 685–94. https://doi.org/10.1098/rspb.2001.1878.

West, S. A., E. Toby Kiers, I. Pen, and R. F. Denison. 2002. “Sanctions and Mutualism Stability: When Should Less Beneficial Mutualists Be Tolerated?” *Journal of Evolutionary Biology* 15 (5): 830–37. https://doi.org/10.1046/j.1420-9101.2002.00441.x.

Westhoek, Annet, Elsa Field, Finn Rehling, Geraldine Mulley, Isabel Webb, Philip S. Poole, and Lindsay A. Turnbull. 2017. “Policing the Legume-Rhizobium Symbiosis: A Critical Test of Partner Choice.” *Scientific Reports* 7 (1): 1419. https://doi.org/10.1038/s41598-017-01634-2.

White, James, Jurgen Prell, Euan K. James, and Philip Poole. 2007. “Nutrient Sharing between Symbionts.” *Plant Physiology* 144 (2): 604–14. https://doi.org/10.1104/pp.107.097741.

Williams, Hywel T P, and Timothy M Lenton. 2007. “Artificial Selection of Simulated Microbial Ecosystems.” *Proceedings of the National Academy of Sciences* 104 (21): 8918–23. https://doi.org/10.1073/pnas.0610038104.

Yasuda, Michiko, Hiroki Miwa, Sachiko Masuda, Yumiko Takebayashi, Hitoshi Sakakibara, and Shin Okazaki. 2016. “Effector-Triggered Immunity Determines Host Genotype-Specific Incompatibility in Legume– Rhizobium Symbiosis.” *Plant and Cell Physiology* 57 (8): 1791–1800. https://doi.org/10.1093/pcp/pcw104.

Yates, Ron John, John Gregory Howieson, Wayne Gerald Reeve, and Graham William O’Hara. 2011. “A Re-Appraisal of the Biology and Terminology Describing Rhizobial Strain Success in Nodule Occupancy of Legumes in Agriculture.” *Plant and Soil* 348 (1–2): 255–67. https://doi.org/10.1007/s11104-011-0971-z.

Yoder, Jeremy B. 2016. “Understanding the Coevolutionary Dynamics of Mutualism with Population Genomics.” *American Journal of Botany* 103 (10): 1742–52. https://doi.org/10.3732/ajb.1600154.

Yoder, Jeremy B., and Peter Tiffin. 2017. “Sanctions, Partner Recognition, and Variation in Mutualism.” *The American Naturalist* 190 (4): 491–505. https://doi.org/10.1086/693472.

Yoshida, Chie, Sachiko Funayama-Noguchi, and Masayoshi Kawaguchi. 2010. “Plenty, a Novel Hypernodulation Mutant in Lotus Japonicus.” *Plant and Cell Physiology* 51 (9): 1425–35. https://doi.org/10.1093/pcp/pcq115.

Zgadzaj, Rafal, Ruben Garrido-Oter, Dorthe Bodker Jensen, Anna Koprivova, Paul Schulze-Lefert, and Simona Radutoiu. 2016. “Root Nodule Symbiosis in Lotus Japonicus Drives the Establishment of Distinctive Rhizosphere, Root, and Nodule Bacterial Communities.” *Proceedings of the National Academy of Sciences* 113 (49): E7996–8005. https://doi.org/10.1073/pnas.1616564113.

Appendices

Appendix 1.1 see attached

Appendix 1.2 see attached

Appendix 2.1 Host and symbiont data collected for the 3.5wpi harvest

The patterns observed here are similar to the 5wpi data set, but with smaller differences among treatments. Nodulation patterns were assessed as the mean number of nodules per plant **(A)**, and the mean nodule to shoot biomass ratio **(B)**. Rhizobial fitness was estimated at the plant level alone **(C)**, and the proportion of MAFF in coinoculated hosts was also estimated at the plant level **(D)**. Host benefits from nodulation was only analyzed as shoot mass of inoculated plant minus shoot mass of uninoculated size-matched control **(E)**. Error bars represent one standard error from the mean. A connecting letter report indicates significant differences among hosts (Standard Least Squares Fit Model, post-hoc LSMeans Tukey HSD test, $\alpha = 0.05$). Asterisks indicate greater proportions of MAFF than expected based on proportion within the inoculum. Hosts receiving MAFF, STM6, or a mixed-strain coinoculum are represented by solid bars, dotted bars, or striped bars, respectively. Green bars = MG-20 host, blue = Gifu, purple = *plenty*, and red = *har1*.

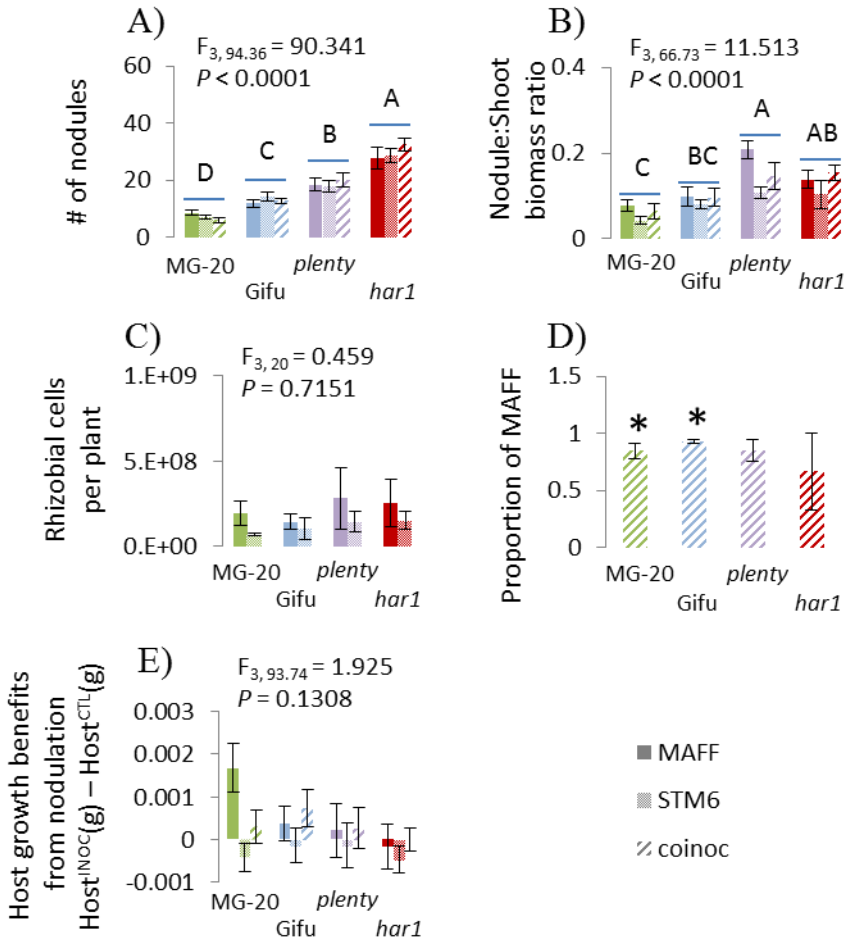

Appendix 2.2 see attached

Appendix 2.3 see attached

Appendix 2.4 see attached

Appendix 2.5 see attached

Appendix 2.6 Fitness functions and corresponding AICc values for host shoot mass dependent on number of nodules formed

Function name	Harvest	Inoculum	y-intercept	Function	# of parameters	n	MSE	AICc
linear	3.5wpi	coinoculum	0.0044684	0.000080878717472121*x	1	38	1.24E-06	-222.33008
square root	3.5wpi	coinoculum	0.0044684	0.000202093662198134(x^1/2) - 0.000031116348501091 1*x	2	38	1.23E-06	-220.25928
Log_{10}	3.5wpi	coinoculum	0.0044684	log10(x+1) * 0.000515466919002561 - 0.000019999581080272 2*x	2	38	1.23E-06	-220.28614
Negative exponential	3.5wpi	coinoculum	0.0044684	0.00047351182518577 2(1-Exp(-0.480247830015179*x)) - (0.000010721017021769 2*x)	3	38	1.25E-06	-217.62041
linear	3.5wpi	MAFF	0.0044684	0.000016432059251421 9*x	1	40	2.98E-06	-218.91503
square root	3.5wpi	MAFF	0.0044684	0.000241961407890998(x^1/2)-0.000032583078865593*x	2	40	2.99E-06	-216.65791
Log_{10}	3.5wpi	MAFF	0.0044684	log10(x+1) * 0.000615160996607869 - 0.000019256448018224 1*x	2	40	2.99E-06	-216.67708
Negative exponential	3.5wpi	MAFF	0.0044684	0.000581218413219208(1-Exp(-0.394035255853711*x)) - (0.000008930134943853 7*x)	3	40	3.06E-06	-213.9549
linear	3.5wpi	STM6	0.0044684	-0.000015111195556854 9*x	1	37	1.27E-06	-216.02082
square root	3.5wpi	STM6	0.0044684	-0.000204223998204155(x^1/2)- (-0.000027345546474363 8*x)	2	37	1.27E-06	-213.82593
Log_{10}	3.5wpi	STM6	0.0044684	log10(x+1) * (-0.000500050390171661) - (-0.000014894285560110 4*x)	2	37	1.27E-06	-213.81075
Negative exponential	3.5wpi	STM6	0.0044684	-0.000398051421338899(1-Exp(-502.264300859076*x)) - (-0.000003040228508877*x)	3	37	1.27E-06	-211.47228
linear	5wpi	coinoculum	0.0047769	0.000162317552114355*x	1	38	5.95E-05	-158.47003
square root	5wpi	coinoculum	0.0047769	0.00317236114985949(x^1/2) - (0.00037662116682609*x)	2	38	4.86E-05	-159.5835
Log_{10}	5wpi	coinoculum	0.0047769	log10(x+1)* (0.00818151925361532) - (0.000206886351018881*x)	2	38	4.84E-05	-159.65155
Negative exponential	5wpi	coinoculum	0.0047769	0.0103314724694257(1-Exp(-0.141572147447448*x)) - (0.000138582468221939*x)	3	38	4.89E-05	-157.12914
linear	5wpi	MAFF	0.0047769	0.000169259841679034*x	1	39	5.94E-05	-162.72661
square root	5wpi	MAFF	0.0047769	0.00365984900951813(x^1/2) - (0.000415212425423131*x)	2	39	3.65E-05	-168.74876
Log_{10}	5wpi	MAFF	0.0047769	log10(x+1)*(0.00941993895378868) - (0.000220750792577468*x)	2	39	3.65E-05	-168.73995
Negative exponential	5wpi	MAFF	0.0047769	0.0140423277388243(1-Exp(-0.0976359554616423*x)) - (0.000181225726111763*x)	3	39	3.69E-05	-166.23732
linear	5wpi	STM6	0.0047769	-0.000031364858377340 4*x	1	38	2.46E-06	-211.04793
square root	5wpi	STM6	0.0047769	-0.000494964793749678(x^1/2) - (-0.000056792369714791 7*x)	2	38	2.21E-06	-210.61343
Log_{10}	5wpi	STM6	0.0047769	log10(x+1)*(-0.0012364996349053) - (-0.000028419604978571 6)	2	38	2.22E-06	-210.52839
Negative exponential	5wpi	STM6	0.0047769	-0.275512344724502(1-Exp(-0.00391963520937539*x)) - (-0.000976191857871114*x)	3	38	2.12E-06	-208.90768

Appendix 2.7 Fitness functions and corresponding AICc values for estimated rhizobia population size per plant dependent on number of nodules formed

Function name	Harvest	Inoculum	y-intercept	Function	# of parameters	n	MSE	AICc
linear	3.5wpi	coinoculum	0	8881373.0589196*x	1	12	1.64E+16	196.901917
square root	3.5wpi	coinoculum	0	94722705.6003285(x^1/2) - (11115326.3151691*x)	2	12	8.48E+15	196.228586
Log_{10}	3.5wpi	coinoculum	0	log10(x+1) * (234752344.979218) - (5495747.30009085*x)	2	12	8.43E+15	196.202076
Negative exponential	3.5wpi	coinoculum	0	179499023.985503(1-Exp(-122634690.927495*x)) - (-402524.689755154*x)	3	12	7.96E+15	199.209647
linear	3.5wpi	MAFF	0	11583291.6762189*x	1	12	2.90E+16	199.889293
square root	3.5wpi	MAFF	0	23514079.4984835(x^1/2) - (-6739990.78223996*x)	2	12	3.13E+16	203.037441
Log_{10}	3.5wpi	MAFF	0	log(x+1) * (60921310.8906118) - (-7967900.9452514*x)	2	12	3.13E+16	203.029109
Negative exponential	3.5wpi	MAFF	0	62361115.0516423(1-Exp(-331097581.806191*x) - (-8781887.52976442*x)	3	12	3.10E+16	206.291294
linear	3.5wpi	STM6	0	5743957.96804458*x	1	12	7.19E+15	192.616979
square root	3.5wpi	STM6	0	42552005.1381313(x^1/2) - (2935145.04001617*x)	2	12	6.16E+15	194.564185
Log_{10}	3.5wpi	STM6	0	log10(x+1) * (104531696.78276) - (359288.357531038*x)	2	12	6.21E+15	194.60633
Negative exponential	3.5wpi	STM6	0	67289734.850404(1-Exp(-3381273.32714893*x)) - (-2812388.97253559*x)	3	12	6.72E+15	198.329207
linear	5wpi	coinoculum	0	6708983.70899168*x	1	12	6.77E+16	204.300397
square root	5wpi	coinoculum	0	104813170.833252(x^1/2) - (11770702.8055149*x)	2	12	6.24E+16	206.635629
Log_{10}	5wpi	coinoculum	0	log10(x+1) * (263121246.940056) - (5793248.06271108*x)	2	12	6.26E+16	206.650634
Negative exponential	5wpi	coinoculum	0	219309435.326318(1-Exp(-7557.90255343837*x)) - (358160.25682523*x)	3	12	6.48E+16	210.1389
linear	5wpi	MAFF	0	16017437.4652128*x	1	12	8.22E+16	205.310527
square root	5wpi	MAFF	0	64367483.6502422(x^1/2) - (-4972124.51142148*x)	2	12	8.34E+16	208.146776
Log_{10}	5wpi	MAFF	0	log10(x+1) * (159746129.837673) - (-8689136.89956412*x)	2	12	8.37E+16	208.166105
Negative exponential	5wpi	MAFF	0	153357489.261753(1-Exp(-8620023.75515224*x)) - (-11230556.2975049*x)	3	12	8.40E+16	211.49011
linear	5wpi	STM6	0	4241681.87252608*x	1	12	9.60E+15	194.117873
square root	5wpi	STM6	0	15120742.0970736(x^1/2) - (-1758859.10281064*x)	2	12	1.01E+16	197.158222
Log_{10}	5wpi	STM6	0	log10(x+1) * (38167789.9844744) - (-2599148.60217653*x)	2	12	1.10E+16	197.59425
Negative exponential	5wpi	STM6	0	33355339.1760357(1-Exp(-6941517.66513112*x)) - (-3285322.72115991*x)	3	12	1.02E+16	200.508309

Appendix 3.1 Relative read depth of each sample

Replicon read depth was standardized by chromosome read depth for each sample. Blue boxplots represent experiment CE3:*har1*_a, red is CE3:*har1*_b, green is CE3:MG-20_a, purple is CE3:MG-20_b, and orange is the CE3 ancestor